

Republic of Iraq
Ministry of Higher Education & Scientific Research
University of Baghdad
College of Education for pure science-ibn al-Hiatham



STUDY OF SOME PHYSICAL PROPERTIES OF EPOXY REINFORCE WITH NANO PARTICLES

A Thesis Submitted to the committee of
Physics Department - Education for pure science-ibn al-Hiatham,
University of Baghdad

In Partial Fulfillment of the Requirements for the

Degree of Doctor of Philosophy

In Physics

By

SAFAA ABED SALIH

M.Sc. In Physics

University of Baghdad

Supervisors

ASSITE Prof. Dr. Widad. Hamdi.J

2016 .A.

1437 H.

DEDICATION:

TO MY FAMILY:

FATHER, MOTHER AND ALL BROTHER RESPECT

WIFE (SORA) LOVE

SONS

HASSAN, MAITH AND AISAM

TO MY COLLEAGUES SPECIALLY

ACKNOWLEDGMENT

It is my pleasure to express my gratitude to supervisors, assist Prof. Dr. Widad. Hamdi.J for her guidance and supporting throughout the period of Ph.D. study.

My deep appreciation to Dr. Muhannad Mahdi Abd for his assistance, supporting and advices in the last two year.

My deep appreciation to the department of Physics, college of Education for pure science-ibn AL-Hiatham – University of Baghdad to give me opportunity to study and finish Ph.D. study

My deep appreciation to the department of Science, College of Basic Education, University of Al-Mustansiriya for its supporting and assistance through all the period of my Ph.D. study.

My deep appreciation to Dr. Adil I . Khadim for his assistance and advices

My deep appreciation to Dr. Abdul Hameed .R. Mahdi for all advices and supporting.



جمهورية العراق
وزارة التعليم العالي
والبحرث العلمي
جامعة بغداد
كلية التربية ابن الهيثم

دراسة بعض الخواص الفيزيائية للايبوكسي المدعم بدقائق نانوية

رسالة مقدمة

الى مجلس كلية التربية-ابن الهيثم - جامعة بغداد
وهي جزء من متطلبات نيل درجة الدكتوراه في علوم الفيزياء

من قبل

صفاء عبد صالح

ماجستير فيزياء – جامعة بغداد

المشرف

أ.م.د. ووداد حمدي جاسم

1437 هجري

2016 ميلاد

Abstract

Epoxy with various mix ratio of concentration 1, 2, 3, 4, 5, 7, 10, 15 and 20% of ZrO₂, MgO nanoparticles and ZrO₂, MgO microparticles were used to prepare epoxy microcomposites and epoxy nanocomposites in order to study the several mechanical properties (flexural strength, flexural modulus, fracture toughness, impact strength and hardness) and electrical properties (dielectrical constant, dissipation factor and thermal conductivity) and thermal properties (thermal conductivity and T_g).

The molding process was used to prepare epoxy and their nanocomposite and microcomposite samples using, ultrasonic homogenizer and shearing mixer. Three point bending examine, impact strength examine, hardness shore D examine, The LCR meter examine, Scanning Electron Microscope (SEM) examine and Differential Scanning Calorimeter (DSC) were used also.

The results where obtained to form 3- point bending examine illustrated that the mechanical properties of EP/ ZrO₂ nanocomposites were increased with increasing concentration of ZrO₂ nanoparticles. The ratio of about 2% vol. fraction lead to Maximum improvement in flexural strength was 52%. flexural modulus improvement was doubled at this ratio of vol. fraction, fracture toughness is improved about 86% at 2% vol. fraction, impact strength is improved about 51% at 2% vol. fraction, while hardness is improved about 5% at 2% vol. fraction comparing with results of epoxy sample. Ductile behavior appears in some stress-strain curves of obtained for EP/ ZrO₂ nanocomposites.

The mechanical properties of EP/ MgO nanocomposites were increased with increasing concentration of MgO nanoparticles at low volume fractions <(5%) of MgO nanoparticles. Flexural strength improved 47% at 4% vol. fraction. Flexural modulus is improvement about 74% at 4% vol. fraction, fracture toughness is rise about four times at 4% vol. fraction. impact strength is improved about 65% at 4% vol.

fraction, while hardness is improved about 3% at 4% vol. fraction . Ductile behavior almost appears in stress-strain curves of EP/ MgO nanocomposites. The mechanical properties for epoxy ZrO₂/ MgO microcomposites reduce with increasing concentration of ZrO₂/ MgO microparticles. this show nanoparticles overcome for others microparticles; thus addition quit small amounts .lead to particularly improvement in mechanical properties ,which can be explain through the pictures .

Scanning Electron Microscope (SEM) pictures show the topography of fractured structure of EP/ ZrO₂ nanocomposites and EP/ MgO nanocomposites with nanocracks of the epoxy structure at some of volume fractions of ZrO₂/ MgO nanoparticles, while the topography of fractured structure show the nanocracks almost vanish from the structure because of adding ZrO₂/ MgO nanoparticles was at minimum value at 2% vol. fraction of ZrO₂ nanoparticles and 4% vol. fraction of MgO nanoparticles . this enhance by experimental results which we got it in the small raito addition .their influence to improve mechanical properties of epoxy.

Dielectrical properties of EP/ ZrO₂ nanocomposites and EP/ MgO nanocomposites show; Dielectric constant improved at low volume fraction of ZrO₂/ MgO nanoparticles, while at higher concentration (> 10%) Dielectric constant of EP/ MgO nanocomposites stile increased and Dielectric constant begin to reduce in EP/ ZrO₂ nanocomposites. Tan delta of EP/ ZrO₂ nanocomposites little increase with increasing volume fraction ZrO₂ nanoparticles, while Tan delta of EP/ MgO nanocomposites begin to reduce with increasing volume fraction of MgO nanoparticles.

Thermal conductivity for EP/ ZrO₂ nanocomposites and EP/ MgO nanocomposites have the same behavior with 1, 2, 3, 4, 5, 7, 10, and 15% vol. fraction. thermal conductivity of both EP/ ZrO₂ nanocomposites and EP/ MgO nanocomposites increase with increasing the volume fraction. EP/ MgO nanocomposites and EP/ MgO nanocomposites have thermal conductivity lower than from EP/ MgO microcomposites and EP/ MgO microcomposites .

Symbols and Abbreviation

Symbols:

A	area(m ²)
E	modulus of elasticity (N/m ²)
E_c	composites modulus of elasticity
E_m	matrix modulus of elasticity
E_f	filler modulus of elasticity
ϵ	flexural strain
Q	heat flux.
k	thermal conductivity
T_1-T_2	difference in temperature
x	thickness of the sample
F	applied force
h	thickness
ΔL	elongation
L_o	original length
M	bending moment
M_m	moment of resistance
E	energy absorbed at fracture
m	mass of pendulum
g	gravitational acceleration
h	displacement
h'	maximum displacement
b	width of the samples
d	thickness of the samples

P load
 P polarization
 S slope of tangent of straight line of load-deflection curve
 T_g glass transition temperature
 V_m volume fraction of matrix
 V_f volume fraction of filler
 α total polarizability
 α_e electronic polarizability
 α_i ionic polarizability
 α_o orientational polarizability
 α_d space charge polarizability
 σ_f flexural stress

Abbreviations

DSC Differential Scanning Calorimeter
 EP Epoxy
 SEM Scanning Electron Microscope
 HSD hardness Shore D
 HRC hardness Rockwell
 HB hardness Brinell
 HV hardness Vickers
 LDPE low density polyethylene
 UV ultraviolet
 PH power of hydrogen
 DGEBA diglycidyl ether of bisphenol-A
 PMMA poly(methyl methacrylate)
 BDH British drug houses
 LCD inductance capacitance Resistance

Tables

Number	Title Table	Page
1-1	Repeated units of the more shared polymeric materials	3
3-1	Materials and some of their properties	46
3-2	Dimension standard of samples	51
4-1	Maximum stress, maximum strain, flexural strength, flexural modulus for EP/ZrO ₂ nanocomposites	63
4-2	Maximum stress, maximum strain, Flexural strength, of epoxy and EP/ ZrO ₂ microcomposites	70
4-3	Maximum stress (MPa), maximum strain (%), flexural strength, flexural modulus of EP/MgO nanocomposites	82
4-4	Maximum stress (MPa), maximum strain (%), flexural strength, of epoxy and EP/MgO microcomposites	88
4-5	Glass transition temperature (T _g) for epoxy, EP/ ZrO ₂ microcomposites	116
4-6	Glass transition temperature (T _g) for epoxy, EP/ MgO microcomposites	119

List of Contents

NO	Subject	Page No.
	List of Contents	
	CHAPTER ONE INTRODUCTION	
1-1	Introduction	1
1-2	Polymer	2
1-2-1	The Classification of Polymer	4
1-2.2-	Epoxy	6
1.3	Nanoparticles	7
1.3.1	Some Physical Properties	9
1.3.2	Zirconia (ZrO₂) Nanoparticles	9
1.3.3	Magnesia (MgO) Nanoparticles	10
4-1	Polymer Nanocomposites	11
1.4.1	The factors that effect on polymer nanocomposites 1 properties Epoxy Nanocomposites	12
5-1	Epoxy Nanocomposites	12
6-1	Rules of Mixtures for Composites	13
7-1	Reinforcement Theory	14
1.7.1	Particle–Particle Interactions	14
1.7.2	Particles – Polymer Interaction	15
1.8	- Literature Survey	16
1.9	Aim of the Work	21
	Chapter Two	
2.1	Mechanical Properties	22
2.1.1	Fracture -	22
2.1.1.1	Ductile Fracture-	23
2.1.1.2	Brittle Fracture	24
1.1.3-2	Polymer Fracture 1.1.3-2	25
1.1.4-2	Nanocomposites Fracture Toughness	28
1.2-2	Stress – Strain Behavior	29
1.3-2	Three Point Bending	30
2.1.4	impact strength 1.4-2	33
2.1.5	Hardness 1.5-2	34
2-2	Electric properties 2-2	35
2.2.1	Dielectric Constant	35
2.2.2	Electric Polarization 2.2-2	36
2.2.2.1	Electronic Polarization1	36

NO	Subject	Page No.
2.2.2.2	Atomic (ionic) Polarization	37
2.2.2.3	Orientational Polarization	37
- .2.2.2.4	Space Charge Polarization	37
2.3-2	Electric Polarization in Frequency Varying Electric Field	39
2.4.2	The Influence of Frequency on Dielectric Loss	41
2.5-2	Dielectric Properties of Nanocomposites	43
2.5.1-2	The Influence of Nanoparticles and Interaction Zones	44
3.3	Thermal properties	44
3.3.1	Thermal conductivity	44
3.3.1.1	Thermal conductivity of polymers	45
3	Chapter Three -	
3.1	Introduction	46
3.2	The Properties of Materials	46
3.3	Preparation Instruments	48
3.4	Samples Preparation Method	59
3.5	Mechanical ,Dielectrical and Thermal Tests Samples	52
3.5.1	Mechanical Tests Samples	52
3.5.2	Dielectrical and Thermal Tests Samples	53
3.6	Measurements Tests 6-3	54
3.6.1	Mechanical Tests 6.1-3	54
3.6.2	Bending test	55
3.6.3	hardness test	56
3.6.2	Dielectrical Tests	57
3.6.3	Thermal Tests	58
3.6.3.1	Thermal conductivity	58
3.6.3.2	Differential Scanning Calorimeter (DSC) Tests	59

	Scanning Electron Microscope (SEM	
4	Chapter Four -	
4.1	Introduction	61
4.2	The Mechanical Properties	61
4.2.1	The Mechanical Properties EP/ZrO₂ Nanocomposite	61
4.2.2	Mechanical properties of EP/ZrO₂ Microcomposites	.69
4.2.3	Scanning Electron Microscope (SEM) image of EP/ ZrO₂ Nanocomposites topography of Fractured	75
4.2.4	Mechanical Properties of EP/MgO Nanocomposites	81
2.2.5	Mechanical Properties of EP/MgO Microcomposites -	87
2.2.6	Scanning Electron Microscope (SEM) image of EP/ MgO Nanocomposite topography of Fractured	92
4.3	Electrical Properties	98
4.3.1	Dielectric constant of EP/ ZrO₂ Nanocomposites	98
4.3.2	Tan Delta of EP/ ZrO₂ Nanocomposites	100
4.3.3	Dielectric constant of EP/ ZrO₂ Microcomposites	102
4.3.4	Tan Delta of EP/ ZrO₂ Microcomposites	103
4.3.5	Dielectric constant of EP/ MgO Nanocomposites	104
4.3.6	Tan Delta of EP/ MgO Nanocomposites	106
4.3.7	Dielectric constant of EP/ MgO Microcomposites	108
4.3.8	Tan Delta of EP/ MgO Microcomposites	109
4.4	Thermal properties	110
4.4.1	Thermal conductivity	110
4.4.1.1	Thermal conductivity of EP/ ZrO₂ nanocomposites	110
4.4.1.2	Thermal conductivity of EP/ ZrO₂ microcomposites	112
4.4.1.3	Thermal conductivity of EP/ MgO nanocomposites	112
4.4.1.4	Thermal conductivity of EP/ MgO microcomposites	113
4.4.2	Differential Scanning Calorimeter (DSC) Spectra of EP/ ZrO₂Nano/Microcomposites	114
4.4.3	Differential Scanning Calorimeter (DSC) Spectra of EP/ MgO Nano/Microcomposites	117
4.5	Conclusions	119
4.6	Future work	121

CHAPTER ONE

POLYMER NANOCOMPOSITES:

PROPERTIES, PREPARATION AND
PERFORMANCE

1-1 Introduction

A polymer composite materials, based on a polymer matrix and inorganic nanoparticle fillers, have dragged great attention in recent years, due to improvements in different properties including thermal, electrical, optical and mechanical properties [1]. The polymer composite collect the advantages of the filler materials (e.g., rigidity, thermal stability) and the advantages of polymer (e.g., ductility, flexibility, dielectric, and processability). Moreover, where filler become nanosized the composites usually contain special properties of nano-fillers conduces to materials with enhanced properties [2]. Inorganic nano-scale fillers involve nanoparticles of metals (e.g., Cu, Au, Ag), metal oxides, nonmetal oxides (e.g., MgO, Al₂O₃, ZrO₂), semiconductors (e.g., PbS, CdS). The nanoparticle has one dimension in nanometer scale, polymer nanocomposites are delineative as follows: zero-dimensional nanocomposites denotes to isolated 0-D nanoparticles in polymer matrix; one-dimensional nanocomposites denotes to 1-D nanotubes in a polymer matrix; two-dimensional nanocomposites denotes to 2-D sheets exfoliated in a polymer matrix (e.g., polymer/layered silicate hybrids); and 3-D nanocomposites denotes to overlap polymer networks [3]. There are many important applications of polymer nanocomposites such as protective coatings, computer chip packaging (insulation), based on their great strength, good processability, high temperature stability, good chemical resistance. thermal stability and improvements in mechanical properties [4-6].

1-2 Polymer

Polymers are macromolecules built up by the linking together, under creation of chemical bonds, of large numbers for much smaller molecules . The small molecules that collect with each other to constitute polymer molecules are called monomers, and the reactions by which they collect are termed polymerizations. There possibly will be hundreds, thousands, tens of thousands, or more monomer molecules linked together in a polymer molecule [7].

Polymers can be classified into naturally occurring and prosthetic polymers. Among naturally occurring polymers are cellulose, proteins, starches, and latex. While prosthetic polymers are produced commercially on a large scale and have a large range of properties and uses.

The term monomer denotes to the small molecule from which a polymer is compound. [8,9].

Table (1-1) illustrated repeated units of the more shared polymeric materials

Table (1-1) Repeated units of the more shared polymeric materials [7-9].

<i>Chemical Name</i>	<i>Repeat Unit Structure</i>
Polyethylene (PE)	$\begin{array}{c} \text{H} \quad \text{H} \\ \quad \\ \text{---C---C---} \\ \quad \\ \text{H} \quad \text{H} \end{array}$
Poly(vinyl X) (PVC)	$\begin{array}{c} \text{H} \quad \text{H} \\ \quad \\ \text{---C---C---} \\ \quad \\ \text{H} \quad \text{X} \end{array}$
Polypropylene (PP)	$\begin{array}{c} \text{H} \quad \text{H} \\ \quad \\ \text{---C---C---} \\ \quad \\ \text{H} \quad \text{CH}_3 \end{array}$
Polystyrene (PS)	$\begin{array}{c} \text{H} \quad \text{H} \\ \quad \\ \text{---C---C---} \\ \quad \\ \text{H} \quad \text{C}_6\text{H}_5 \end{array}$
Polyoxymethylene	$\begin{array}{c} \text{H} \\ \\ \text{---C---O---} \\ \\ \text{H} \end{array}$
Polyoxymethylene	$\begin{array}{c} \text{H} \quad \text{H} \\ \quad \\ \text{---C---C---O---} \\ \quad \\ \text{H} \quad \text{H} \end{array}$
Epoxy group	$\begin{array}{c} \text{O} \\ / \quad \backslash \\ \text{CH}_2 \quad \cdot \text{CH} \end{array}$
Poly(methyl methacrylate) (PMMA)	$\begin{array}{c} \text{H} \quad \text{CH}_3 \\ \quad \\ \text{---C---C---} \\ \quad \\ \text{H} \quad \text{C} \\ \quad \quad \quad // \quad \backslash \\ \quad \quad \quad \text{O} \quad \text{O} \\ \quad \quad \quad \quad \\ \quad \quad \quad \quad \text{CH}_3 \end{array}$
Nylon-n,m	$\begin{array}{c} \text{O} \quad \quad \quad \text{O} \\ \quad \quad \quad \\ \text{---N---(CH}_2)_n\text{---N---C---(CH}_2)_{m-2}\text{---C---} \\ \quad \quad \quad \\ \text{H} \quad \quad \quad \text{H} \end{array}$

1-2-1 The classification of polymer

There are many probable classifications of polymers. According to [10].

a) The structure of polymer:

1- Linear polymers: Van der Waals bonding between chains as illustrated in figure (1-1 a). Examples: poly(vinyl chloride), polyethylene, Polystyrene and nylon.

2- Branched polymers: Chain packing efficiency is decrease compared to linear polymers - lesser density as illustrated in figure (1-1 b). For example, low density polyethylene (LDPE) contains short chain branches.

3- Cross-linked polymers: Chains are linked by covalent bonds As in figure (1-1 c).

4- Network polymers: Multifunctional monomers creating three or more active covalent bonds create three dimensional networks as shown in figure (1-1 d)

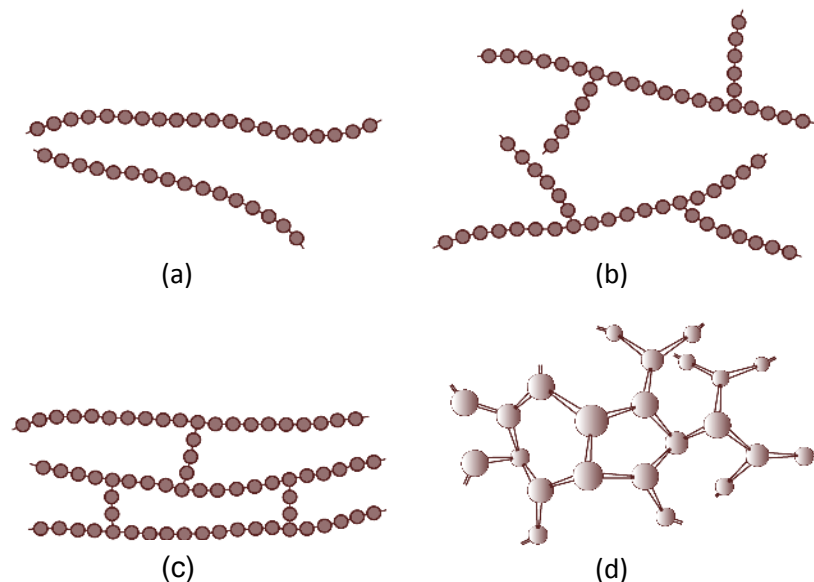


Fig. (1-1) Graph representations of (a) linear, (b) branched, (c) crosslinked, and (d) network (3-dimensional) molecular structures. Circles designate individual repeated units [10].

b) The behavior of polymers with increase temperature

[11, 12].

1- Thermoplastic polymers

Thermoplastic have linear one-dimensional polymers and have strong intermolecular covalent bonds and weak van Der Waals bonding between chains. At elevated temperature, it is easy to "melt" these bonds and have molecular chains readily slide past one another. These polymers are capable of flow at raised temperatures. They can be formatively into different forms and in general are dissolvable.

2- Thermosetting polymers

These are 3-dimensional amorphous polymers which are highly Cross-linked (strong, covalent bonds between chains) networks with no long-range order. Once the chemical reaction or polymerization is complete, the polymer becomes a hard, difficult fusion, insoluble material which cannot be softened, melted or molded devastatingly. A good example of a thermosetting plastic is a two part epoxy systems in which a resin and hardener (both in a viscous state) are mixed and within several minutes, the polymerization is complete resulting in a hard epoxy plastic.

3- Rubbers and Elastomers polymers

rubber material is one which can be stretched to at least twice its original length and rapidly contract to its original length. Rubber must be a high polymer (polymers with very long chains) as rubber elasticity,

"Natural rubber" is a thermoplastic, and in its normal form it becomes "soft" and sticky" on hot days (not a better property for an automobile tire). In fact, until discovered a curing reaction with sulfur in 1839, rubbers were not cross-linked and did not have unique mechanical properties, rubber-elastic properties.

1-2-2 Epoxy

Epoxy resin is one of important thermosets which is broadly used for plenty applications from microelectronics to spaceships in modern technology (encapsulating, packing for electronic circuits, thin film coating ,protective coatings etc.) because of its mechanical and electrical properties, easily processed and low cost. The epoxy resins have poor thermal, electrical and mechanical stability, so the various methods have been used to improve these properties. Because of its good adhesive properties, many modifiers can be simply doped to the resins . An epoxy resin is defined as a molecule with more than one epoxy group, which can be hardened into a plastic. The epoxy group as shown in fig (1-2), called the glycidyl group [10, 13].

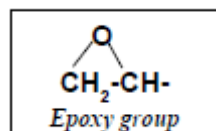


Fig (1-2) epoxy group

Epoxy resin is manufactured from simple basic chemicals that are easily available. as shown in fig (1-3)

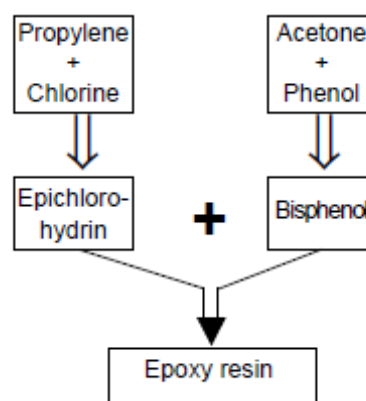


Figure (1-3).Epoxy resin manufacture

1-3 Nanoparticles

Nanoparticles are defined as solid particles with a size in the range of 1-100nm. There are some methods for synthesis nanoparticles like; Physical Vapor Deposition, the Sol-Gel manner, Chemical Vapor Deposition, Micelle and Inverse Micelle manner, Hydrothermal method, and Grinding with Iron Balls [14, 15]. The conversion from microparticles to nanoparticles yields considerable changes in physical properties. Every property has a specific length scale, and if a nano-scale item is made smaller than the critical length scale, the fundamental physics of that property change drastically [13] as shown in Fig. (1-4).

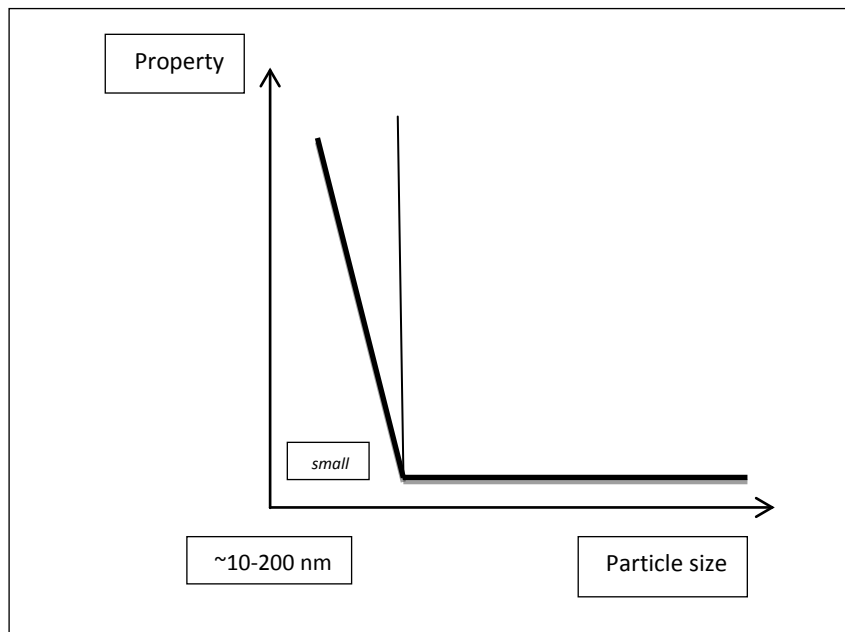


Fig. (1-4): Illustration of the change of a physical property as a function of particle size. [13]

Nanoscale materials have a large surface area for a given volume, in the case of particles, the surface area per unit volume is inversely

proportional with the particle diameter, thus, the smaller the diameter the greater the surface area per unit volume. Therefore, a change in particle diameter, from micrometer to nanometer range, the influence surface area-to-volume ratio by 3- orders of magnitude. Since many important physical and chemical interactions are ruled by surfaces and surface properties, a nanostructured material can have substantially different properties from a larger-dimensional material of the same composition, therefore the properties of nanoparticles are usually size dependent, and, when prepared in nanometer-size, materials exhibit unique properties. [1, 13]. Nanoparticles are generally described as primary or ultimate particles, aggregates and agglomerates as shown in fig (1-5). In some instance these particles types are easily distinguishable but in others there can be noticeable overlapping. The need is to distinguish between collections of particles that are weakly and strongly bonded together the term agglomerate for weakly bonded particle groups and aggregate for strongly bonded ones[16].

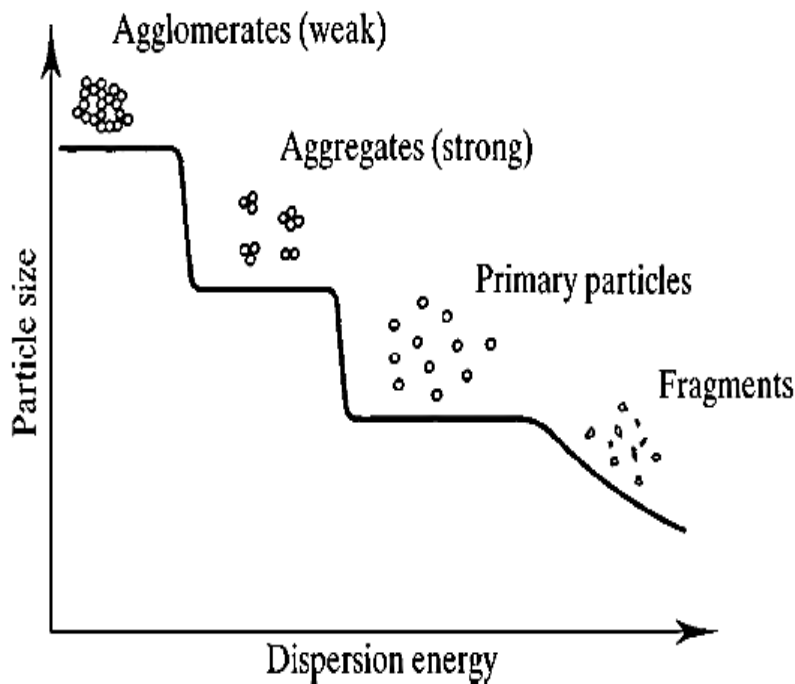


Fig. (1-5) Idealized view of the dispersion of filler particles [16].

1-3-1 Some Physical properties

Many physical attributes are depend size like [17, 18].

(a) improved sintering and hardness attributes, where the process of heat treatment of porous structures, which occur through the pressing of powders, resulting in a reduced of the porosity of the compressed material, so the successful sintering improving the hardness of materials.

(b) decrease brittleness and improved ductility and super plasticity, where the brittle materials can be ductilized by decrees their grain size and super the brittle materials can be ductilized by decrees their grain size .

(c) an increase in dielectric constant and electrical resistance can be observed.

(d) an effect on optical properties like TiO_2 were found to become most efficient UV absorbers

1-3-2 Zirconia (ZrO_2) Nanoparticles

Zirconium dioxide, which is also denoted to as zirconium oxide or zirconia, is an inorganic metal oxide that is largely used in ceramic materials[19]. Many different ways of producing (ZrO_2) nanosize powders , such as hydrothermal processing, sol-gel processing, and ion exchange manufacture methods[20]. pure ZrO_2 exhibits three crystalline forms. Pure zirconia is monoclinic (M) at room temperature. This phase is stable up to 1170 °C. It will transform into a tetragonal (T) phase under higher temperatures and later into a cubic phase (C) at 2370 °C as shown in fig (1-6) which illustrate (ZrO_2) nanoparticles in three main crystalline structure phases: (a) cubic; (b) tetragonal and (c) monoclinic [21].

Zirconia is used in different fields of chemistry such as ceramics and catalysis[22]. Nano-zirconia ceramics are of great attention for their obvious enhancement in strength and toughness. Its high hardness, low

reactivity, and high melting point (2715 °C) which change mechanical property, , thermal performance ,electrical performance and optical performance of ceramic components[23].

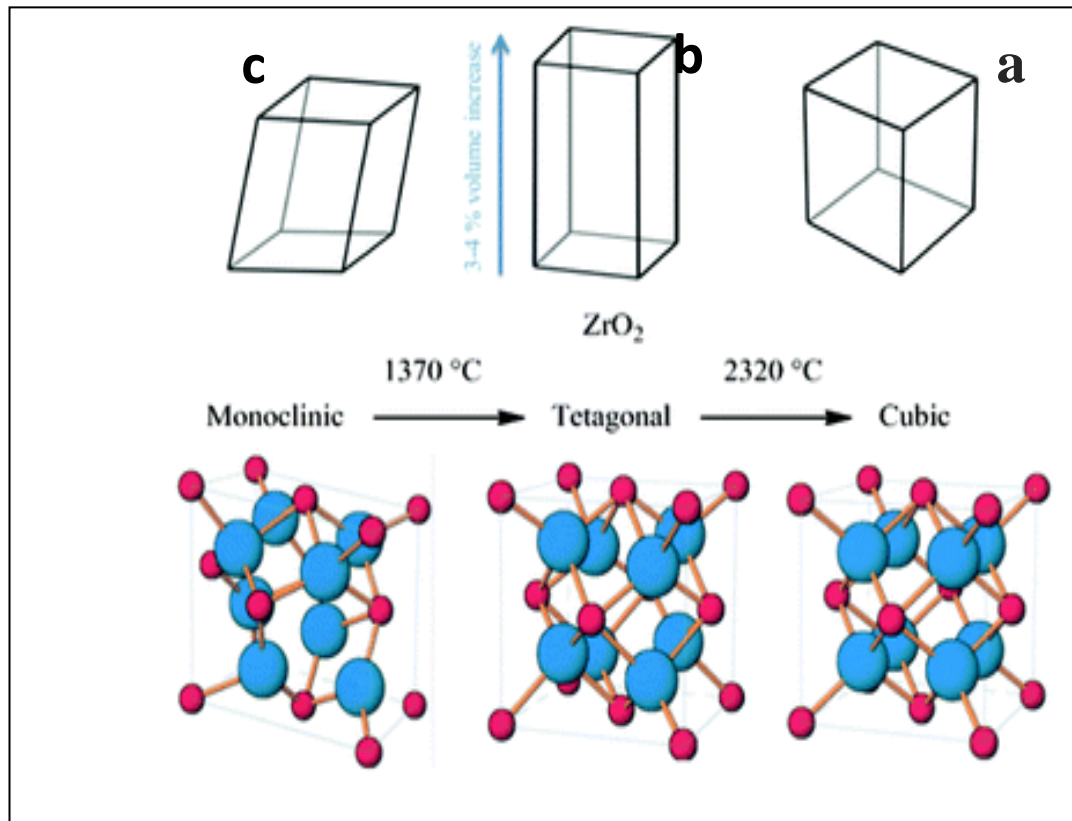


Fig.(1-6): Illustration of three polymorphs of ZrO₂; (a) cubic; (b) tetragonal and (c) monoclinic [21]

1-3.3 Magnesia (MgO) Nanoparticles

The magnesium oxide (MgO) is a very suitable material for insulation applications due to their low heat capacity and high melting point (2850 °C). MgO is obtained by thermal decomposition of different magnesium salts .The crystal structure of magnesium oxide is cubic, as shown in fig (1-7)[24].

MgO is used as dielectric layer due to its excellent properties such as high dielectric constant (~ 9.8), large band gap in the range of (7.3 eV -7.8 eV) and higher breakdown field. (12 MV/cm) compared to commonly used dielectric layer [25]. Magnesium oxide nanoparticles can be applied in electronics and coatings fields [26].

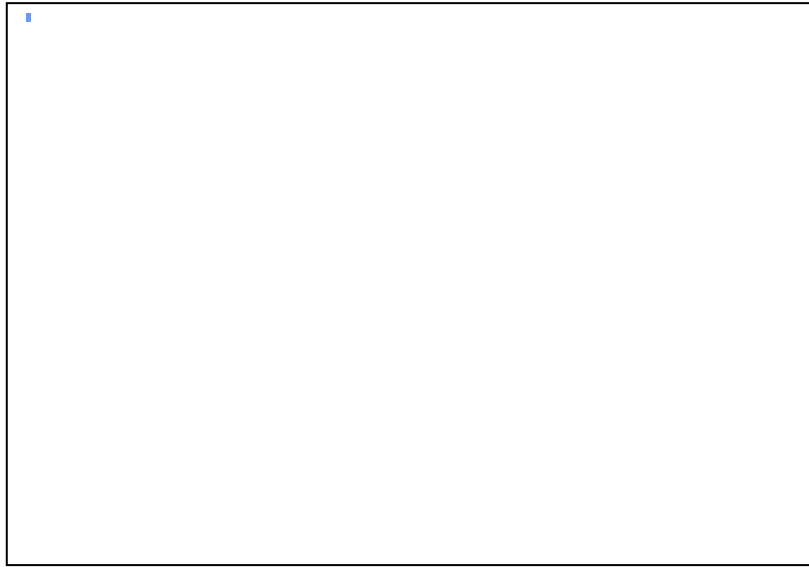


Fig. (1-7) Graphic shapes of MgO nanoparticles structures) [25]

1 -4 Polymer Nanocomposites

Polymer nanocomposites are defined as an interacting mixture of two phases, a polymer matrix and a solid phase which is in the nanometer size range in at least one dimension. Very significant feature for polymer nanocomposites is that the small size of the fillers leads to a dramatic increase in interfacial area creates significant volume fraction of interfacial polymer interaction with nano-fillers forming properties unlike from the bulk polymer until at low concentration of nanofillers[26]. In particle - polymer structure creation, two effects plays an significant roles in the reinforcement; particle -

polymer and particle-particle interactions, when particle – polymer interactions are generally the determining operator for the strength of the structure of polymers. Therefore polymer nanocomposites complete significant enhancements in mechanical, thermal ,electrical and optical properties at low filler concentrations, without increase in density [27-29].

1-4.1 The factors that affect on polymer nanocomposites properties

There are many operator that affect on the polymer nanocomposite properties [1, 8, 30].

- (a) Kinds of nanoparticles and their surface curing, distribution and dispersion of nanoparticles in the polymer matrix, size and shape.
- (b) The kinds of synthesis methods.
- (c) Polymer nanocomposite morphology.
- (d) Polymer matrix crystallinity, molecular weight, polymer chemistry and the kind of polymer; thermoplastic, thermosetting or elastomers.

1-5 Epoxy Nanocomposites

Epoxy nanocomposites is one of the most significant polymer nanocomposites because of the wide range of epoxy applications in industry, the epoxy resin have low density of epoxy about 1.05 - 1.3 g/cm², and good adhesive. Epoxides are amorphous structure and highly cross-linked polymers, the structure of cross-linked polymer also preform to an unwanted properties such as; poor resistance to crack initiation and growth. relatively brittle materials, One way to enhance these disadvantages can be complete by filling with nanoparticles when the special properties of nanoparticles leading to enhance the material properties [30]. Some advantages predictable from the reinforcement of nanoparticles are like improved some mechanical properties;

(fracture toughness, modulus of elasticity and impact strength, scratch and abrasion resistance) improved dielectric properties, improvement of heat distortion ,chemical resistance , weathering stability and durability [3,31].

1-6 Rules of mixtures for composites

The rule of mixtures equations predict that the elastic modulus of composites(E_c) depends on the volume fraction of the component phases for a two-phase composite.

$$E_c = E_m V_m + E_f V_f \quad \dots \dots (1 - 1)$$

Where E the modules of elasticity and V the volume fraction of the component phases and the subscripts c ,m and f represent the composite matrix and the fillers components respectively. The concentrations are expressed by volume fractions for, matrix V_m , and filler V_f , found from the volumes of individual components, ϕ_m for matrix, and ϕ_f for fillers,

$$V_m + V_f = 1 \quad \dots \dots \dots (1 - 2)$$

$$V_m = \frac{\phi_m}{\phi_m + \phi_f} = \frac{\phi_m}{\phi_c} \quad \dots \dots \dots (1 - 3)$$

$$V_f = \frac{\phi_f}{\phi_m + \phi_f} = \frac{\phi_f}{\phi_c} \quad \dots \dots (1 - 4)$$

$$\phi_f = \frac{W_f}{\rho_f}, \quad \phi_m = \frac{W_m}{\rho_m}$$

Where w and ρ are the mass and density of matrix and fillers for the prepared composite [32].

1-7 Reinforcement Theory

Nanostructures created through the introduction of discrete nanoscale fillers of different structural, physical and chemical properties into a continuous solid matrix (e.g., polymer) Such structural (nanocomposite) features, together with the unique properties of nanoparticles, lead to many new phenomena and promising applications [33]. Because of electrostatic particle–particle and polymer–particles interactions, two kinds of structures were usually creating in filled polymers, namely: (i) coagulated network, formed by particle–particle aggregation; and (ii) structural network, created by the absorbed polymer layers and the filler particles percentage, [18]. At low filler content, weak coagulated structures of particle aggregates are created through a bound polymer layer leading to a reinforcement of the matrix polymer. At sufficiently high filler content, the entire amount of polymer come from the bulk is absorbed at the inorganic interfaces, resulting in the creation of a structural network, which involves of a coagulated network of particles and absorbed polymer layer. The process of structure creation in filled polymers is commonly dominates by chemical modification of the filler [34].

1-7.1 Particle-Particle Interaction

A primary finically is the proper dispersion of the fillers. Without proper distribution and dispersion of the fillers, the high surface area is compromised and the aggregates can act as defects, which limit properties. Distribution of nano-filler describes the homogeneity throughout the sample, and the dispersion refer to the level of agglomeration.as shown in Figure (1-8) schematically shows good distribution but poor dispersion (a), poor

distribution and poor dispersion (b), poor distribution but good dispersion (c), and good distribution and good dispersion (d). [18].

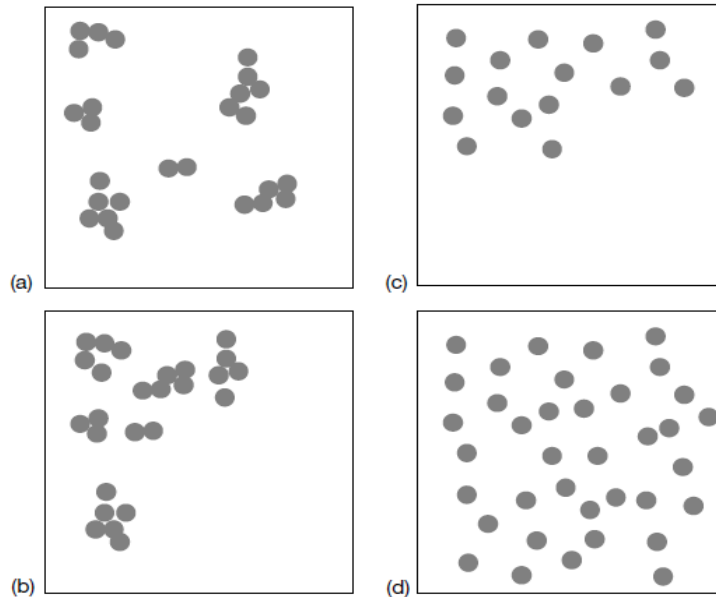


Fig. (1-8) A schematic showing the difference between dispersion and distribution, (a) good distribution with poor dispersion; (b) poor distribution and dispersion; (c) poor distribution with good dispersion and (d) good distribution and dispersion [35].

1-7.2 Particles – Polymer Interaction

The formation of three-D structure (a network) of nanoparticles in a polymer matrix is probable by two mechanisms; either by agglomeration or chain interlocked .where the stronger effects may be predictable when chains of macromolecules are tethered at the nanoparticles surfaces (physical interaction; Vander walls interaction, dipole interaction ,hydrogen interaction). In this state the mobility of the chains inside a few nanometers of the surface is decrease while leaving the bulk relatively unaffected, and this has been called a bond polymer layer. The surface may act to constrains chains because of adsorption, thus restricting the general chain mobility of the

molecules polymer both near to and far from the nanoparticles surface (happen due to the dipole attraction of some nanoparticles such as metal oxides). The other strongest effects may be predictable by directly bonded (chemical interaction) to the nanoparticles surfaces by active groups [36,37].

1-8 Literature Survey

In (2001) Siegel et al. , studied the EP/TiO₂ nanocomposites; they found an increase of 15% of the strain to failure filling an epoxy resin with 10% wt. percentage of TiO₂ nanoparticles. The performed on spherical nanoparticle titania filled epoxy had shown that the strength, modulus, strain-to-failure and scratch resistance could be increment simultaneously at a certain volume fraction of filler [38].

In(2004) Y.shan. studied the glass transition temperature and the micrograph of fractured surface of ZrO₂ filled in epoxy nanocomposite .The dispersion of particle in the matrix is clearly evident from the micrographs .The results showed that the incorporation of ZrO₂ in the epoxy matrix increases glass transition temperature. This may be due to the restricted chain mobility imparted by the nano sized particles [39].

Federica Bondioli (2006) studied the characterization of epoxy resins filled with submicron spherical zirconia particles .Zirconia particles were prepared by sol-gel method. Precipitation of zirconia nanoparticles .matrix properties by introducing ZrO₂ nanoparticles filler content, in the range of 1—5 vol. a systematic increase in elastic modulus was obtained by increasing the filler content [40]

In the same year Wazzan et al. , studied EP/TiO₂ nanocomposites using titanium dioxide (TiO₂) in changed weight fractions as a toughening agent for amine-cured epoxy resin. The composites were characterized by impact and

tensile testing, followed by scanning electron microscope of the fracture surfaces. The results showed that the nanoparticles TiO₂ toughening particles obviously improved the mechanical properties of the cured epoxy resin compared to the untoughened epoxy resin. The optimal properties were achieved at a TiO₂ concentration of 4% wt [41].

In (2007) Singha et.al., studied the dielectric properties of epoxy nanocomposites with (TiO₂) insulating nanoparticles at low concentrations filler by weight. The measurement of dielectric constant (relative permittivity) and tan delta was at range (400 Hz- 1MHz). At very low nanoparticle loadings, results demonstrate some interesting dielectric performances for nanocomposites and some of the electrical properties were found to be unique and advantageous for use in several existing and potential electrical systems [42].

Chatterjee et.al., (2008) studied the EP/TiO₂ nanocomposites and the matrix properties by introducing TiO₂ nanoparticles (5–40 nm, 0.5–2% wt. percentage) fillers into an epoxy resin .using Ultrasonic mixing process. The nanoparticles improves the thermal and mechanical properties of the epoxy resin. The nanocomposites show increase in storage modulus, glass transition temperature, tensile modulus, flexural modulus and short beam shear strength from neat epoxy [43]

Nelson et al. (2005) studied the incorporation of TiO₂ (38 nm) nanoparticles into thermosetting resin. Although the improvements in dielectric constant (relative permittivity (real part)) and tan delta are accompanied by the mitigation of internal charge in the materials, the nature of the interfacial region was shown to be pivotal in determining the dielectric behavior. In particular, it was shown that the conditions and enhanced area of the interface

changes the bonding that may give rise to an interaction zone, which affects the interfacial polarization through the formation of local conductivity. [44].

A. Dorigato (2010) studied the improving Epoxy Adhesives with Zirconia Nanoparticles . According to preliminary tensile mechanical tests on bulk nanocomposites samples, zirconia nanoparticles were selected for the preparation of adhesives with various filler contents. The glass transition temperature increased up to a filler content of 1 vol% and then decreased . Also tensile modulus, stress at break and fracture toughness of bulk adhesives samples were positively affected by the presence of an optimal amount of zirconia nanoparticles. [45]

In the same year Bum Jeong studied the Electrical insulation properties of Nanocomposites with MgO Filler. The results show that the gradient of the dielectric breakdown strength of specimens with added MgO is slow at both low and high temperatures [46].

Sung-Hoon Cho in(2011) studied the Electrical and Thermal Characteristics of Nano-Micro Epoxy Composite .which were produced by mixing several kinds of nanofillers such as MgO, CuO, C, Ag and ZnO with basic epoxy resin. The AC insulation breakdown test revealed breakdown strength values of approximately 17-31 kV/mm. Large improvements in breakdown strength at high temperature were composite materials filled with MgO, Ag, and ZnO .it was found that the thermal conductivity with addition of nanofillers tended to show similar or slightly lower values than the average value in most cases, compared with the thermal conductivity in a conventional molded transformer of approximately 0.8 W/m·K. Among the specimens. confirmed in the epoxy[47].

In the same year M. A. Sithique studied the effect of reinforcement (ZrO_2) nanoparticles on various properties such as mechanical, thermal and morphology of soy based epoxy matrix. It was the impact testing finds that the incorporation of soy epoxy in the DGEBA improved the impact strength [48].

Sudipta Halder (2012) studied the influence of ultrasonic dual mode mixing (UDMM) on morphology and mechanical properties of ZrO_2 -epoxy nanocomposite. It was shown that the a ZrO_2 -epoxy nanocomposite with the effect of the UDMM process on the dispersion characteristics of particles in ZrO_2 -epoxy nanocomposite and its improved mechanical properties has been compared with that of the mechanically mixed ZrO_2 -epoxy nanocomposite [49].

In the same year Wang studied the relative permittivity (real part) and tan delta of EP/ SiO_2 nanocomposites in a frequency range of (1 - 1 MHz). The permittivity for EP/ SiO_2 nanocomposites decreases at lower concentration (less than 1% wt.). When the nanoparticles content is above 1% wt. value, the permittivity of nanocomposites begins to increase with nanoparticles concentration. Such increase is believed to be due to the higher permittivity of inorganic nanoparticles [50].

K.S. Harishanand (2013) studied the mechanical properties of Epoxy composites filled with ZnO, ZrO_2 and CeO_2 with various content of 0-3 wt%. It was observed that the inclusion of metal oxide affected most of the mechanical properties of neat epoxy. Density, hardness, tensile, flexural, compression and impact strength of neat epoxy were found to increase with increasing of the metal oxide content up to certain wt%. Metal oxide filler

addition shows significant improvement in tensile and flexural properties only at certain Content (up to 1 wt %) [51].

In the same year Andrew A. Wereszczak studied the thermally conductive and electrical insulator of MgO-Filled Epoxy Molding Compounds. The addition of filler increased the elastic modulus over that of unfilled epoxy and MgO filler is better at increasing the elastic modulus than is SiO₂ [52].

ZHAO Xia1(2014) studied the corrosion resistance of modified nano- in ZrO₂/epoxy.It show that the dispersion effect of nano- ZrO₂ was improved epoxy coating. The adhesive strength of the epoxy coating decreased with the increaseing of nano- ZrO₂ content. The nano- ZrO₂ /epoxy coating containing 1% (mass fraction) nano- ZrO₂ exhibited a high electric resistance.[53]

Najiba Abdullah Al-Hamadan (2015) studied the dielectric properties of ZrO₂/PMMA Nanocomposites.It was shown that the dielectric constant, dissipation factor and dielectric loss of composites behaves nonlinearly as frequency increases over the range 50Hz -3 MHz, whereas above 3 MHz the values of dielectric constant remain constant[54].

In the same year Widad Hamdi used the brown chicken egg shells wast as a bio-CaCO₃ particles with different volume fraction (1-5%) to reinforced the epoxy .At 3% of loading the hardness ,thermal conductivity and electrical properties are a good improvement [55].

1-9 Aim of the work

The aim objective of this work is to study the physical property represented by mechanical , electrical and thermal behavior of epoxy reinforced by nanoparticle and microparticle such as ZrO_2 and MgO with different volume fraction 1, 2, 3, 4, 5, 7, 10, 15 and 20% of ZrO_2 , MgO nanoparticles and ZrO_2 , MgO microparticles respectively. In order to compare between some of their properties and determine the optimum values of fracture stress, flexural strength, flexural modulus ,dielectric properties and thermal properties. These information's of measurements could be beneficial in a variety of applications in aerospace, military aircraft, automotive, helicopters, and electronic devices by addition of low concentration of Zirconia (ZrO_2) nanoparticles and magnesia (MgO) nanoparticles.

CHAPTER TWO

MECHANICAL ,ELECTRICAL AND THERMAL
PROPERTIES

2-1 Mechanical Properties

The mechanical behavior of materials describes the response of materials to mechanical force or deformation. Important mechanical properties are flexural strength, flexural modulus, fracture toughness, hardness and impact strength [9, 56]. In general, the addition of inorganic fillers into a polymer produces an increment in stiffness, but losses toughness, whereas addition of rubber particles increases toughness, but decreases stiffness. The addition of nanoparticles into polymer matrix at low fillers concentrations has caused in remarkable combination of high toughness and stiffness [57].

2-1-1 Fracture

Fracture is the divided of a body into two or more pieces in response to an imposed stress that is static (i.e. constant or slowly change with time) and at temperatures that are low relative to the melting temperatures of material. The imposed stress may be compressive, tensile, flexural, shear, or torsion [58, 59] There are two kinds of fracture are probable: brittle and ductile classification built on the ability of material to experiment plastic deformation [60].

Fracture process includes two steps; crack creation and propagation in response to an applied stress. The creation of cracks may be capable to appear into a Structure by three methods. First they can presence in a material because of its composition, as second- particles phase de-bonds in composites, and third, they can be generated during the service life of a element similar fatigue cracks. Crack creation also strongly relies on the microstructure of a specific crystalline or amorphous solid, imposed loading, and environment. The microstructure plays a very significant role in a fracture process because of dislocation motion, , grain size, and kind of phases creation up the microstructure. All these microstructural features are

imperfections and can act as fracture nuclei under unfavorable conditions [9, 61].

2-1.1.1 Ductile Fracture

Ductile fracture is characterized by extensive plastic deformation in the vicinity of an advancing crack (Ductile fracture occurs well after the maximum load is reached and a neck has formed). Furthermore, the process proceeds relatively slowly as the crack (Such a crack is often said to be stable) length is extended. That is, it resists any further extension unless there is an increase in the applied stress. Figure (2-1) shows schematic representations for two characteristic macroscopic ductile fracture profiles [9]. The configuration shown in figure (2-1c) founded for extremely soft metals, such as pure gold and lead at room temperature, and other metals, polymers, and inorganic glasses at elevated temperatures. Figure (2-1b) is moderately ductile fracture after some necking [62].

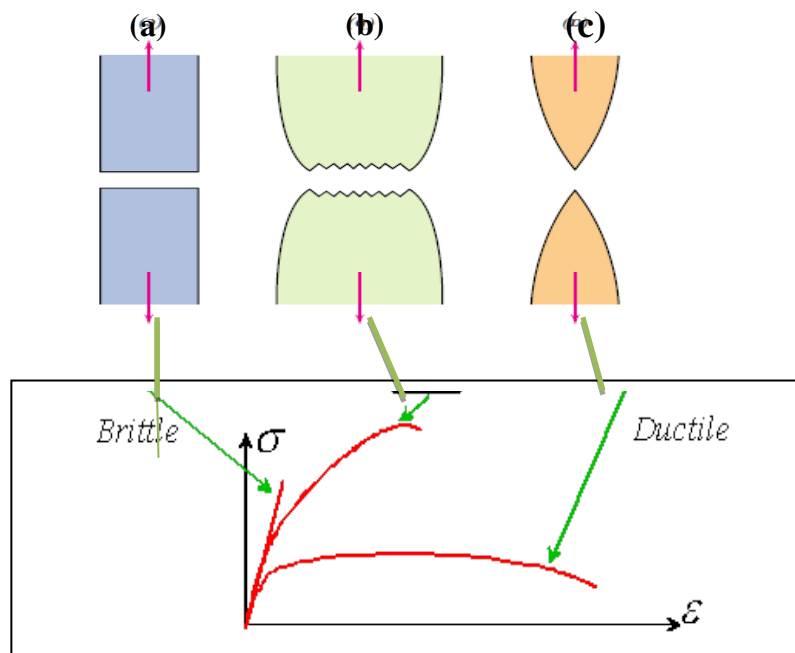


Fig. (2-1) (a) Brittle fracture none any plastic deformation (b) Moderately ductile fracture after several necking (c) Highly ductile fracture in which the sample necks down to a point [9].

Ductile fracture has two distinguished features, as the plastic deformation gives warning that fracture is imminent, allowing protective

measures to taken, second, extra strain energy is needed to induce ductile fracture in as much as ductile materials are normally tougher. Under the action of an imposed tensile stress, most metal alloys are ductile, whereas ceramics are especially brittle, and polymers may show both types of fracture [63].

2-1-1.2 Brittle Fracture

The word ‘brittle’ is related with a minimum of plastic deformation, i.e. with a brittle fracture the material fractures with very fast propagation of crack (propagates fast without Increase in imposed stress) with very little or no plastic deformation [64, 65]. For example, in some steel pieces, a series of V-shaped markings may form; near the center of the fracture cross section that point back toward the crack initiation site (Figure 2-2-a). Other brittle fracture surfaces contain lines or ridges that radiate from the origin of the crack in a fanlike pattern; (Figure 2-2-b). Often, both of these marking shapes will be sufficiently rough to be recognized with the naked eye. For very stiff and fine-grained metals, there will be no discernible fracture shape . Brittle fracture into amorphous materials, for example ceramic glasses, yields smooth surface and a relatively shiny [66]

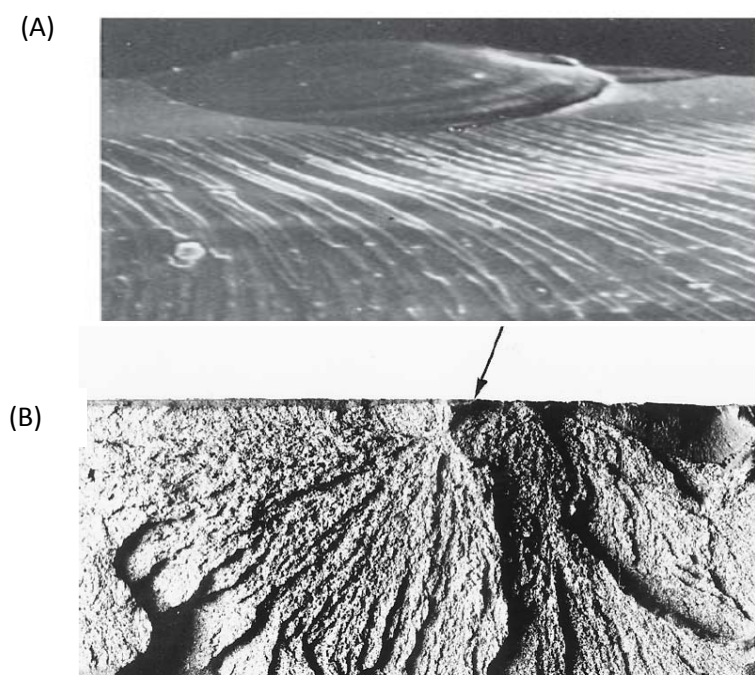


Fig. (2-2) Brittle fracture surface, (A) very smooth mirror region near the origin of the fracture, with tear lines involving the remainder of the surface [67]. (B) surfaces have lines or ridges that radiate from the origin of the crack into a fanlike pattern [9].

2-1.1.3 Polymer Fracture

large ranges of fracture modes are observed into polymers, depending on the underlying polymer structure and microstructure. Fracture in amorphous polymers tends to occur by craze creation due to the stretching of polymer micro-fibrils that give increase to gaps between polymer chains. These gaps are observed as microcracks or crazes when seen under a light microscope [59].

Three stages of cracking are typically observed as a crack advances through an amorphous polymer. The first stage, Stage A in figure (2-3), includes crazing through the middle plane. This results in the creation of a mirror zone by the growing of voids along the craze. The second stage, Stage B includes crack growing between the craze/matrix interfaces. This results in so-called mackerel patterns. Finally, the third stage, Stage C includes cracking through craze bundles. This enhancing the creation of hackle bands, as cracking happens through bundles of crazes. The resulting coarse fracture surface has a misty look, and parabolic (hyperbolic marks) voids are noticed on the fracture surfaces as in figure (2-3). These voids are somewhat similar to those observed on the fracture surfaces of ductile metals in the exist of shear [58, 68].



Figure (2-3) Shows diagram of stages of cracking into amorphous polymers. Region A: crack advance by void creation; region B: crack advance along alternate craze–matrix interfaces; region c: crack advance through craze bundle to form hackle bands [58].

The fracture surface look and mechanisms for composites depend on the fracture characteristics of the matrix and reinforcement materials and on the effectiveness of the bonding between the two[58]. The damage in composite

materials may happen by Interfacial/interphase cracking and de-bonding ,Particle pull-out or fibril cracking [58].

The creation of cracks may be a compound fracture process, which strongly depends on the microstructure of a specific crystalline or amorphous solid, imposed loading, and environment. The microstructure plays a very significant role in a fracture process because of dislocation motion, inclusions, precipitates, grain size, and kind of phases making up the microstructure. All these microstructural features are defect and can act as fracture nuclei under negative conditions. For instance, Brittle Fracture is a low-energy process (low energy dissipation). On the other hand, Ductile Fracture is a high-energy process in which a large amount of energy dissipation is related with a large plastic deformation before crack instability happens. Consequently, slow crack growth happens due to strain hardening at the crack tip area [69, 70].

Inorganic fillers particles were generally addition to polymer to improve the stiffness, if there is a strong interfacial strength also to rise the yield stress. In case of low or lost interfacial strength (adhesion), no-bonding and cavitation seems during loading. The micro-voids about the filler particles action as stress concentrators (like the elastomeric particles in rubber particle toughening) and can start local yielding processes. In dependence on particle distribution and particle size, several cases often seem as in figure (2-4):[71]

- a. The basic effect is no-bonding/cavitation and local stress concentration.
- b. Big particles create great voids with the disadvantage of void coalescence and construction of cracks of overcritical lengths.
- c. Agglomerates of small particles can break, constructing sharp cracks.

d. Small, homogeneously distributed particles start local yielding among the particles/micro-voids

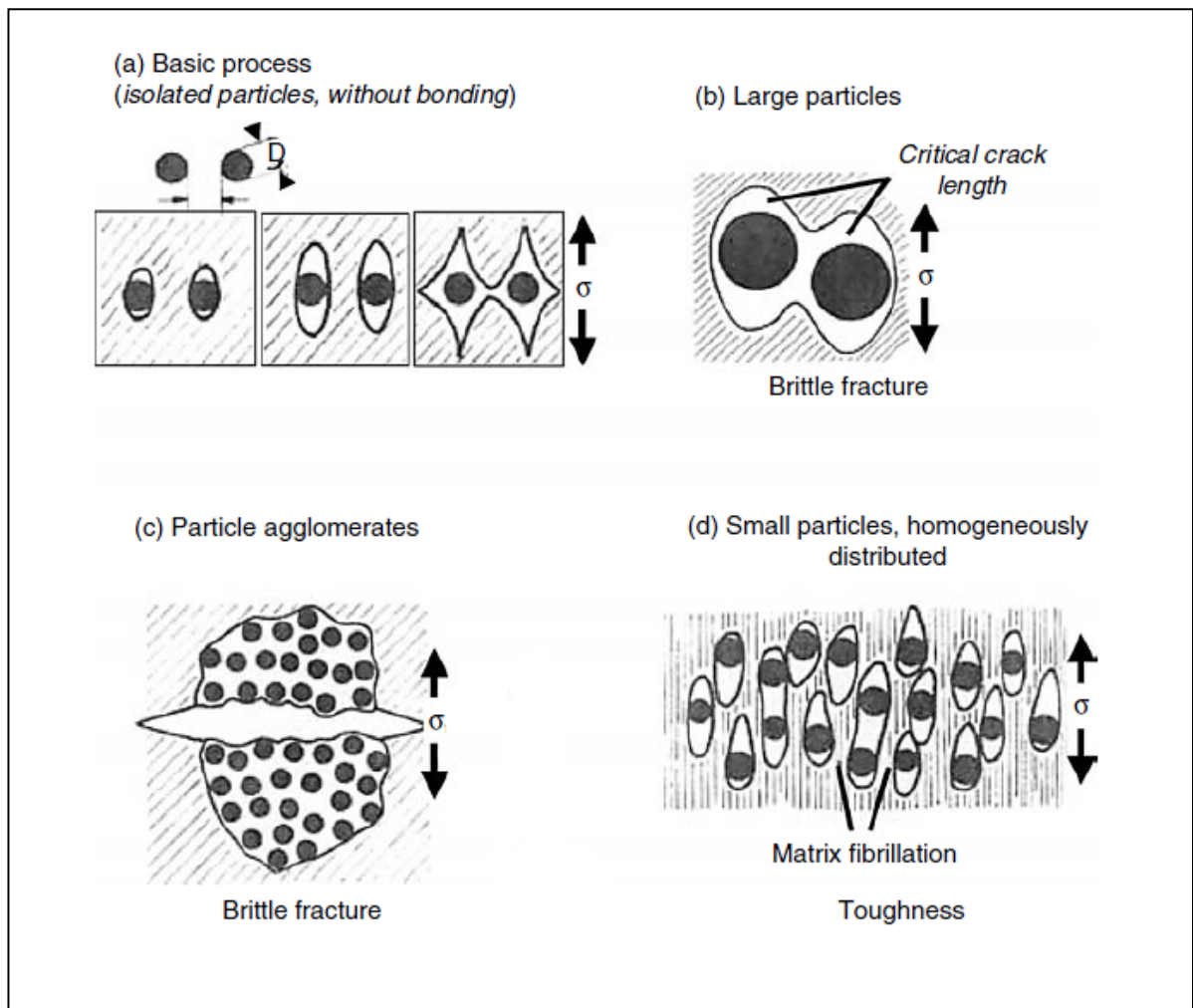


Fig. (2-4) Illustrations of particle-filled polymers and changed cases of local processes, depending on distribution and particle size [71].

2-1.1.4 Nanocomposites Fracture Toughness

Nanoparticles can overcome the infarct of traditional toughening kinds by simultaneously refining the toughness and strength of polymer (epoxy)

without losing thermal or mechanical properties. The main toughening mechanisms due to nanoparticles-toughened matrices are; plastic deformation ,crack pinning of the matrix, filler induced crazing, (crack interaction with microstructure) and interfacial non-bonding/void growth by the rigid nanoparticles [72]. . As a crack begins to propagate inside a composite material, the crack front meets particle fillers and bows out among the rigid particles as shown in figure (2-5), while still remaining pinned at all the locations where it has encountered the filler particles. The pinning process can create secondary cracks then combine after transient the particles. As the strain energy increases, local step fracture occurs and the pinning point released leaving a “tail-like” feature on the fracture surface. Energy is absorbed and dissipated through the cracks-pinning process, which leads to an increase in the fracture toughness of the material [73].

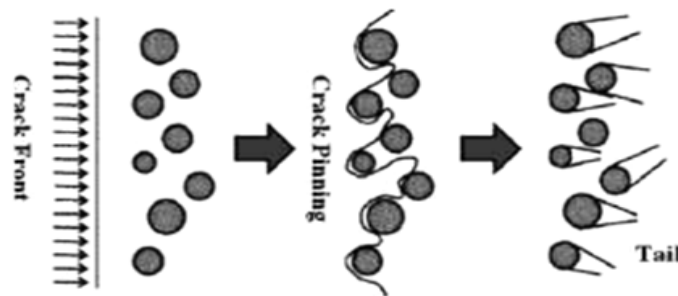


Fig. (2-5) Crack pinning for toughening of composite materials [73].

Crack deflection near or at particle/polymer interfaces is a source of energy dissipation through the crack propagation for particles filled polymer. As the crack front is approaching a polymer/particle interface, the crack can tilt and change direction when it encounters the rigid particles and passes about them. This process is showed in figure (2-6) such deflection reason a continuous change in the local stress state from mode I to mixed- mode. To propagate a crack below mixed mode conditions needs a higher driving force than in pure mode I, which consequences in a higher fracture toughness of the material [73].

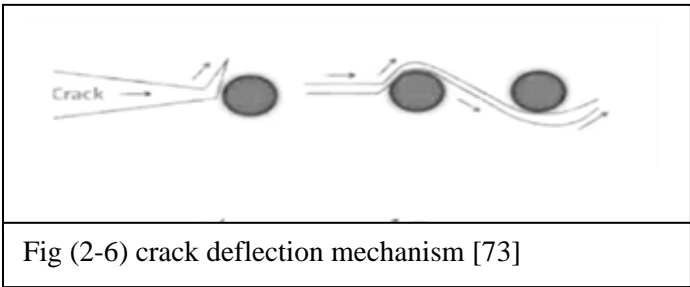


Fig (2-6) crack deflection mechanism [73]

2-1.2 Stress-Strain Behavior

The stress-strain performance is the degree to which a structure deforms or a strain depends on the value of an applied stress. For most metals that are stressed in tension at relatively low levels, stress and strain are proportional to each other through the relationship [57].

$$\sigma = E\epsilon \quad \dots \dots \dots (2 - 1)$$

This is called Hooke's law, when (E) the modulus of elasticity (Young's modulus), where strain (ϵ) and stress (σ) are given by

$$\sigma = \frac{F}{A} \quad \dots \dots \dots (2 - 2)$$

$$\epsilon = \frac{\Delta L}{L_o} \quad \dots \dots \dots (2 - 3)$$

Where; A is the area of a plane, F is the force, the elongation $\Delta L = L - L_o$ and L , L_o the instantaneous and original length. Deformation in which stress and strain are proportional is named elastic deformation; a plot of stress (ordinate) vs. strain (abscissa) results in a linear relationship, elastic deformation as illustrated in figure (2-7A). The slope of this linear share corresponds to the modulus of elasticity E . Elastic deformation is nonpermanent, which means that where the imposed load released, the piece returns to its cardinally shape [57, 58 and 81].

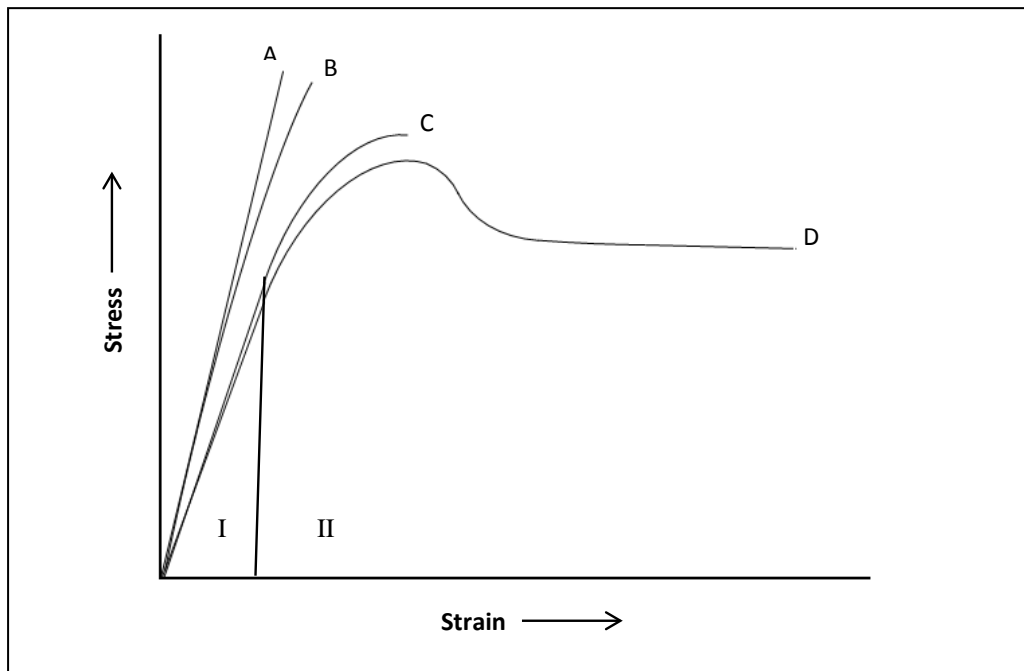


Fig. (2-7). Schematic stress–strain diagram, A- linear elastic deformation, B - nonlinear elastic behavior. C, D - plastic deformations, where region I is linear elastic deformation (brittle behavior) and region II is plastic deformation (ductile behavior) [57].

. There are some materials (e.g., many polymers) for which this elastic portion of the stress–strain curve is not linear as in figure (2-7B), hence, it is not possible to determine a modulus of elasticity as described above. For this nonlinear behavior, either tangent or secant modulus is normally used. As the material is deformed beyond this point (P) the proportional limit, the stress is no longer proportional to strain (Hooke’s law, equation 2.1, ceases to be valid), and permanent, non-recoverable, or plastic deformation occurs shown in figure 2-7C, D. The transition from elastic (region I – brittle behavior) to plastic (region II – ductile behavior) is a gradual one for most metals; some curvature results at the onset of plastic deformation, which increases more rapidly with increasing stress [58, 67].

2-1-3 Three-Point Bending

The three-point bending test showed schematically in figure (2-8), a flat rectangular sample is simply supported close to its ends and either centrally loaded in three-point bending [67].

The three points bending flexural test provides values for the modulus of elasticity (E_f), flexural stress (σ_f), flexural strain (ϵ_f), and the flexural stress-strain response of the material [75].

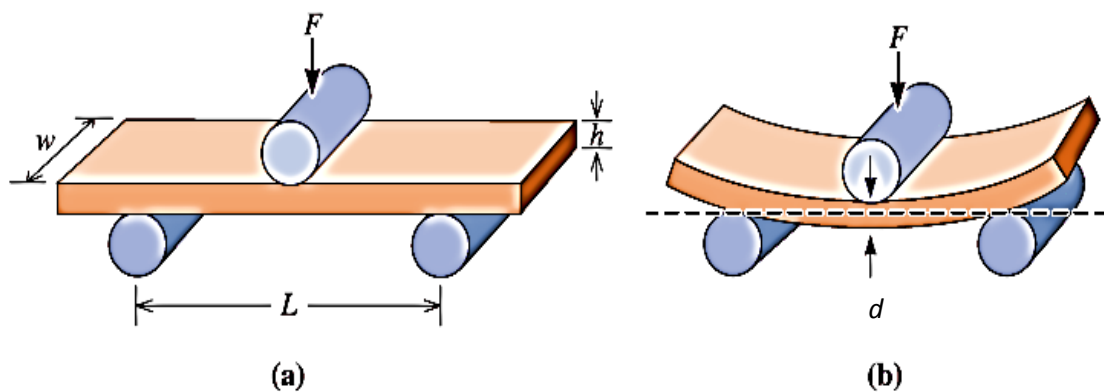


Fig. (2-8) (a) The three-point bend test (b) the deflection d obtained by bending [67].

The material properties supposed uniform through the thickness. Under these circumstances (force distribution, uniform material) the usual stress varies linearly from a maximum in compression on one surface to an equal maximum in tension on the other surface, When the imposed force at the sample midpoint cause in bending this constitutes a bending moment (M) close to sample ends while (M_m) is the moment of resistance figure (2-9) [9].

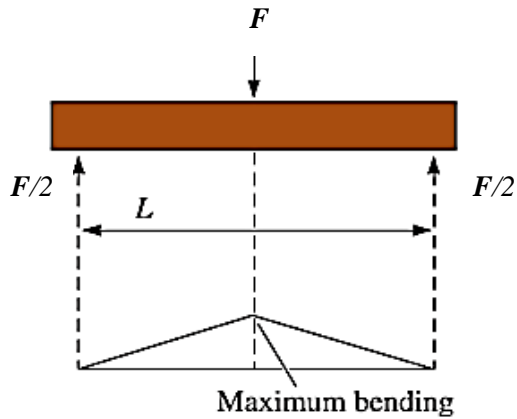


Fig. (2-9) Three-point bending test setup and force distribution [67].

Where:

$$M = \frac{FL}{4} \quad \dots \dots \dots (2 - 4)$$

$$M_m = \frac{hw^2}{6} \quad \dots \dots \dots (2 - 5)$$

For rectangular beam the flexural strength (σ_f), or modulus of rupture, describes the materials strength [67]:

$$\sigma_f = \frac{M}{M_m} \quad \dots \dots \dots (2 - 6)$$

$$\sigma_f = \frac{3FL}{2hw^2} \quad \dots \dots \dots (2 - 7)$$

The modulus of elasticity in bending, The Young modulus in bending or the flexural modulus calculated in the elastic region of figure (2-7):

$$E_f = \frac{L^3 S}{4hw^3} \dots \dots \dots (2 - 8)$$

Where (S) is the slope of the straight-line portion of force-deflection curve [9]. stress and strain are proportional to each other through the relationship

2-1.4 impact strength

Impact strength refers to ability of material to absorb the energy. The measurement of impact strength is most commonly made by the izod or charpy impact test as shown in figure(2-10)

The principle of both methods is to strike a small bar of polymer with a heavy pendulum swing. In the izod tests the bar is held vertically by gripping one end in a vice and the other free end is struck by the pendulum. In the charpy test the bar is supported at its ends in a horizontal plan and strike in the middle by the pendulum, and the impact bars are normally notched, the impact –strength test are carried out at very high strain rates. The weight end of the pendulum is raised to a fixed height (h) and is then released . The maximum displacement is noted down as h' the difference in height (h-h') The energy absorbed at fracture *E* can be obtained by simply calculating the difference in potential energy of the pendulum before and after the test such as,

$$E = m g (h-h ') \dots \dots \dots (2-9)$$

where *m* is the mass of pendulum and *g* is the gravitational acceleration. The geometry of 55mm long, standard Charpy test specimen is given in Figure(2-10) .If the dimensions of specimens are maintained as indicated in standards, notched-bar impact test results are affected by the lattice type of materials, testing temperature, thermo-mechanical history, chemical composition of materials, degree of strain hardening [76].

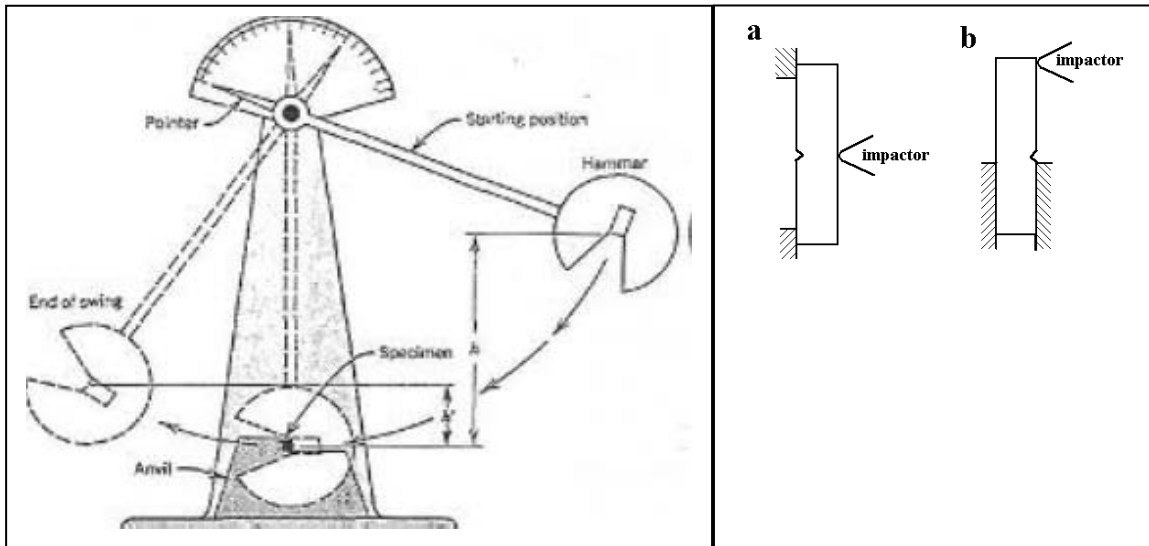


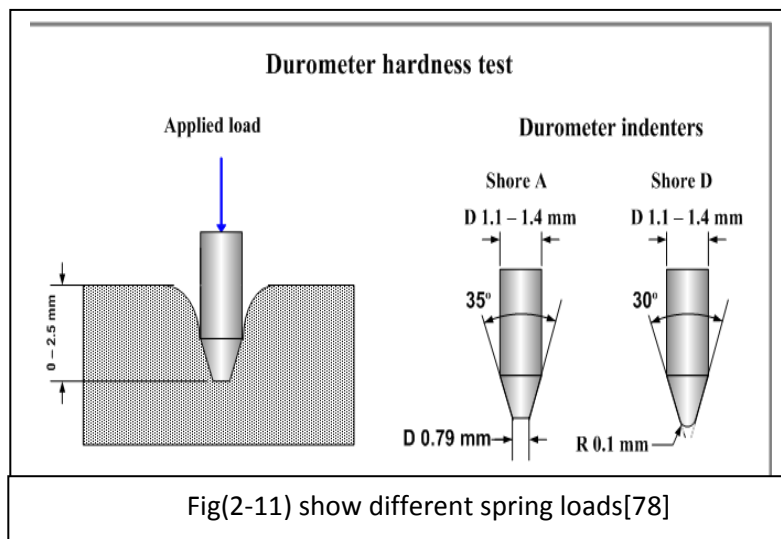
Figure (2-10): Apparatus for impact testing of materials ,Specimen and loading configuration for a) Charpy pendulum and b) Izod pendulum[77]

2-1-5 Hardness

Hardness is the property of a material that enables it to resist plastic deformation, usually by penetration. However, the term hardness may also refer to resistance to bending, scratching and abrasion. Quantitative hardness techniques is a small indenter is forced into the surface of the material . to be tested , under controlled conditions of load and rate of application .The depth or size of the resulting indentation is measured hardness test are performed more frequently . Rockwell (HRC), Brinell (HB), Vickers (HV) and Shore (HS).[76]

Shore hardness is a measure of the resistance of a material to penetration of a spring loaded needle-like indenter. Shore A scale is used for testing soft Elastomers (rubbers) and other soft polymers. Hardness of hard elastomers and most other polymer materials (Thermoplastics, Thermosets) is measured

by Shore D scale. Shore hardness is tested with an instrument called Durometer . Durometer utilizes an indenter loaded by a calibrated spring. The measured hardness is determined by the penetration depth of the indenter under the load. Two different indenter as shown in figure (2-11) and two different spring loads are used for two Shore scales (A and D). The loading forces of Shore A: 1.812 lb (822 g), Shore D: 10 lb (4536 g). [78]



2-2. Electric properties

2-2.1 Dielectric Constant

The dielectric constant relates to the permittivity of the material (symbol use here ϵ). The permittivity indicates the ability of a material to polarize in response to an imposed field. It is the ratio of the permittivity of the dielectric to the permittivity of a vacuum. Physically it means the greater the polarization developed by a material in an imposed field of given strength, the greater the dielectric constant will be [79]. Polymers and the atoms that create them up have their electrons tightly bound to the central long chain and side groups during 'covalent' bonding. Covalent bonding makes it much more difficult for most conventional polymers to support the movement of electrons and so they act as insulators[80].

2-2.2 Electric Polarization

When a dielectric material placed in static electric field (\mathbf{E}), electric charges do not flow through the material, but only slightly shift (creating electric dipoles) from their average equilibrium positions producing electric polarization (\mathbf{P}) also can be thought of as charge redistribution into a material affected by an external electric field. The electric moment obtained by an atom or a molecule under the effect of an electric field is proportional to the imposed field. The relation between polarization and the electric field is given by [81].

$$\mathbf{P} = \chi' \epsilon_0 \mathbf{E} \quad \dots \dots \dots (2 - 10)$$

$$\chi' = \epsilon' - 1 \quad \dots \dots \dots (2 - 11)$$

Where (χ') is the electrical susceptibility of material, vacuum and (ϵ') is the permittivity of the material, (ϵ_0) the permittivity of vacuum. There are four basic kinds of electric polarization: Electronic polarization, ionic or Atomic polarization, Dipolar polarization and space charge or Interface polarization. The total polarization of an arbitrary dielectric material is contributing of all kinds of polarization; as shown in fig(2-12) [82].

2-2.2.1 Electronic Polarization

The electric field causes deformation or translation of the originally symmetrical distribution of the electron clouds of atoms or molecules. This is basically the displacement of the outer electron clouds with respect to the internal positive atomic cores[83]. This effect is shared to all materials. This

polarization effect is small, despite the vast number of atoms within the material, since the moment arm of the dipoles is very short, which maybe comprises only a small fraction of an Angstrom[84].

2-2.2.2 Atomic or Ionic Polarization

The electric field reasons the ions or atoms of a polyatomic molecule to be displaced relative to each other. This is essentially the distortion of the normal lattice vibration, and this is why it is sometimes denoted to as vibrational polarization .Ionic displacement is common in ceramic material [83].

2-2.2.3 Orientational Polarization

Orientation (dipolar polarization) polarization this polarization occurs only in materials consisting of particles or molecules with a permanent dipole moment. The electric field reasons the reorientation of the dipoles toward the direction of the field [84].

2-2.2.4 Space Charge Polarization (Interface)

interfacial polarization or the space charge, , produce by the separation of movable positively and negatively charged particles under an imposed field, which form negative and positive space charges in the bulk of the material or at the interfaces between different materials. These space charges, in turn, modify the field distribution. This occurs mainly in polycrystalline solids or amorphous or in materials consisting of traps [83].

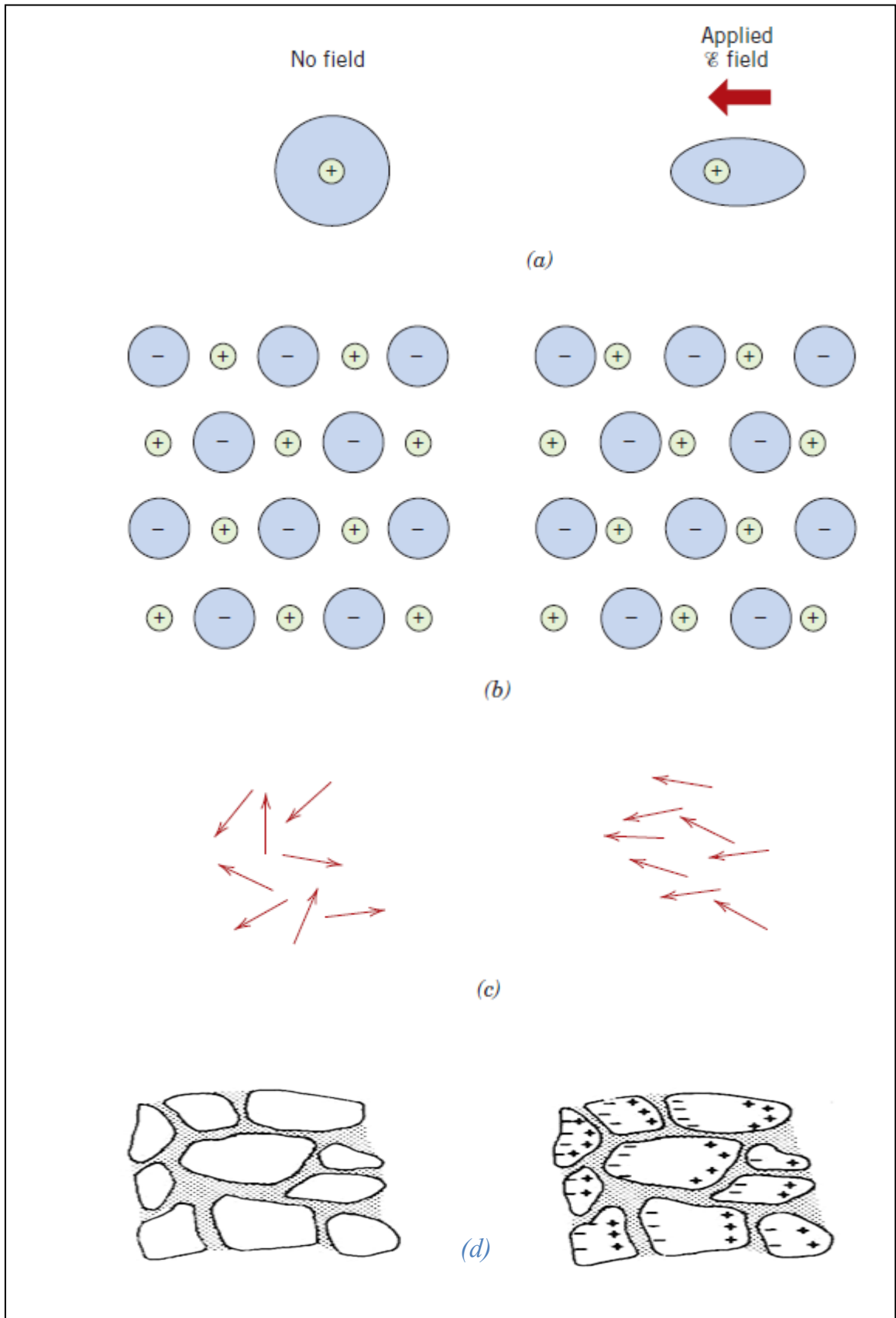


Figure (2-12) Basic kinds of electric polarization: (a) Electronic polarization, (b) Atomic or ionic polarization, (c) Dipolar polarization and (d) Interface or space charge polarization [85].

2-2.3 Electric Polarization in Frequency Changing Electric Fields

In the frequency-domain method, we mainly measure the dielectric constant at different frequencies of alternating excitation fields. In each kind of polarization needs time to perform; so the degree of the total polarization depends on the time difference of the electric field(frequency). The relation between the polarization \mathbf{P} and electric field \mathbf{E} is given by eq. (2-10) still holds, but the susceptibility χ is now a complex number [86],

$$\mathbf{P} = \chi \epsilon_0 \mathbf{E} \quad \dots (2 - 12)$$

$$\chi = \chi' - j\chi'' \quad \dots \dots (2 - 13)$$

Where χ' indicates its real part (given in eq. 2-11) and χ'' its imaginary parts, taking account of eq. (2.10 – 2.13) we find.

$$\chi'' = \epsilon'' \quad \dots \dots (2 - 14)$$

The dielectric constant ϵ_r (the relative permittivity of material) defined as the ratio of the static field strength of a vacuum to that in the material at the same distribution of charge. In m.k.s. system the dielectric constant (the permittivity of vacuum) ϵ_0 of free space is $8.854 \cdot 10^{-12}$ farad per meter, and also and may be defined as the measure of a material's ability to store electric charge equal to [87]:

$$\epsilon_r = \frac{\epsilon}{\epsilon_0} \quad \dots \dots (2 - 15)$$

Where ϵ is the permittivity of the material which will be greater in magnitude than ϵ_0 , and relative permittivity is greater than unity [88]. When a time-

varying electric field is applied the complex dielectric constant ϵ^* appear which is introduced to allow for dielectric losses due to the friction accompanying polarization and orientation of electric dipoles. This may be written as.

$$\epsilon^* = \epsilon - j\epsilon' = (\epsilon_r - i\epsilon_r')\epsilon_0 \quad \dots \dots (2 - 16)$$

Where ϵ_r called the dielectric constant (relative permittivity (real part)) and ϵ_r' called the loss factor. The dielectric constant depends strongly on the frequency of the alternating electric field or the rate of the change of the time-varying field .Dielectric constant ϵ_r , the loss factor ϵ_r' and tangent of loss angle ($\tan \delta$) calculated according to the following relations [88].

$$\epsilon_r = \frac{C d}{\epsilon_0 A} \quad \dots \dots (2 - 17)$$

$$\epsilon_r' = \frac{d}{2\pi f \epsilon_0 R A} = \frac{d}{w \epsilon_0 R A} \quad \dots \dots (2 - 18)$$

$$\tan \delta = \frac{\epsilon_r'}{\epsilon_r} \quad \dots \dots (2 - 19)$$

Where, d is a thickness of specimen, R is a Resistance of specimen, A is a Effective area. C is a Capacitance and ϵ_0 is a Permittivity of free space. Information about conduction mechanism of materials can found from a.c electric conductivity. A frequency dependence of (a.c) conductivity $\sigma_{A.C}(w)$ has been observed in many amorphous semiconductors and insulators both inorganic and polymeric materials, the empirical relation for the frequency dependence a.c conductivity is given by [89] .

$$\sigma_{A.C}(\omega) = A\omega^s \quad \dots \dots \dots (2-20)$$

Where, s is the exponential factor, it is usually less than or equal to one, and ω is the angular frequency ($\omega = 2\pi f$) which defines the frequency as

$$s = \frac{d[\ln(\sigma)]}{d[\ln(\omega)]} \quad \dots \dots \dots (2 - 21)$$

have the following relations with a.c electric conductivity according to the following relations; [88 and 90]:

$$\sigma = \frac{d}{R.A} \quad \dots \dots \dots (2 - 22)$$

$$\epsilon_r' = \frac{d}{\omega \epsilon_0 R A} = \frac{\sigma_{a.c}}{\omega \epsilon_0} \quad \dots \dots \dots (2 - 23)$$

$$\sigma_{a.c} = \omega \epsilon_0 \tan \delta \epsilon_r \quad \dots \dots \dots (2 - 24)$$

2-2.4 The Influence of Frequency on Dielectric Loss.

The difference of the dielectric constant with frequency is similar to the difference of polarizability and polarization. At low frequencies of the order of

a few Hz, the dielectric constant is made up of contributions from electronic, atomic and space charge polarization [91]. When measurements are carried out as a function of frequency, the space charge polarization ends after a certain frequency and the dielectric constant becomes frequency independent. The frequency beyond which the variation ends may fall in the certain range. The frequency-independent value is taken as the true static dielectric constant [92]. By measuring the dielectric constant as a function of frequency, one can discrete the different polarization components. Each polarization mechanism has a bounding properties frequency.

Electrons have very small mass and are therefore able to follow high frequency fields up during the optical range. Ions are a thousand times heavier but continue to follow fields up to the infrared range. Molecules—especially those in liquids and solids—are heavier yet and are severely constraining by their surroundings. Most rotational effects, like those in water, are bounded to microwave frequencies. Space charge effects are often in the kilohertz range or even lower Frequency has an significant effect on the polarization mechanisms of a dielectric. When the frequency of the imposed field is quite large as compared to the inverse of the relaxation time for a particular polarization process, the contribution of that process to the polarizability is negligible. As relaxation time is maximum for the space charge polarization, the space polarization vanishes first followed by dipolar, ionic, and electronic contributions. Figure (2-13) shows a typical frequency spectrum of a dielectric containing all four kinds of polarization [91, 88]

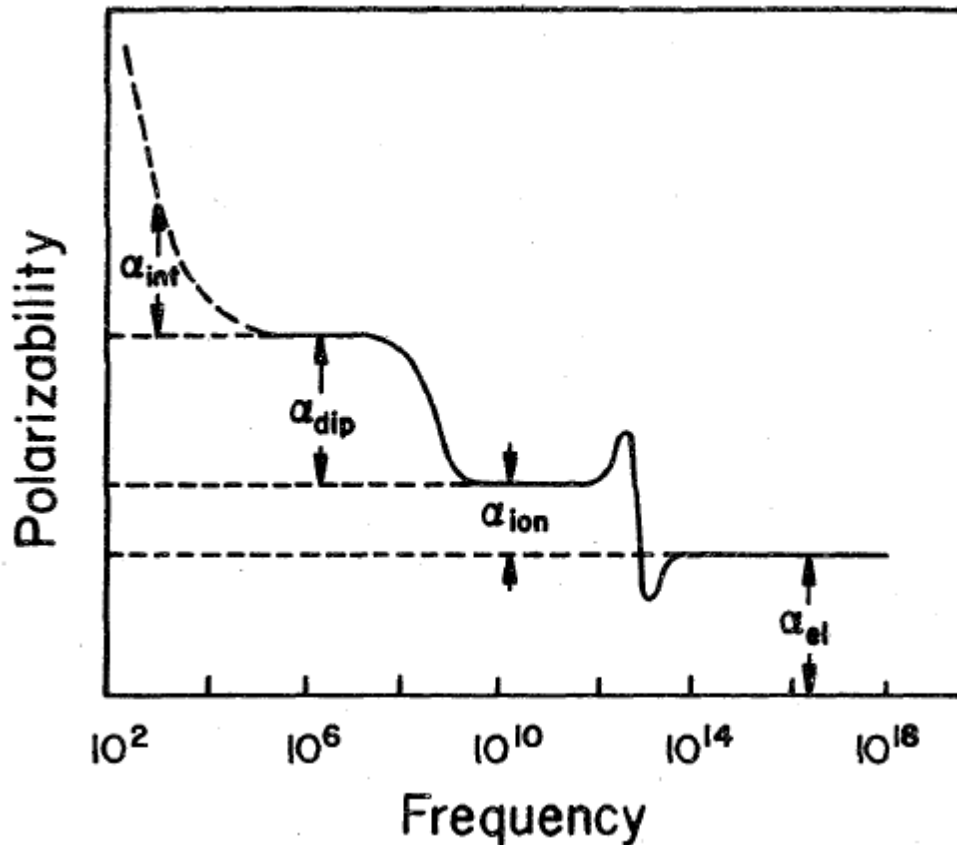


Figure (2-13): The frequency dependence of polarizability showing some contribution mechanisms [92].

2-2.5 Dielectric Properties of Nanocomposites

The polymer matrix composites classified as insulators. The electrical response for polymer matrix nanocomposites refers to their conductivity and dielectric performance. Since the primary electrical character of polymers is insulating, polymer composites seem to be dielectrics, (which can be polarized under the effect of an external electric field). Considering the character of the employed nanofiller or nano-inclusions, polymer nanocomposites categorizes in two major classified: first the insulating matrix-dielectric reinforcing phase and second the insulating matrix-conductive reinforcing phase. The nature of the nanofiller will defers in kinds, shape, and properties where it could be organic, inorganic, conductive, insulation, spherical, non-spherical [88].

2-2.5.1 The Influence of Nanoparticles and Interaction Zones

In considering the influence of the insertion of nanoparticles in an insulator there are two essential factors to take into account. First, the effect of nanoparticles happened on the physical and chemical structure of the material. Second, how the nanoparticles changed the electrical properties of the material surrounding it. The percolation effects characterized by increasing in electrical conductivity by several order of magnitude. This interaction zone may overlap giving rise to effects related with percolation through the interaction zone as shown in figure (2-14) [73,88].

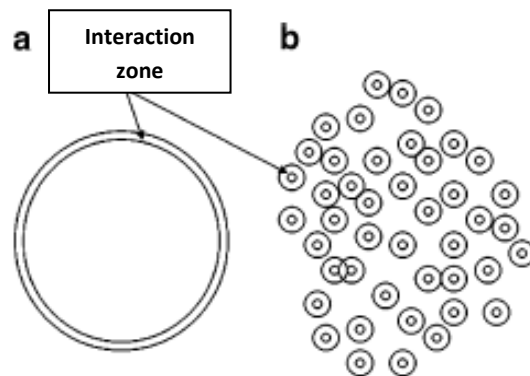


Fig. (2.14) Illustration of interaction zones for (a) a microparticles and (b) an assembly of nanoparticles [73].

2.3. Thermal properties

2-3.1 Thermal conductivity

The thermal conductivity is the property of a material that indicates its ability to conduct heat. This physical constant is defined as the amount of heat that passes during a unit cube of a material in a unit of time, when the variance in temperature between the opposite sides of the cube is 1K. along the direction of the heat flow. Both parameters are related by the equation(2 .25)

$$Q = -k A (T_1 - T_2) / x \quad \dots\dots\dots (2-25)$$

Where Q is the heat flux (W), K is the thermal conductivity (W/m-K), A is the cross sectional area (m²) T_1-T_2 is the difference in temperature (K), x is the thickness of the sample (m) [94].

2.3.1 Thermal conductivity of polymers

Polymer materials show a weak thermal conductivity. Thermal conductivities of insulating polymer materials are generally 1-3 orders lesser than those of ceramics and metals. Due to the chain-like structure of polymers, the heat capacity involves of the contribution of two mechanisms: (a) lattice vibrations and (b) characteristic vibrations, which originate from inner motions of the repeating unit. The lattice (skeleton) vibrations are acoustic vibrations, which give the main contribution to the thermal conductivity at low temperatures. The characteristic vibrations of the side groups of the polymer chains are optical vibrations, which become visible at temperatures above 100 K [95].

For polymers reinforced with different kinds of fillers this is even more important. Enhanced thermal conductivity in polymers may be achieved either by molecular orientation or by the addition of highly heat conductive fillers [96, 97].

There are many factors may affect the thermal conductivity of polymers: Temperature, pressure, density of the polymer, orientation of chain segments, crystal structure, the degree of crystallinity and many other. The thermal conductivity of filled polymers is primarily determined by the kind and amount of fillers used. The thermal properties of the filler, the size, shape, and orientation of filler particles or fibers in polymer matrix, and the percentage of fillers are all important factors that determine the thermal conductivity of reinforced polymers [98].

CHAPTER THREE

MATERIALS AND PREPARATION METHOD

3-1 Introduction

This chapter is studying the properties of the materials and the preparation process that was used to prepare the epoxy and nano/microcomposites which determined for mechanical ,dielectrical and thermal tests. measurement techniques and Instruments were described.

3-2 The Properties of Materials

The raw materials used to prepare the specimen are; Epoxy as a matrix (Nitofill, EPLV with Nitofill EPLV hardener from Fosroc Company). The mixing ratio for resin and hardener is 3:1 and gelling time 40 minute and mixed viscosity 1.0 Poise at 35 °C; The particle fillers are; Magnesia nanoparticles by (Nanoshel.com.USA) .; Magnesia microparticles by . (BDH Chemical Ltd Pool England); zirconia nanoparticles were purchased from(Sigma Aldrich Germany) and macro zirconia was Mallinckrodt produced by Cambridge lab .Table (3-1) shows some of raw the materials properties.

Table (3-1) Materials and some of their properties

Materials	Density g/cm ³	Particle Size	Surface area (m ² /g)	Purity %
Epoxy (EPLV)	1.04	-----	-----	-----
Nano- Magnesia (MgO)	0.18	100 (nm)	200±25	99.8
Micro- Magnesia (MgO)	1.1	0.1 (µm)	-----	99.99
Nano- Zirconia (ZrO ₂)	0.5	100 (nm)	210±10	99.99
Micro- Zirconia (ZrO ₂)	2.6	100 (µm)	-----	99.99

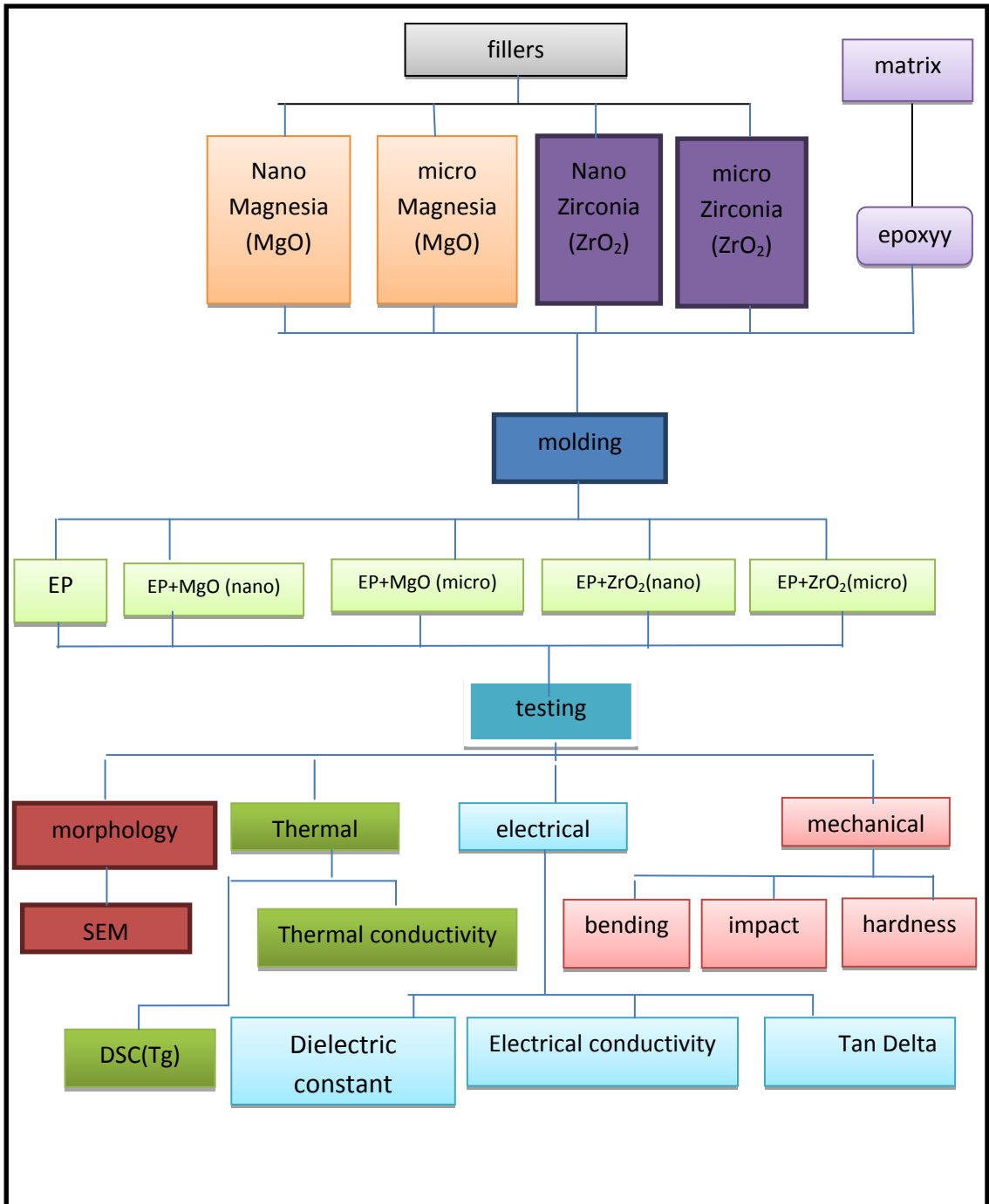


Figure (3-1)The step experimental work of the research

3-3 Preparation Instruments

The instruments were employed to prepare the specimens for both mechanical, electrical and thermal tests of nano/microcomposite. The following instruments were;

- i. Gloves box (handmade by researcher) in illustration (3-2) was used to get nitrogen atmosphere surround weight process and manually mixing process of epoxy resin and nanoparticles to avoid interaction of nanoparticles with unwanted impure particles from the environment.
- ii. Sartorius BL 210S ($d = 0.1\text{mg}$) balance was used to weigh the epoxy resin and fillers.
- iii. Shearing mixer with multi-revolution speed 0-2500 rpm used to get better distribution for fillers.
- iv. Homogenizer (50Watt, 23KHz, 110Volt) as shown in illustration (3-3) was used to get good dispersion for fillers in epoxy resin



illustration (3-2) Gloves box



Fig.(3-3) Homogenizer (50Watt, 23KHz, 110Volt)

3-4 Samples Preparation Method

The preparation trends of the neat epoxy, epoxy nanocomposites and epoxy microcomposites for mechanical , electrical and thermal tests were prepared by mixing process which involves of three steps.

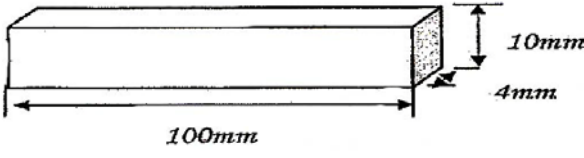
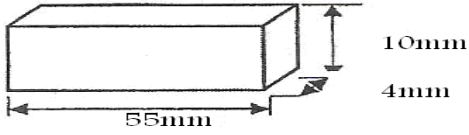
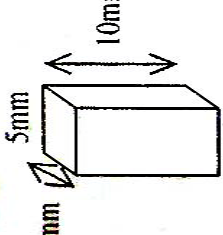
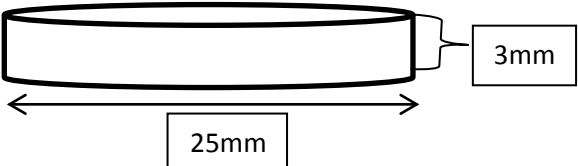
Neat epoxy preparation; firstly epoxy resin and hardener are weighted for suitable mixing ratio, and manually mixed then epoxy resin and hardener were mixed by shearing mixer at 800 rpm for 15 minutes to have good homogeneous between epoxy resin and hardener, secondly, for better homogeneous ultrasonic homogenizer used for 4 minutes. The third step was using vacuum system to remove the bubble before molding the epoxy.

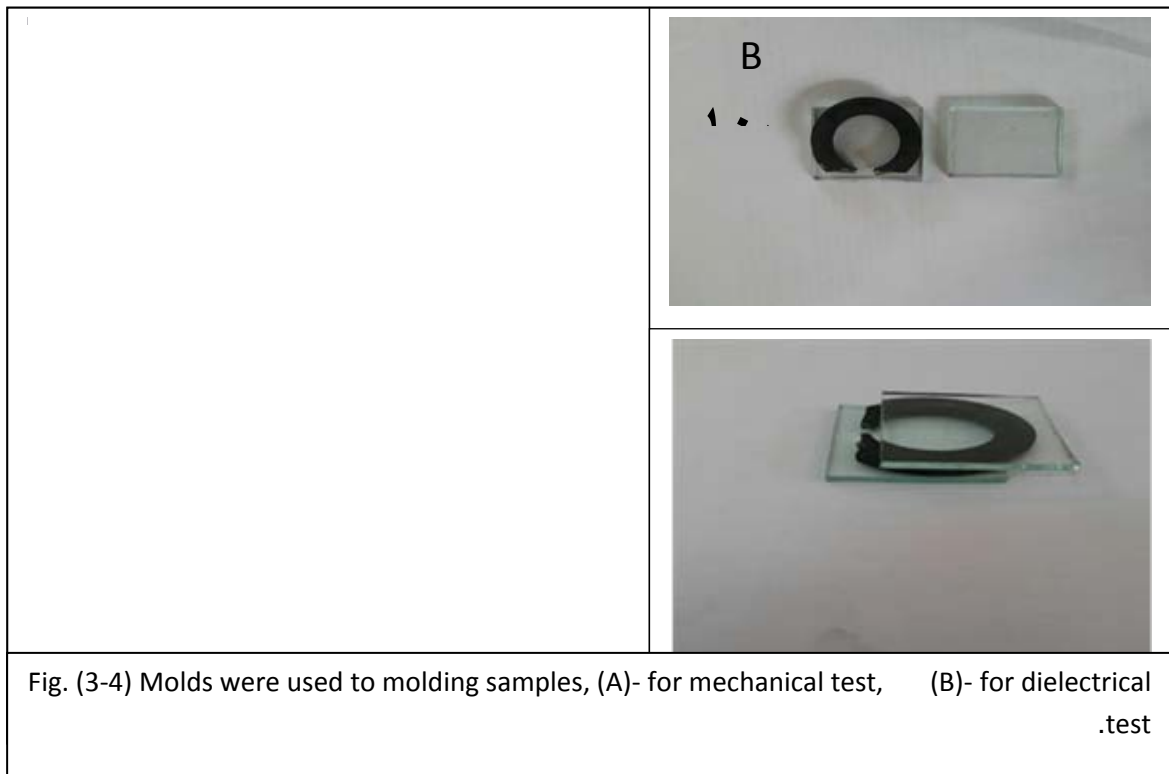
Epoxy nanocomposites preparation; firstly, the nanoparticles are weighted and manually mixed with epoxy resin under gloves box in nitrogen atmosphere to avoid interaction of nanoparticles with unwanted particles from the environment. Interaction with water vapor specially increase particles agglomeration and decrease any interaction (chemical or physical) of particles with polymer chain in the matrix. Nanoparticles with epoxy resin were mixed by shearing mixer at 800 rpm for 15 minutes to have good distribution and less agglomeration.

The second step involves using ultrasonic homogenizer for 4 minutes to get good dispersion. The hardener was mixed with nanoparticles/epoxy resin for 4 minute by ultrasonic homogenizer. Using ultrasonic may cause to decrease viscosity and increase epoxy resin temperature then sample container should be put in a cold water container to avoid high temperature which decrease time of gelling making the composite hard to mold,

The third step was using vacuum system (10^{-2} bar) to remove the bubble before molding the composites in earlier prepared mold as in figure (3-4). All the above steps were done for microcomposites to neutralize the effect of samples preparation that may affect the composites. The epoxy and their nano and micro composite were molded with a standard dimension to different tests. As shown in table (3-2) and fig (3-4).

Table (3-2) Dimention standard of samples

Type of test	Dimention standard of samples	standard Specification
Bending test	 <p>A 3D perspective drawing of a rectangular sample. The length is indicated by a horizontal double-headed arrow at the bottom, labeled '100mm'. The height is indicated by a vertical double-headed arrow on the right side, labeled '10mm'. The width is indicated by a diagonal double-headed arrow at the bottom right, labeled '4mm'.</p>	ASTM-D790
Impact test	 <p>A 3D perspective drawing of a rectangular sample. The length is indicated by a horizontal double-headed arrow at the bottom, labeled '55mm'. The height is indicated by a vertical double-headed arrow on the right side, labeled '10mm'. The width is indicated by a diagonal double-headed arrow at the bottom right, labeled '4mm'.</p>	ASTM-D256
Hardness test	 <p>A 3D perspective drawing of a rectangular sample. The length is indicated by a horizontal double-headed arrow at the top, labeled '10mm'. The height is indicated by a vertical double-headed arrow on the left side, labeled '5mm'. The width is indicated by a diagonal double-headed arrow at the bottom left, labeled '5mm'.</p>	ASTM D2240
Thermal and electrical test	 <p>A 3D perspective drawing of a circular sample. The diameter is indicated by a horizontal double-headed arrow at the bottom, labeled '25mm'. The thickness is indicated by a vertical double-headed arrow on the right side, labeled '3mm'.</p>	ASTM-D150



The samples were left for 48 hours before pulling out from molds and left in the vacuum chamber for 7 days before any test to get better curing conditions. The epoxy composites were prepared with nano/microparticles with volume fractions 0,1, 2, 3, 4, 5, 7, 10, 15 and 20%

3-5 Mechanical , electrical and thermal Tests Samples

3-5.1 Mechanical Tests Samples

The final samples shape prepared for mechanical test are identical to the specification of ASTM (D790) as in illustration (3-5).

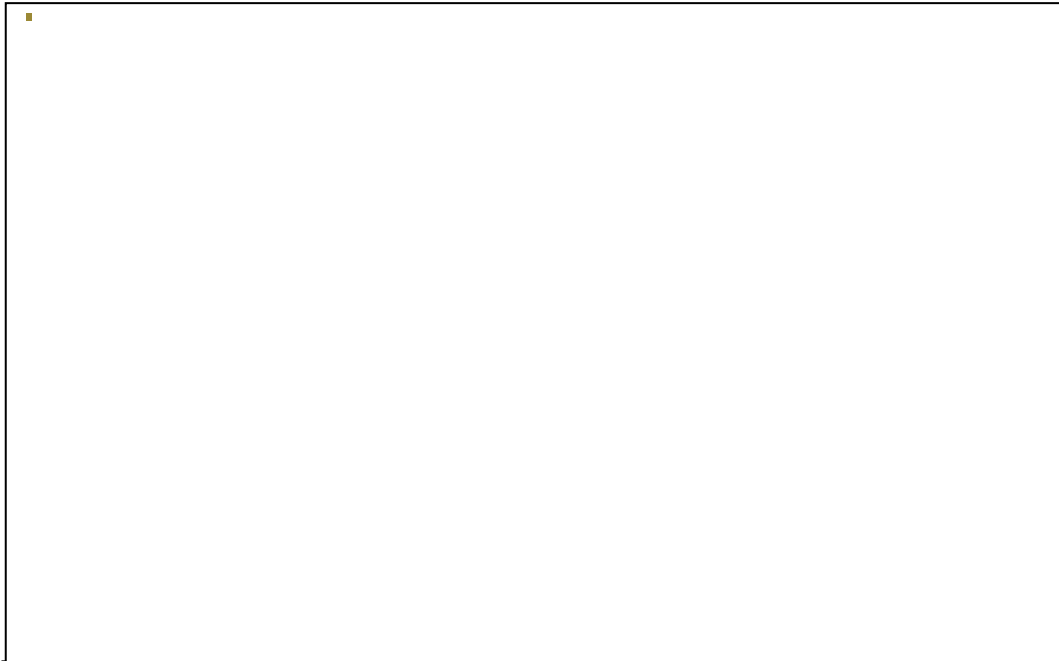


Fig. (3-5). Final epoxy and epoxy nano/microcomposite samples prepared for mechanical test.

3-5.2 Dielectrical and Thermal Tests Samples

The final samples shape prepared for dielectrical test identical to the specification of ASTM (D150) as in illustration (3-6)



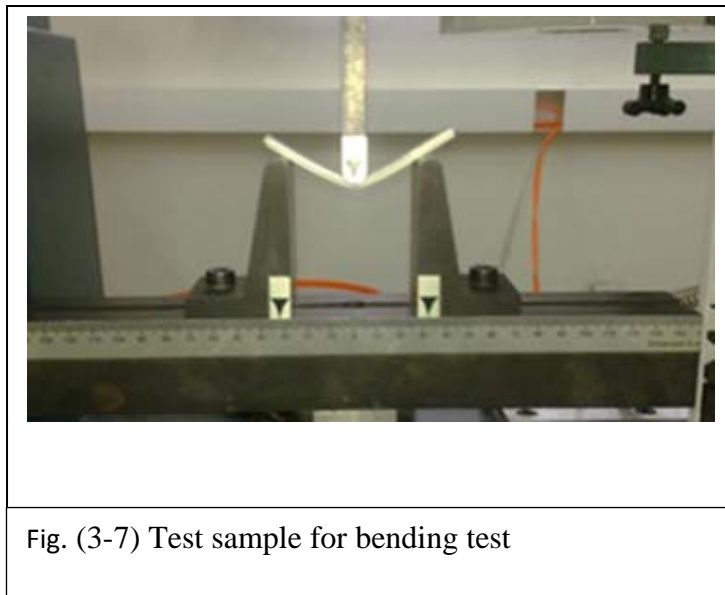
Fig. (3-6). Final epoxy and epoxy nano/microcomposite samples shape prepared for dielectrical test

3-6 Measurements Tests

3-6.1 Mechanical Tests

3-6.1.1 Bending test

Three point bending exam was carried out to exam epoxy and epoxy nano/microcomposites by using Instron 1122 with 10kN full scale load capacity. The force (load) was imposed on the middle of specimen supported by two spans as shown in illustration (3-7). The test was with cross head speed (2mm/min).



From force-deflection curves which was obtained from the testing machine, it can be possible to determine and calculate the flexural strength and flexural modulus by using the equations (2-7) and (2-8) respectively .

The toughness of the specimens was calculated by determining the area under the curve for specimen load-displacement curve [9].

3-6.1.2. Impact test

A Charpy impact testing was completed using pendulum kind of impact testing machine (Max. capacity 25J). Unnotched samples were fractured by impact energy. The impact exams were performed using a Charpy impact tester . The scale reading gave the impact energy absorbed to fracture the sample in joules when struck by a sudden blow as shown in illustration (3-8). The charpy impact strength of unnotched sample was calculated in KJ/mm² as given by the following equation:

$$\text{Impact strength} = \frac{E}{b.d} \times 10^3 \dots\dots\dots 3-3$$

Where: E: is the impact absorbed energy in joules. b: is the width in millimeters of the test samples. d: is the thickness in millimeters of the test samples.



Fig. (3-8) Apparatus for Impact test

3-6.1.3. hardness test

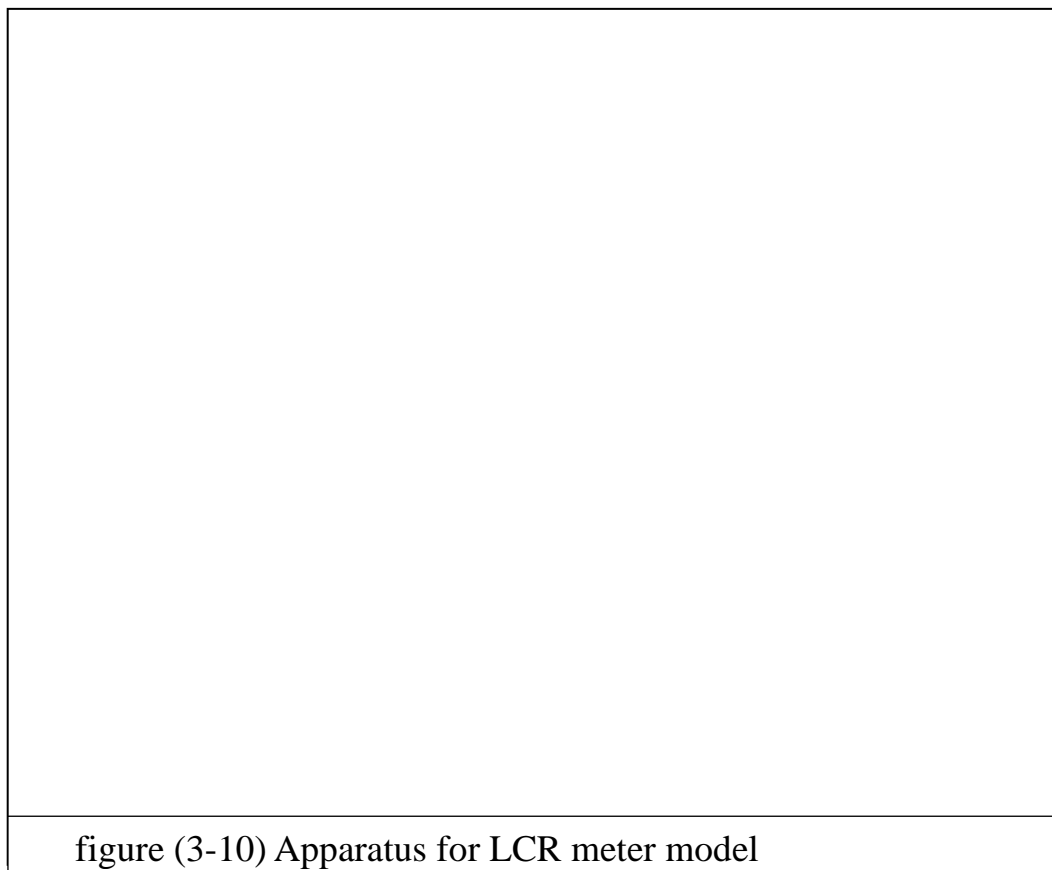
Shore D hardness was used to measure the surface hardness as shown in the figure (3-9), the indenter was attached to a digital scale that is graduated from 0 to 100 unit the usual method was to press down firmly and quickly on the indenter and recording the maximum reading as the shore D hardness measurements were taken directly from the digital scale reading Hand – operated durometer was used to measure the surface hardness (shore D) of epoxy pure and composites (epoxy with ZrO_2 and epoxy with MgO). Hardness results are average of four measurements taken from different parts of the sample.



Fig. (3-9) Apparatus for Hardness test

3-6.2 Dielectrical Tests

The dielectric properties of epoxy and epoxy nano/microcomposites are measured using LCR meter model (GW INTEK,LCR-8105G,Precision LCR-Meter, 20 Hz-5MHz,GPIB,RS-232, Taiwan) as shown in figure (3-10).The device range of frequency 20Hz – 5MHz, electrode diameter 1.25 cm. The dielectric properties (dielectric constant and tan delta) of the epoxy and epoxy nano/microcomposites are exam over the frequency range 2×10^3 - 5×10^6 Hz. The dielectric constant and tan delta are measured at room temperature, the imposed voltage was 500 mV. All the specimen were prepared and measured over a period of 40 days. The numbers of measurement points were 20 for each test for above frequency range. The dielectric constant (relative permittivity – real part)) ϵ_r , the loss factor ϵ_r' and tangent of loss angle ($\tan \delta$) calculated according to the relations (2-17),(2-18) and (2-19) respectively The a.c electrical conductivity $\sigma_{a.c}$ measure according to the following equation (2-22).



3-6.3 Thermal Tests

3-6.3.1 Thermal conductivity

The thermal conductivity of the different samples was measured by Lee's disc method. Lee's disc, Thermometers, steam generator, Screw Gauge and Vernier caliper were used for this method. The mean thickness of sample and the thickness of the disc were determined by Screw Gauge. The diameter of the disc was measured by using Vernier Caliper. The mass of the disc was found by spring balance. The thickness of the sample and Lee's disc were 3 mm. The radius of the disc was found as 5.52 cm. The mass of the disc was 0.79 kg. The given sample was placed between the disc and steam chamber. The two thermometers were inserted into the radial holes drilled on the side of the metallic discs. Steam was then passed through the steam chamber from a boiler until the steady state condition. The steady temperatures of the disc and steam chamber were recorded by the thermometers as shown in figure(3-11).



Fig. (3-11) Apparatus for thermal conductivity test

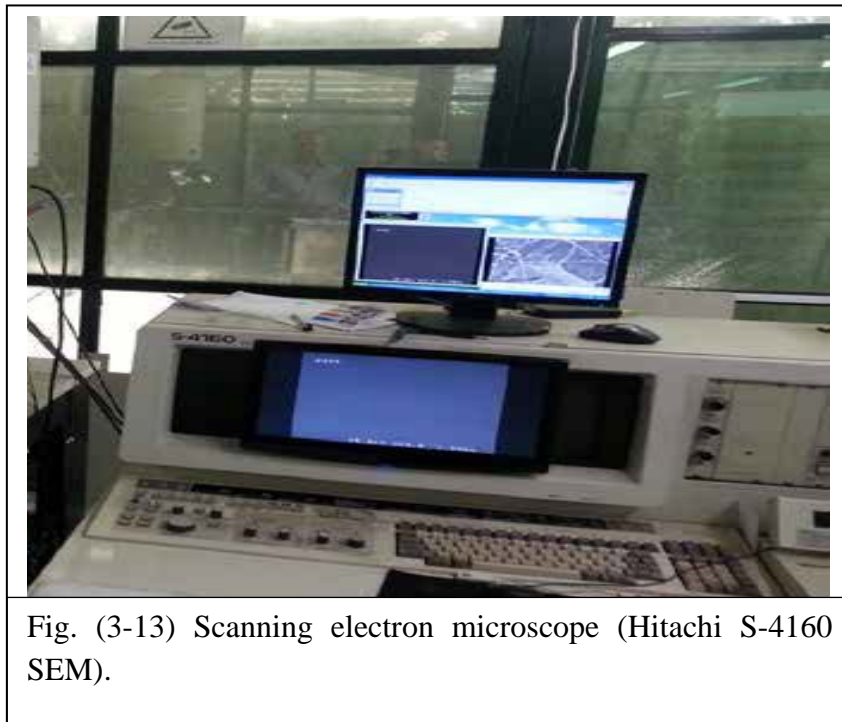
3-6.3.2 Differential Scanning Calorimeter (DSC) Tests

The measurements of DSC was completed on neat epoxy resin, micro/nanocomposites by using(STAPT-1000 linseis) by company-Germany, the glass transition temperature (T_g) of the samples were determined from the tangents of DSC spectra as a function of temperature. The weight of the sample was 10mg, and the experiments were performed at 5°C/minute rate for the rise of temperature with scanning up to 200 °C as shown in figure(3-12).



3-6.4 Scanning Electron Microscope (SEM)

Scanning Electron Microscope (SEM) technique used to image the topography of fracture structure (image range calibration of 1 μm), of zirconia and magnesia nanocomposites. The images were captured by using (Hitachi S-4160 SEM device by company-Germany) Figure (3-13), shows the device that was using in image capturing.



CHAPTER FOUR

RESULTS AND DISCUSSION:

MECHANICAL, ELECTRICAL AND THERMAL
PROPERTIES

4-1 Introduction

This chapter is studying the experimental results values of tested neat epoxy and epoxy with different ratio of volume fractions 1, 2, 3, 4, 5, 7, 10, 15 and 20% of MgO, ZrO₂ nanoparticle and microparticles MgO, ZrO₂ which are used to prepare epoxy magnesium nanocomposites (EP/MgO nanocomposites), epoxy zirconium nanocomposites (EP/ZrO₂ nanocomposites), Epoxy magnesium microcomposites (EP/MgO microcomposites) and epoxy zirconium microcomposites (EP/ZrO₂ microcomposites), in order to test and study several of their mechanical properties like flexural strength, flexural modulus, fracture toughness which are determined by using stress –strain curve (in bending test), hardness and impact are also determined using the hardness shore D and impact test respectively.

To explain the mechanical behaviour of the epoxy / composites. The Scanning Electron Microscope (SEM) are used for imaging fractured structure. The electrical properties like the dielectric constant and tan delta are studied for different specimens obtained from dielectric constant measurement. The thermal properties are determined for epoxy /composites using Lee disc to measuring the thermal conductivity and Differential Scanning Calorimeter (DSC) test to determine glass transition temperature T_g. Three specimens tested (minimum) for each preparation condition, the average of best two values were calculated.

4-2 The Mechanical Properties

4-2-1 The Mechanical Properties EP/ZrO₂ Nanocomposite

From load-deflection or stress-strain curves in flexural test we can get the flexural strength, flexural modulus and fracture toughness for neat epoxy and EP/ZrO₂ composite. The figure (4-1) shows stress-strain curves for the epoxy which agreed with material data sheet provided by manufactured Company .and for EP/ZrO₂ with different volume fractions of addition from (1-20%).

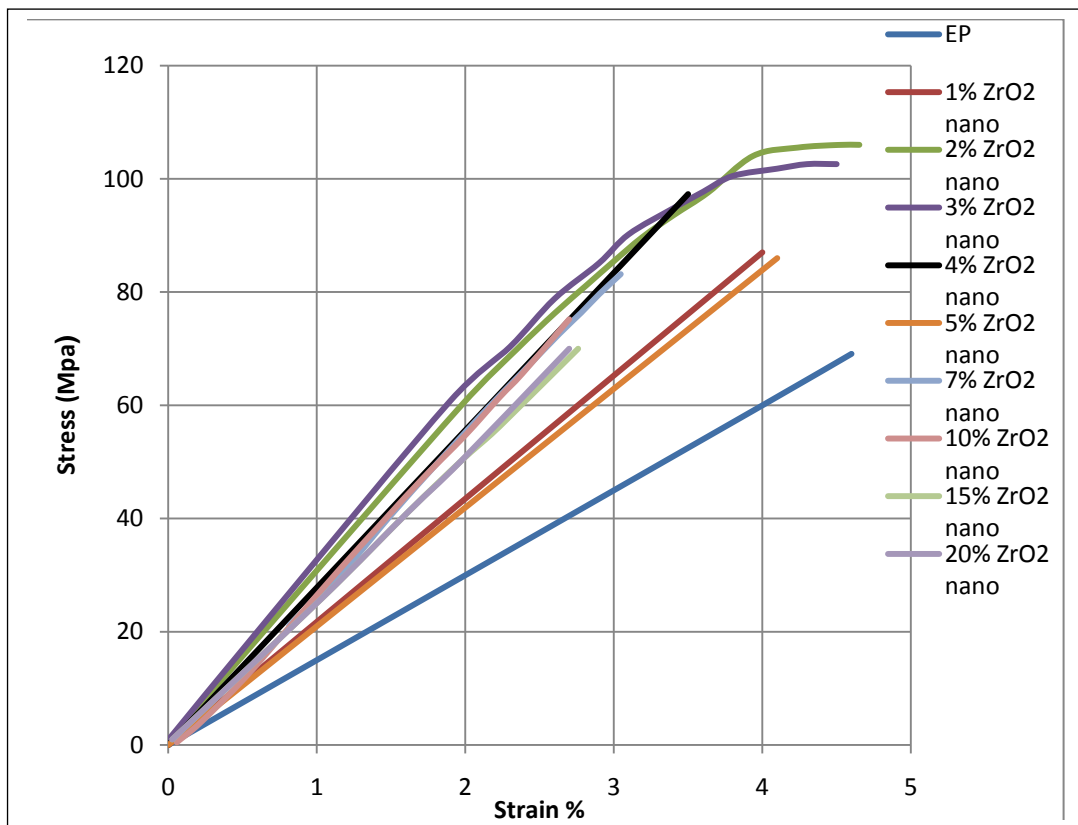


Fig. (4-1) Stress-strain curves of epoxy and EP/ZrO₂ nanocomposites with 0,1, 2, 3,4,5, 7 ,10,15 and 20 % vol. fraction of ZrO₂ nanoparticles

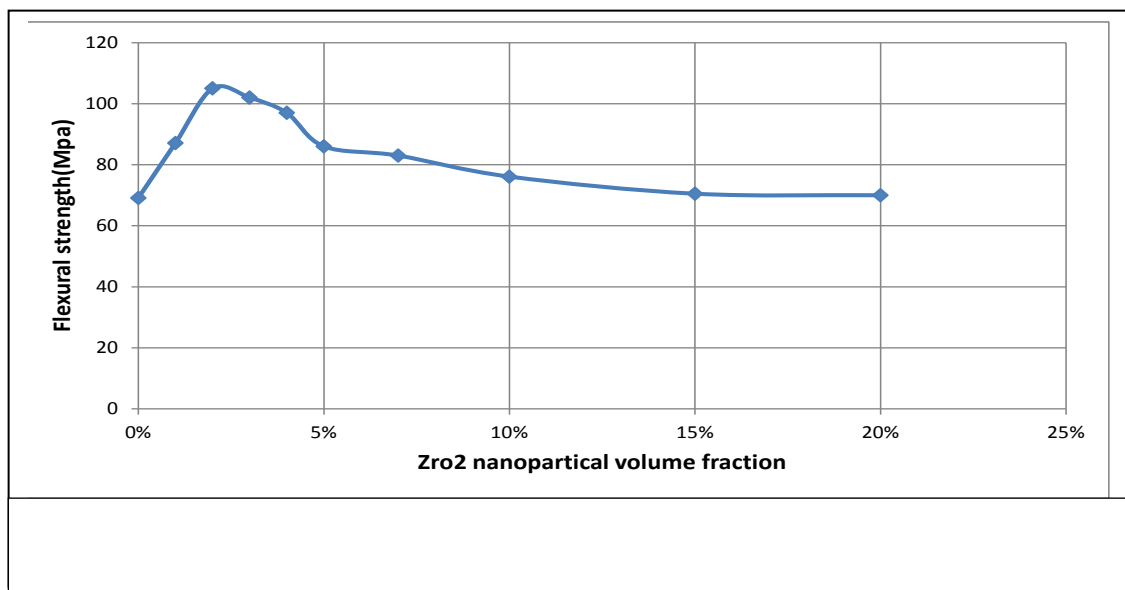
Table (4-1) Maximum stress, maximum strain, flexural strength, flexural modulus and fracture toughness for EP/ZrO₂ nanocomposites with 0, 1, 2, 3, 4, 5, 7, 10, 15, and 20% vol. fraction.

Sample	Maximum stress (MPa)	Maximum strain (%)	Flexural strength (MPa)	flexural modulus (GPa)	Fracture Toughness (J/m ²)
EP	69.1	4.6	69.1	1.5	158.9
EP / 1% nano ZrO ₂	87.1	4	87.1	2.25	180.2
EP/ 2% nano ZrO ₂	105.6	4.6	105.6	3.02	296.5
EP/ 3% nano ZrO ₂	102.4	4.5	102.4	3.1	287.5
EP/ 4% nano ZrO ₂	97.3	3.5	97.3	2.81	177.3
EP/ 5% nano ZrO ₂	86.2	4.1	86.2	2.25	176.4
EP/ 7% nano ZrO ₂	83.1	3.0	83.1	2.65	126.6
EP/ 10% nano ZrO ₂	76.1	2.7	76.1	2.72	106
EP/ 15% nano ZrO ₂	70.5	2.76	70.5	2.51	100
EP/ 20% nano ZrO ₂	70.0	2.69	70.1	2.52	98.5

The results values of flexural strength of EP/ ZrO₂ nanocomposites in figure (4-2) and Table (4-1) show the difference of flexural strengths of EP/ ZrO₂ nanocomposites vs. ZrO₂ nanoparticles volume fraction. The results values of flexural strength have most possibly high values at low volume fraction of ZrO₂ nanoparticles, specifically at 2% vol. fraction maximum increment obviously appeared, this behaviour in a good agreement with Kurahatti [99]. At higher addition of ZrO₂ nanoparticles, flexural strengths of EP/ ZrO₂ nanocomposites decrease with increasing concentration of ZrO₂ nanoparticles but the results values of flexural strengths still higher than that of neat epoxy in a good agreement with the performance obtain by Kurahatti

[99] .While strain changed in random method with increasing concentration of Zirconia nanoparticles.

The influence of several factors explain this behaviour in EP/ ZrO_2 nanocomposites, where the presence of ZrO_2 nanoparticles into the epoxy matrix leads to some change in the epoxy chains and structures, where good dispersion and distribution of nanoparticles into epoxy matrix perform decrease the mobility to the epoxy chains because of creation high immobility nano-layer about each nanoparticles, while the matrix chains (epoxy chains de-bonded to nanoparticles) bonded to that nano-layer constrained the de-contact matrix chains therefore, the network of nanoparticles decrease the total mobility of the nanocomposites system.



Mechanical attributes of epoxy relied highly on the length of the epoxy chains, nanoparticles perform to decrease the chains length to a critical length (where maximum improvement occur) at this addition all mechanical attributes of EP/ ZrO₂ nanocomposites rises as shown in the results of mechanical test. More addition of ZrO₂ nanoparticles lead to reduce in space distance (decrease free space distance) between epoxy chains when the addition of ZrO₂ nanoparticles which are polar particles [41], perform to filling free space among chains and attract resin molecules and therefore epoxy chains through curing processes generating more complex network chains, also ZrO₂ nanoparticles generating Van der-Waals bonding among chains and particles lead to rise constraint between; polymer chains itself and particles/polymer chains, leading chains to stand extra-forces, which causes to varying the mechanical properties of EP/composite.

Figure (4-3) shows the difference of flexural modulus with increasing of ZrO₂ nanoparticles concentration of EP/ZrO₂ nanocomposites. flexural modulus has a random performance with increasing volume fraction of ZrO₂ nanoparticles of EP/ZrO₂ nanocomposites, at 3% vol., fraction of Zirconia nanoparticles ,flexural modulus reach maximum increase, in general all the value obtained after the addition of ZrO₂ nanoparticles to epoxy were higher than that of epoxy specially at low concentration of ZrO₂ nanoparticles, This behaviour of EP/ZrO₂ nanocomposites in good agreement with the behaviour obtained by K.S. Harishanand[51]. The increase of concentration of ZrO₂ nanoparticles lead to rise constraint of epoxy chains when chains deflections and mobility will decrease, so all the results of flexural modulus were higher than that of epoxy.

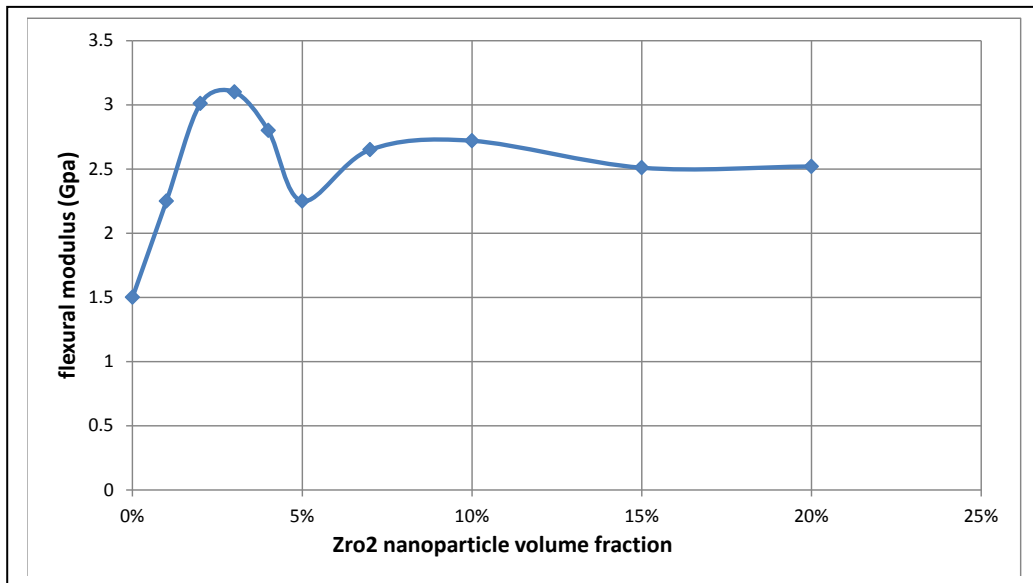


Fig. (4-3). flexural modulus versus ZrO₂ nanoparticle volume fraction of epoxy and EP/ZrO₂ nanocomposites.

Fracture toughness rise with increasing concentration of Zirconia nanoparticles, until 2% vol. fraction, then fracture toughness begin to reduce from and going down, this behaviour is in better agreement with the performance obtained by Mohamed Ashour [48]. fracture toughness Increase due to increasing crack deflections (generating more than one crack propagation direction) which implies crack propagation resistance and rise chains supporting causing from nanoparticles presence. The behaviour of reducing fracture toughness because of nanoparticles agglomerations cause rise the space distance (free volume space) among epoxy chains, therefore, increasing free volume space perform epoxy chains to stand lesser-forces, Figure (4-4) shows the variation between fracture toughness and Zirconium nanoparticles volume fraction.

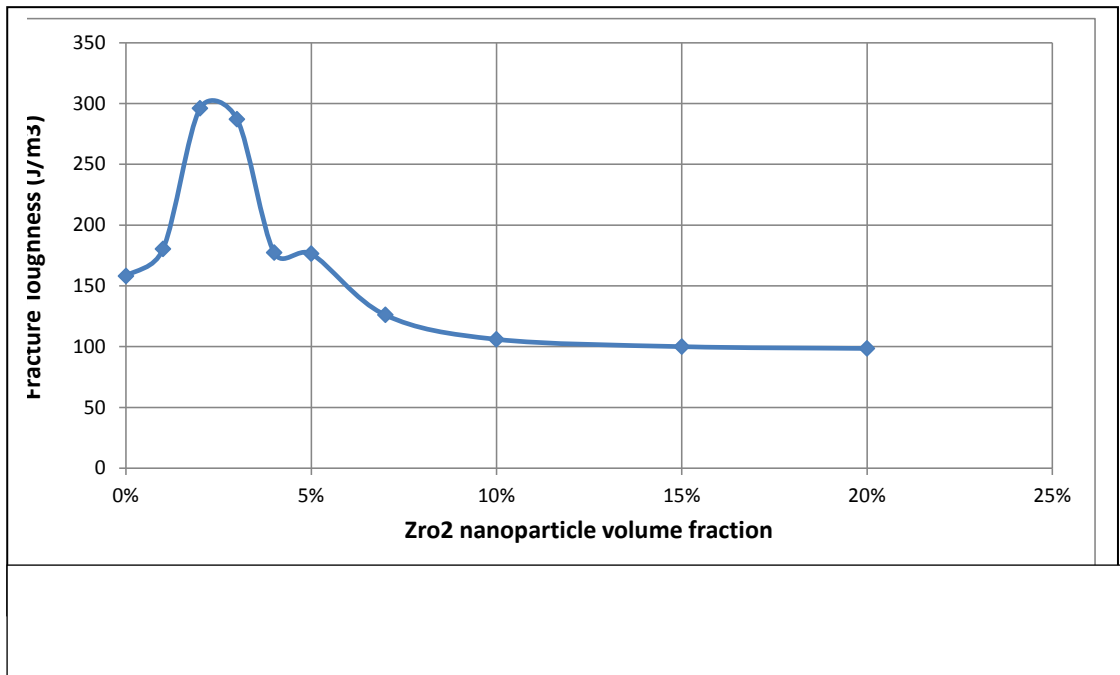
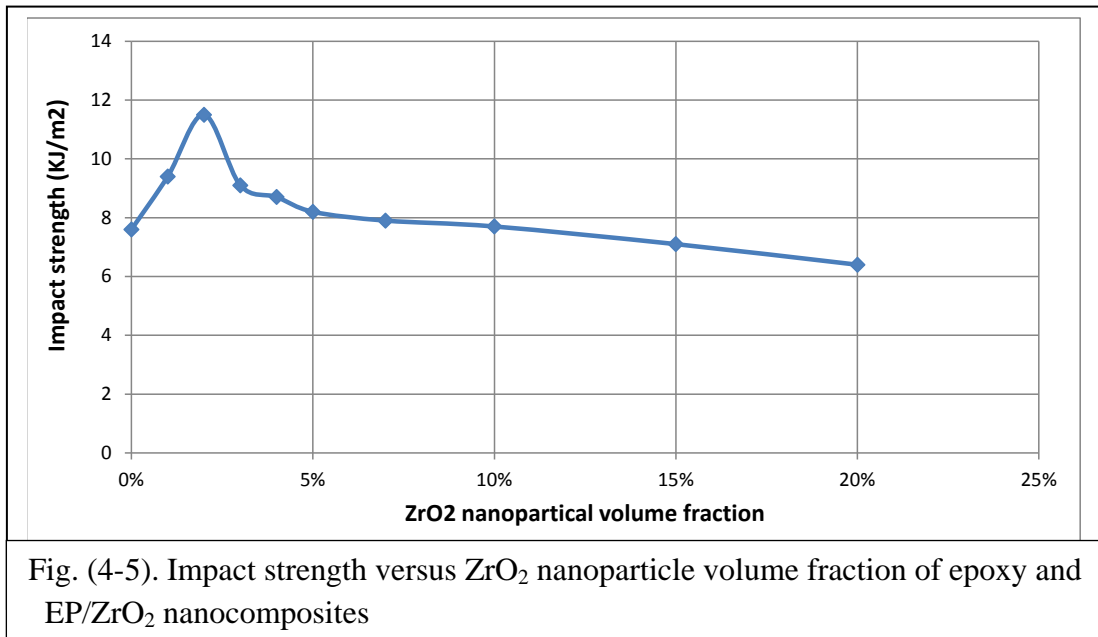
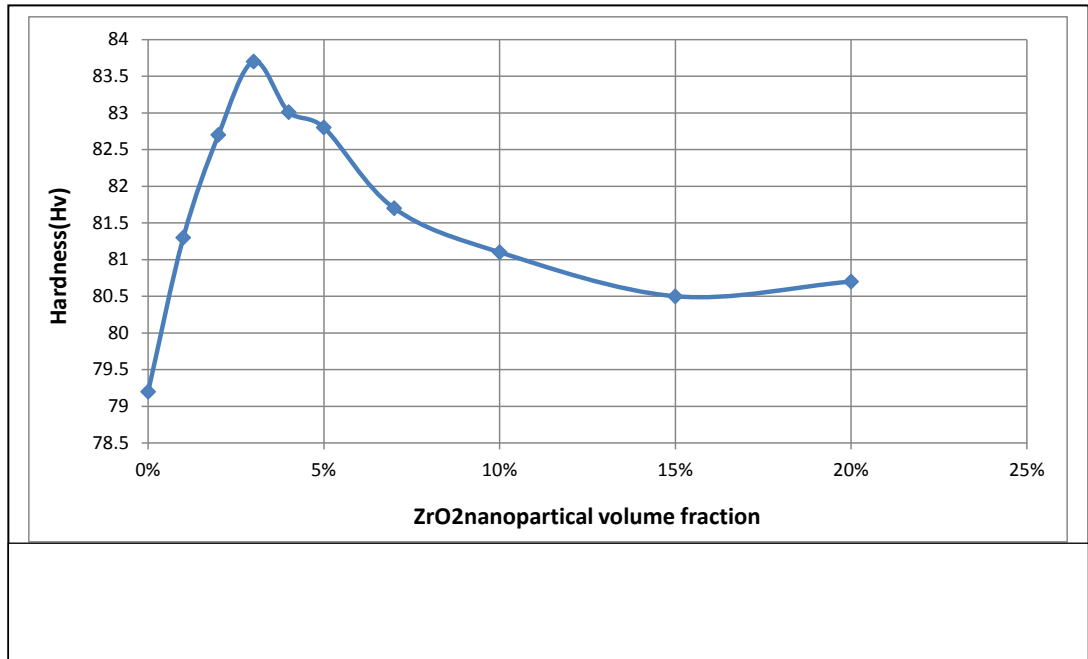


Figure (4-5), show that Impact strength increase with increasing volume fraction of Zirconia nanoparticles, until 2% vol. fraction, then Impact strength begin to reduce from maximum increment this may be due reduce mobility of polymer chains because of hard ceramic nano filler can be the reason for high Impact strength exhibited by slabs at 2% filler content. Higher surface area of ZrO_2 nanoparticle reinforces larger volume of resin matrix and stress can be moved to nanoparticles more competently owing to high interfacial area between resin and filler. , this behavior is in good agreement with the behavior obtained by R.V. Kurahattia [99] and. Hussein K. H. [100].



ZrO₂ nanoparticle was found to increase the hardness of neat epoxy shown in Fig.(4-6), Increase in hardness of neat epoxy with the increase in the concentration of ZrO₂ nanoparticle can be attributed to uniform dispersion of the ZrO₂ nanoparticle in epoxy matrix. A significant enhancement in hardness was observed for 3% vol. fraction. High strength ZrO₂ nanoparticle reinforcements may result in creating a network structure that improves the hardness of the composites. When filler loading was increased beyond 3% vol. fraction a reduce in hardness is observed and value drops down this behaviour is in good agreement with the behaviour obtained by K.S. Harishanand1[51] and. Hussein K. H [100]



4-2.2 Mechanical properties of EP/ZrO₂ Microcomposites

Stress-strain curves of epoxy and EP/ZrO₂ microcomposites with 1, 2, 3, 4, 5, 7, 10, 15 and 20% vol. fraction of ZrO₂ microparticles, was shown in figure (4-7).

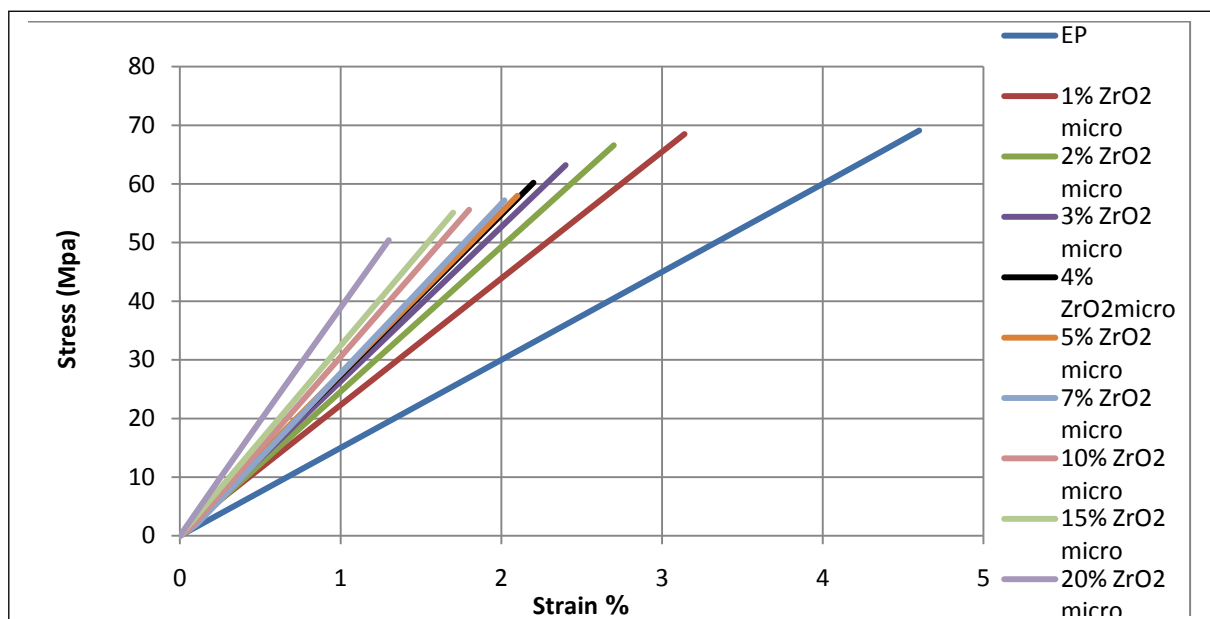


Fig. (4-7) Stress-strain curves of epoxy and EP/ZrO₂ microcomposites with 1, 2, 3, 4, 5, 7, 10, 15 and 20 % vol. fraction of ZrO₂ microparticles

Table (4-2). Maximum stress, maximum strain, Flexural strength, flexural modulus and fracture toughness of epoxy and EP/ ZrO₂ microcomposites.

Sample	Maximum Stress (MPa)	Maximum strain(%)	Flexural strength (MPa)	flexural modulus (GPa)	Fracture Toughness (J/m²)
EP	69.1	4.6	69.1	1.5	158.2
EP/ 1% microZrO ₂	68.5	3.1	68.5	2.25	105.7
EP/ 2% micro ZrO ₂	66.5	2.7	66.5	2.46	89.9
EP/ 3% micro ZrO ₂	63.4	2.4	63.4	2.64	76.8
EP/ 4% micro ZrO ₂	60.2	2.2	60.2	2.73	66.9
EP/ 5% micro ZrO ₂	58.6	2.1	58.6	2.8	61.7
EP/ 7% micro ZrO ₂	57.2	2.0	57.2	2.87	57.7
EP/ 10% micro ZrO ₂	55.6	1.8	55.6	3.08	50.8
EP/ 15% micro ZrO ₂	55.1	1.7	55.1	3.34	47.5
EP/ 20% micro ZrO ₂	50.4	1.3	50.4	3.87	33.2

Flexural strength value of EP/ ZrO₂ microcomposites are shown in table (4-2), where the flexural strength values reduce with increasing the concentration of ZrO₂ microparticles. This performance in microcomposites is due to low or lost interfacial strength (gluing), where microparticles have gluing with epoxy chains less than the gluing of ZrO₂ nanoparticles with epoxy chains because of the properties of microparticles surface (low porosity) where approximately the interactions of epoxy with the surface of microparticles are very poor.

Also, microparticles size rise space distance among epoxy chains which leads to increment bad bonding between epoxy chains, these reasons perform to reduce flexural strength of EP/ZrO₂ microcomposites with increasing the concentration of ZrO₂ microparticles as shown in figure(4-8) .

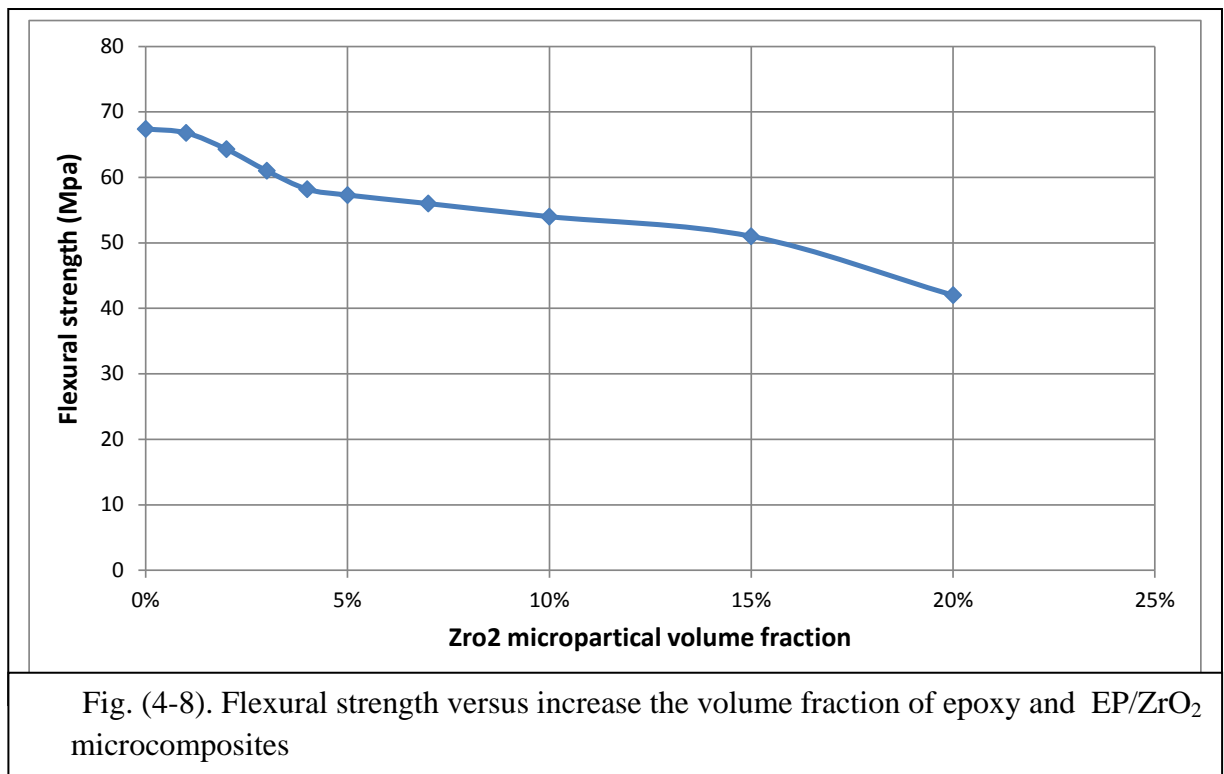
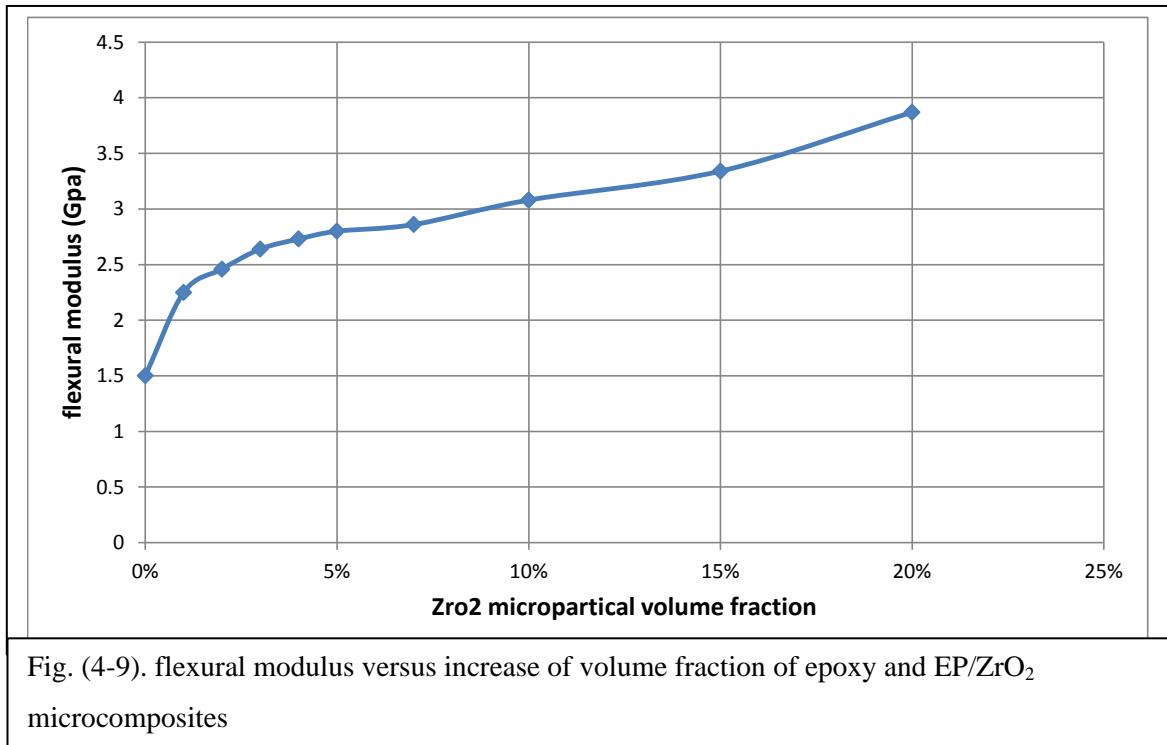


Figure (4-9), shows that the flexural modulus of EP/ZrO₂ microcomposites increase of flexural modulus with increasing the ZrO₂ microparticles volume fraction, this behaviour is due to presence ZrO₂ microparticles in epoxy matrix causing an increase of the immobility of epoxy chains. The mechanism of flexural modulus increases in the presence of microparticles variation of the mechanism of flexural modulus increases in the presence of ZrO₂ nanoparticles, where rise immobility of epoxy chains in presence of ZrO₂ microparticles act as rigid particles impede epoxy chains mobility ,but with use of ZrO₂ nanoparticles not decrease the mobility of the

epoxy chains because of creation high immobility nano-layer about each nanoparticle.



Fracture toughness of EP/ZrO₂ microcomposites decreases with increasing the volume fraction of Zirconium microparticles as shown in Figure (4-10) illustrate the behaviour of difference fracture toughness of EP/ZrO₂ microcomposites vs. ZrO₂ microparticles volume fraction. Gathering all the causes pointed previously like; (i) low porosity of microparticles surface perform to de-bonding and cavitation seems (ii) microparticles size rise space distance among epoxy chains, (iii) increasing concentration of ZrO₂ microparticles leads to forming new crack path near to the surface of microparticles which reduce plastic deformation into epoxy matrix when interfacial space among microparticles and epoxy consider a weak zone which is weaker than epoxy matrix, therefore, fracture toughness of EP/ZrO₂ microcomposites reduce with increasing the concentration of zirconia microparticles.

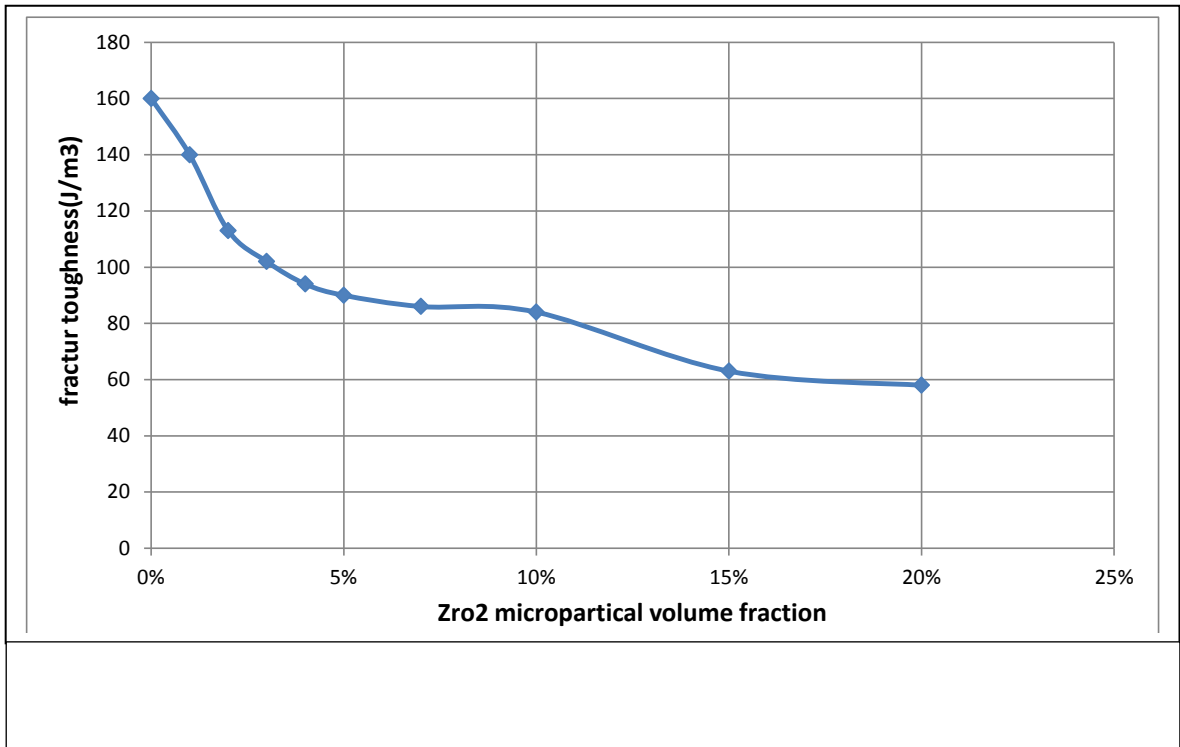


fig (4-11) show; the decreases in impact strength of EP/ZrO₂ microcomposites with increasing the vol. fraction of Zirconium because low porosity of microparticles surface perform to de-bonding and cavitation appears .

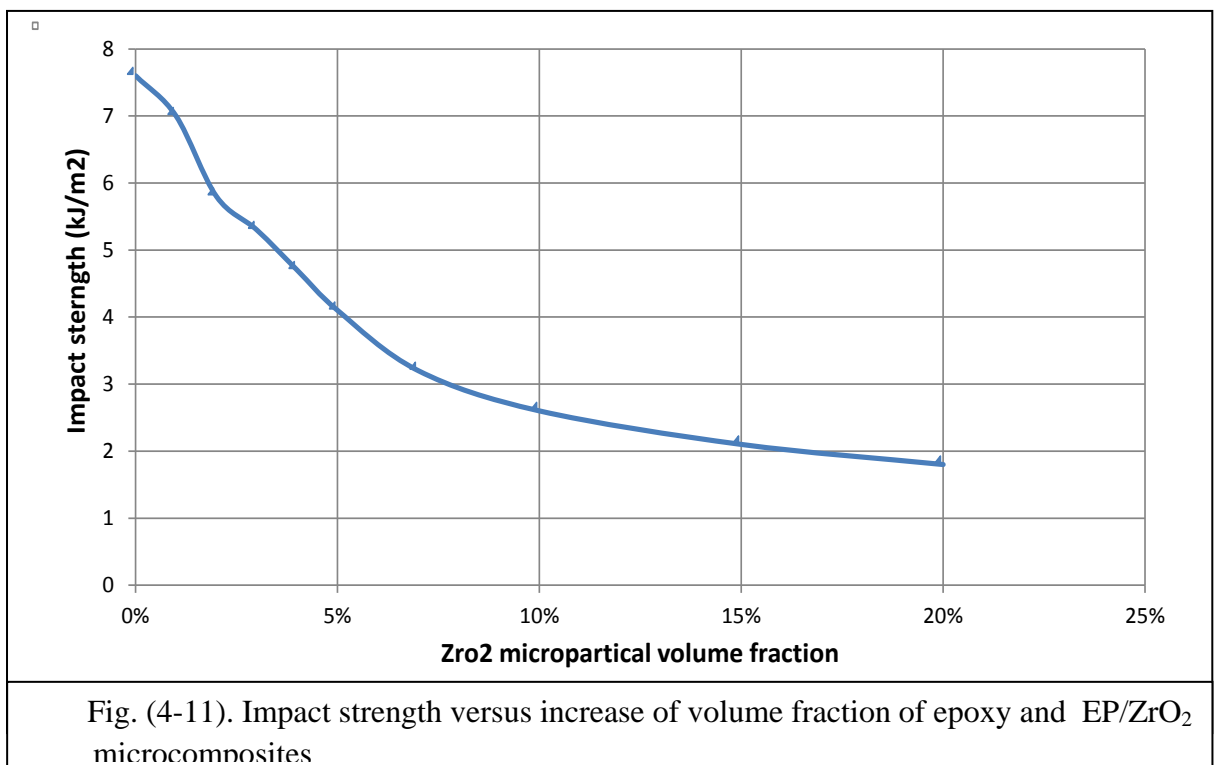
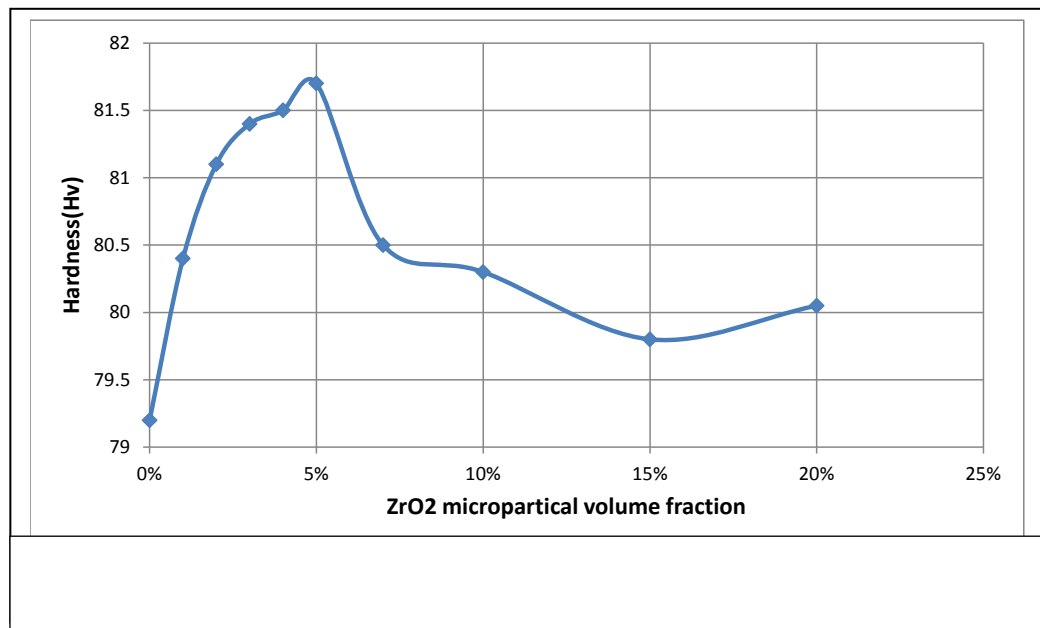


figure (4- 12) show that the hardness increase with increasing volume fraction of ZrO_2 microparticles, until 5% vol. fraction, then hardness begin to reduce from maximum increment because of increasing volume fraction of ZrO_2 microparticles leads to formation new crack path near to the surface of microparticles which reduce plastic deformation into epoxy matrix where interfacial space among microparticles and epoxy consider a weak region which is weaker than epoxy[51].



4-2.3 Scanning Electron Microscope (SEM) image of EP/ ZrO_2 Nanocomposites topography of Fractured Structure

Figures (4-13) – (4-20) illustrate the SEM image for topography of fractured structure of epoxy and EP/ ZrO_2 nanocomposites magnified to 30,000X its original scale.

Figure (4-13) illustrate, Nanocracks of the epoxy structure signed by arrows were formed because of polymerization which start at numerous zones and speeds, according to the nature of chemical reaction of resin and hardener, in which polymerized regions are formed faster than others, applying different stresses on epoxy structure forming nanocracks (which is nano-defect formed

at early stage of polymerization). Nanocracks are of average width equal to 21 nm, and modifier length equal to 199 nm seemed in the SEM image.

Figure (4-14) illustrate SEM image of the of fractured structure of EP/ ZrO₂ nanocomposites of (1 % vol. fraction of ZrO₂ nanoparticles) have nanocracks of mode like to that of fractured epoxy structure and have particles non-bonding also seemed signed by circle shown in figure (4-21) but less length, and less width, this improvement in reducing nanocracks creation was due to ZrO₂ nanoparticles addition.

Figures (4-15) illustrate SEM picture of the Fracture structure of EP/ ZrO₂ nanocomposites with (2 % vol. fraction of ZrO₂ nanoparticles) have different mode of nanocracks comparing with epoxy structure illustrated in figure (4-13). The nanocracks almost disappear from the structure due to adding ZrO₂ nanoparticles, which have; good adhesion force between nanoparticles/epoxy chains emergent from; Van der-Waals bonding and the polar of ZrO₂ nanoparticles, high porosity, increment resin viscosity, filling space distance among epoxy chains, all these causes lead to chains connect one another and overcome issues of polymerisation start at numerous zones and speeds, so, decreasing nanocracks in nanocomposites structure backing matrix to stand extra-forces because of remove structure defects ,therefore has the best improvement in remove nanocracks from the structure between other EP/ ZrO₂ nanocomposites with various volume fraction. This behaviour perform to the expectation that the better mechanical properties could be appeared in such samples because of; more hard crack initiations, more than one crack propagation directions, less voids defect appeared in matrix.

Figures (4-16, 4-17, 4-18, 4-19, and 4-20) illustrate SEM image of the of fractured structure of EP/ ZrO₂ nanocomposites with (3, 4, 5, 7 and 10 % vol. fraction of ZrO₂ nanoparticles), they have a good accord with mode of

nanocracks at figures (4-14), where growing ZrO_2 nanoparticles above certain critical concentration perform to high rise resin viscosity in which dispersion and distribution of ZrO_2 nanoparticles were hard also hardener could be hard to distributed in a good manner with resin (reducing crosslink density), large agglomeration start to appear, therefore, improvement in epoxy matrix will be decrease from maximum improvement to a degree varying inversely with growing concentration of ZrO_2 nanoparticles addition. Figures (4-17, 4-18, 4-19, and 4-20) show ZrO_2 nanoparticles agglomerations (signed by square) due to high concentration of volume fraction of ZrO_2 nanoparticles and bad dispersion of ZrO_2 nanoparticles.

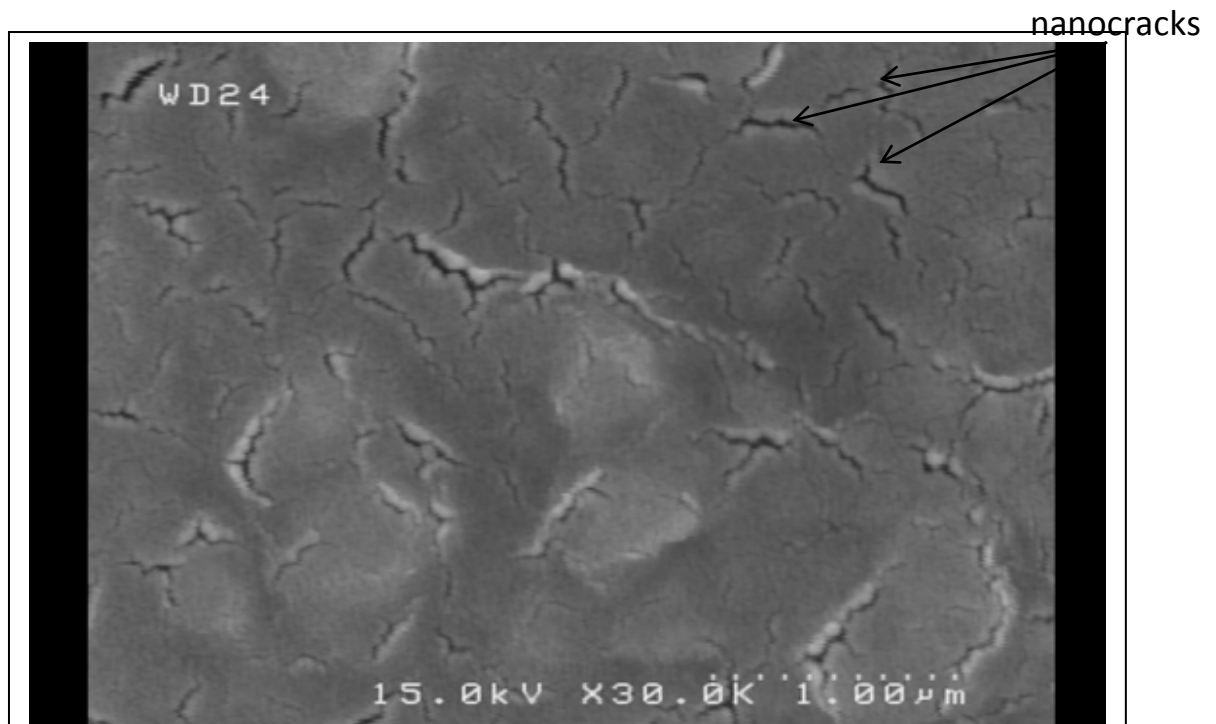


Fig. (4-13). topography of fractured structure of neat epoxy resin.

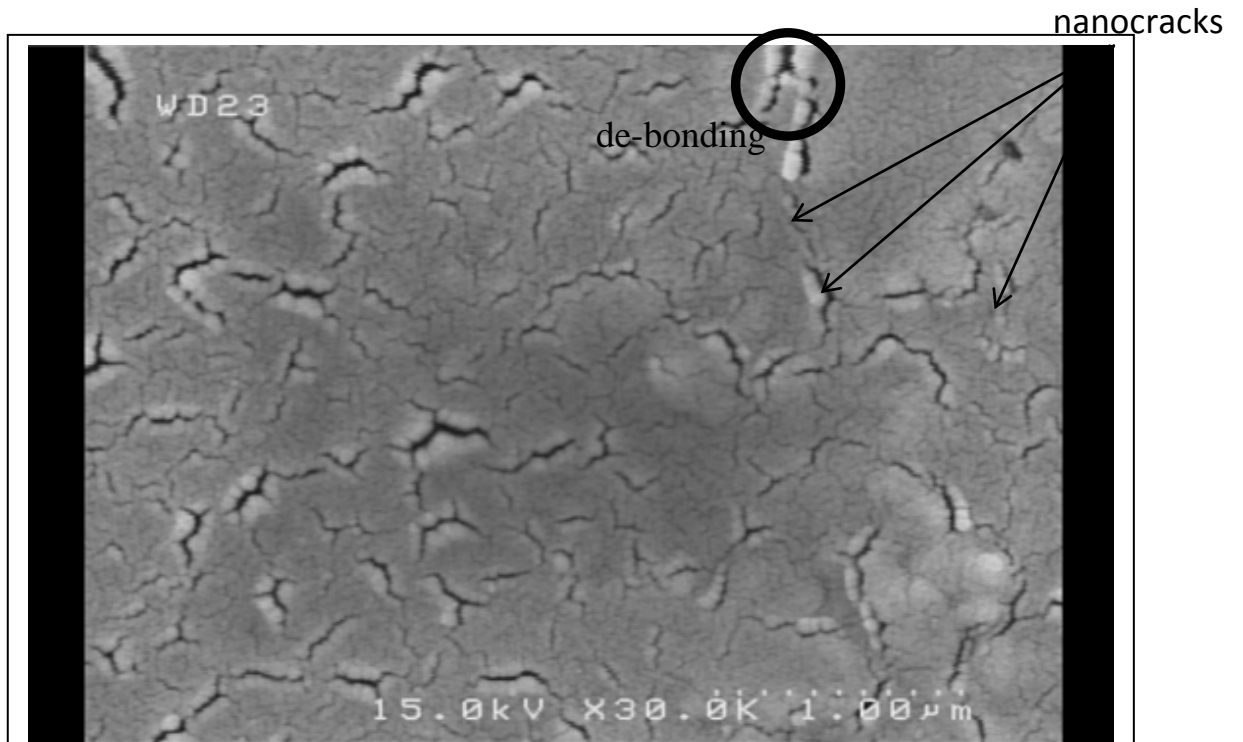
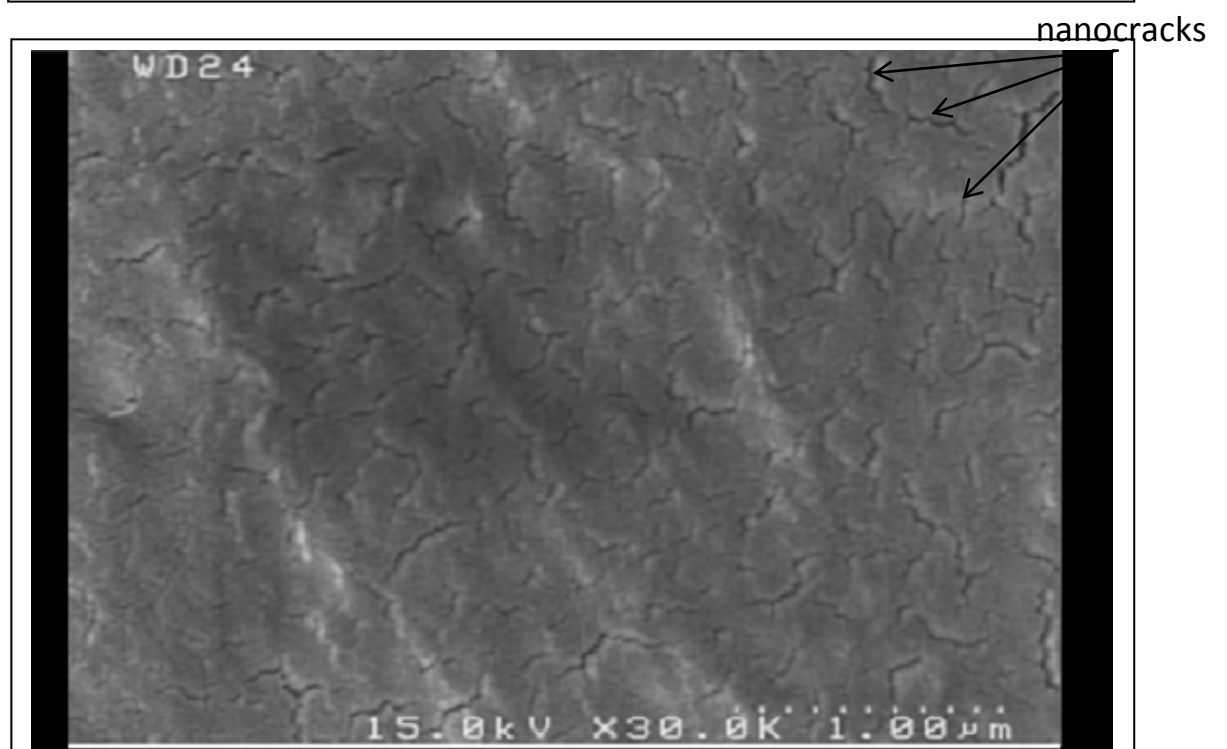
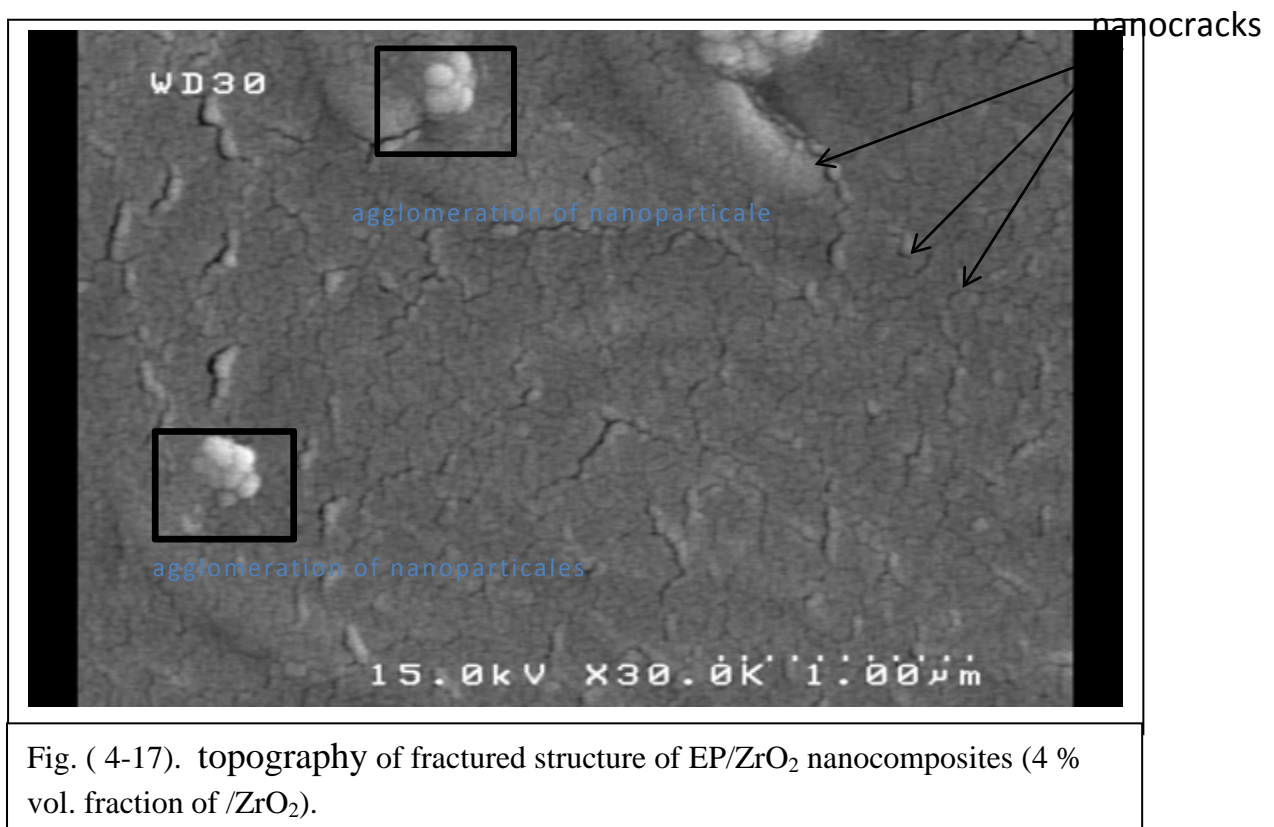
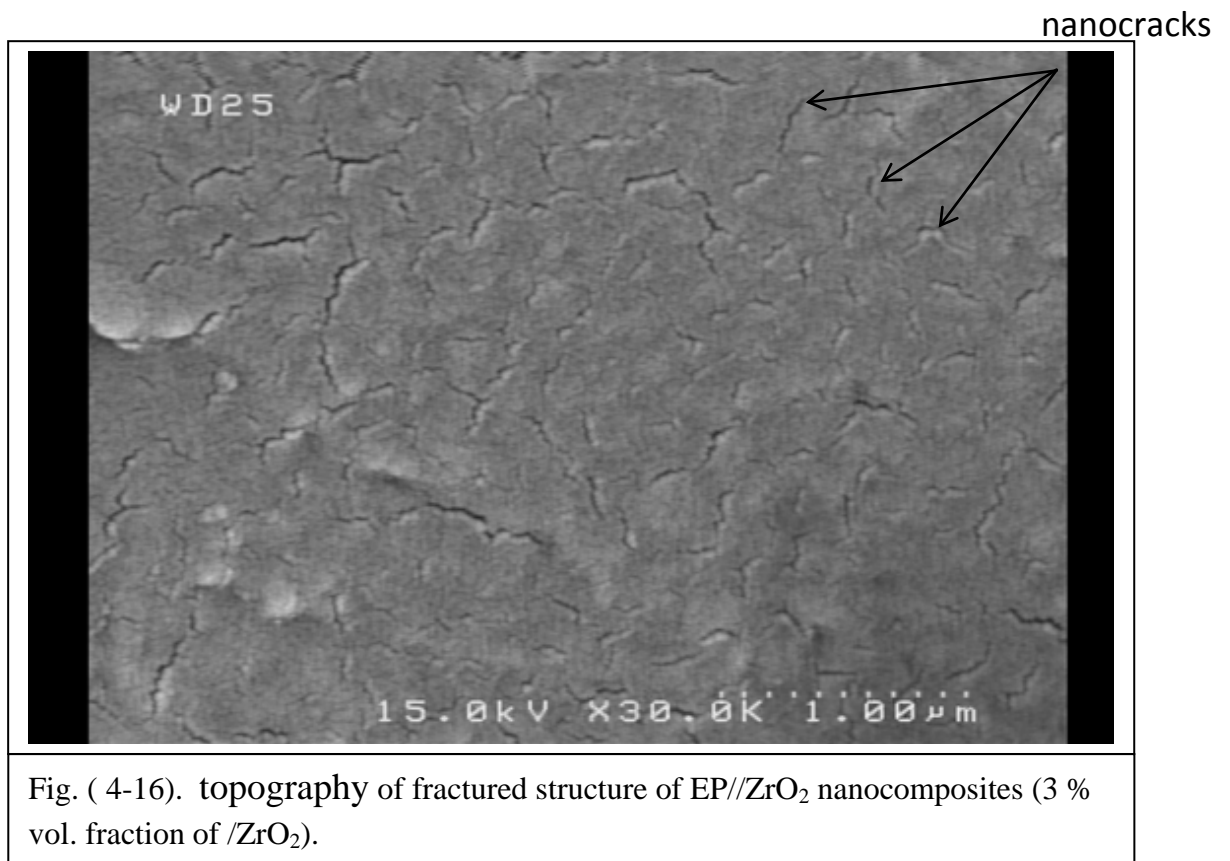
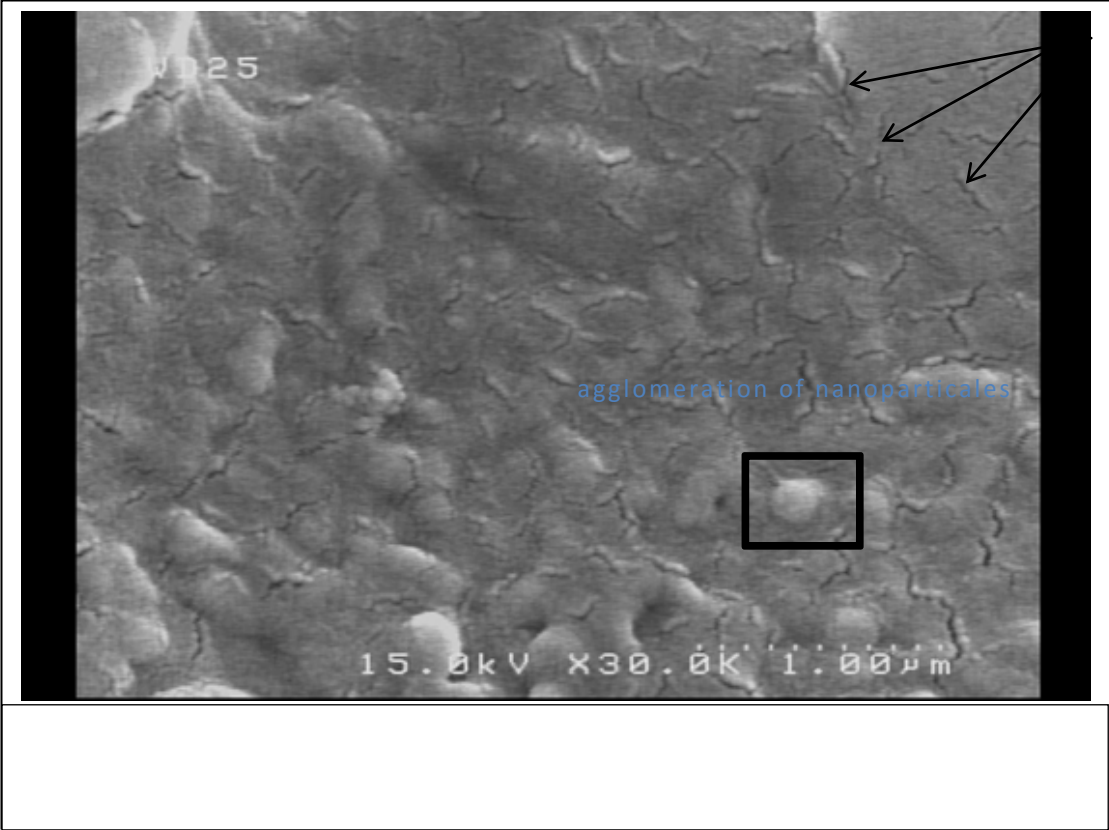


Fig. (4-14). topography of fractured structure of EP//ZrO₂ nanocomposites (1% vol. fraction of /ZrO₂).

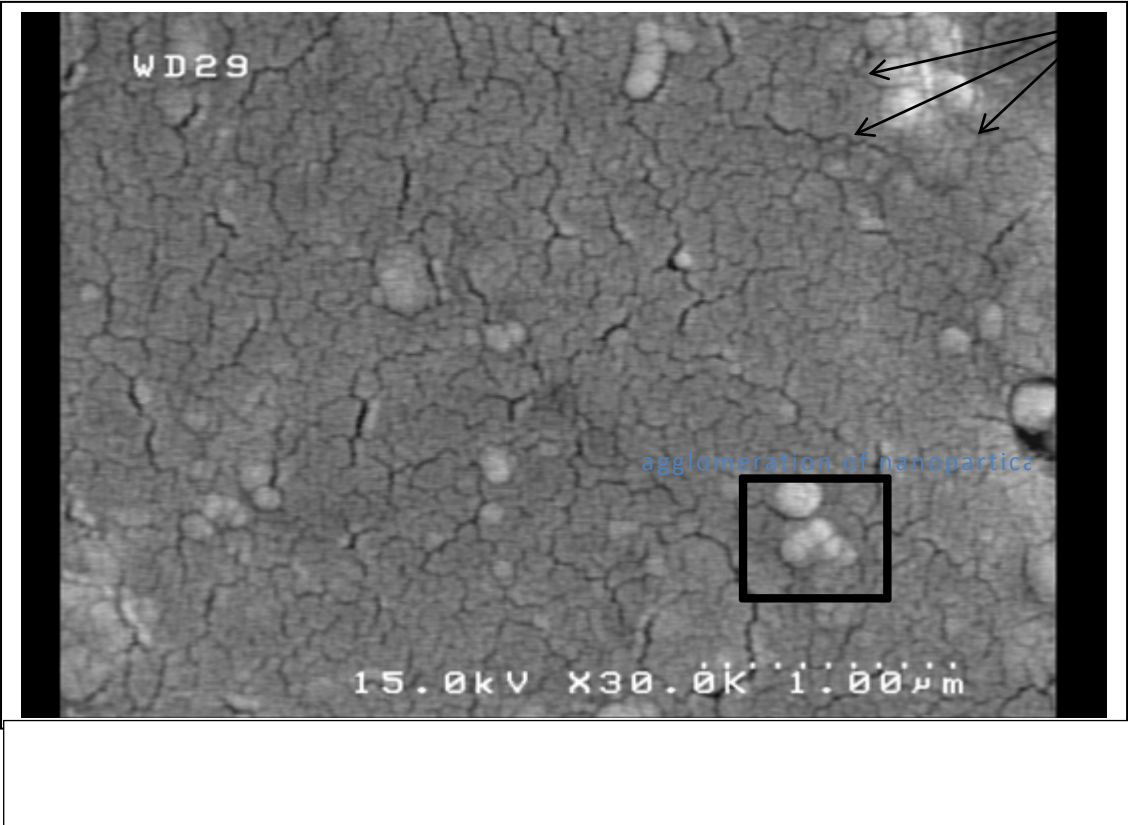




nanocracks



nanocracks



nanocracks

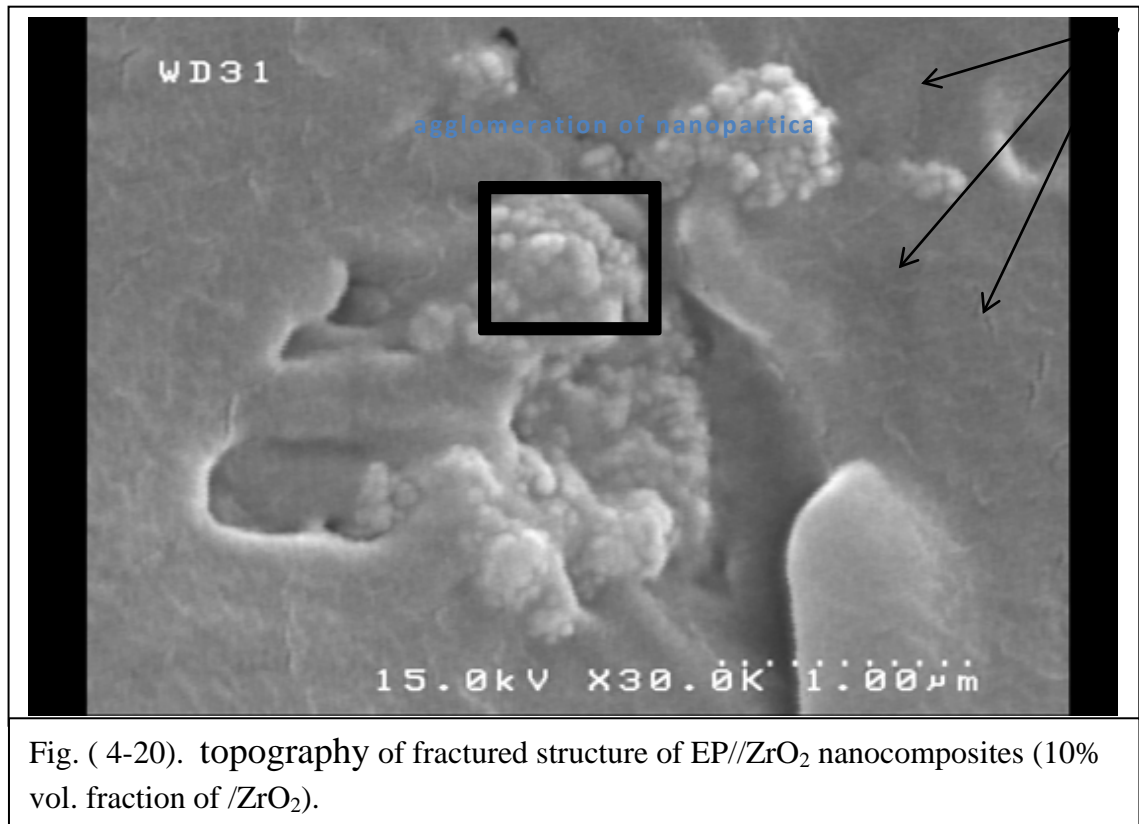


Fig. (4-20). topography of fractured structure of EP//ZrO₂ nanocomposites (10% vol. fraction of /ZrO₂).

4-2.4 Mechanical Properties of EP/MgO Nanocomposites

Stress-strain curves for epoxy and samples of EP/MgO nanocomposites with 1, 2, 3, 4, 5, 7, 10, 15 and 20% vol. fraction are shown in figure (4-21).

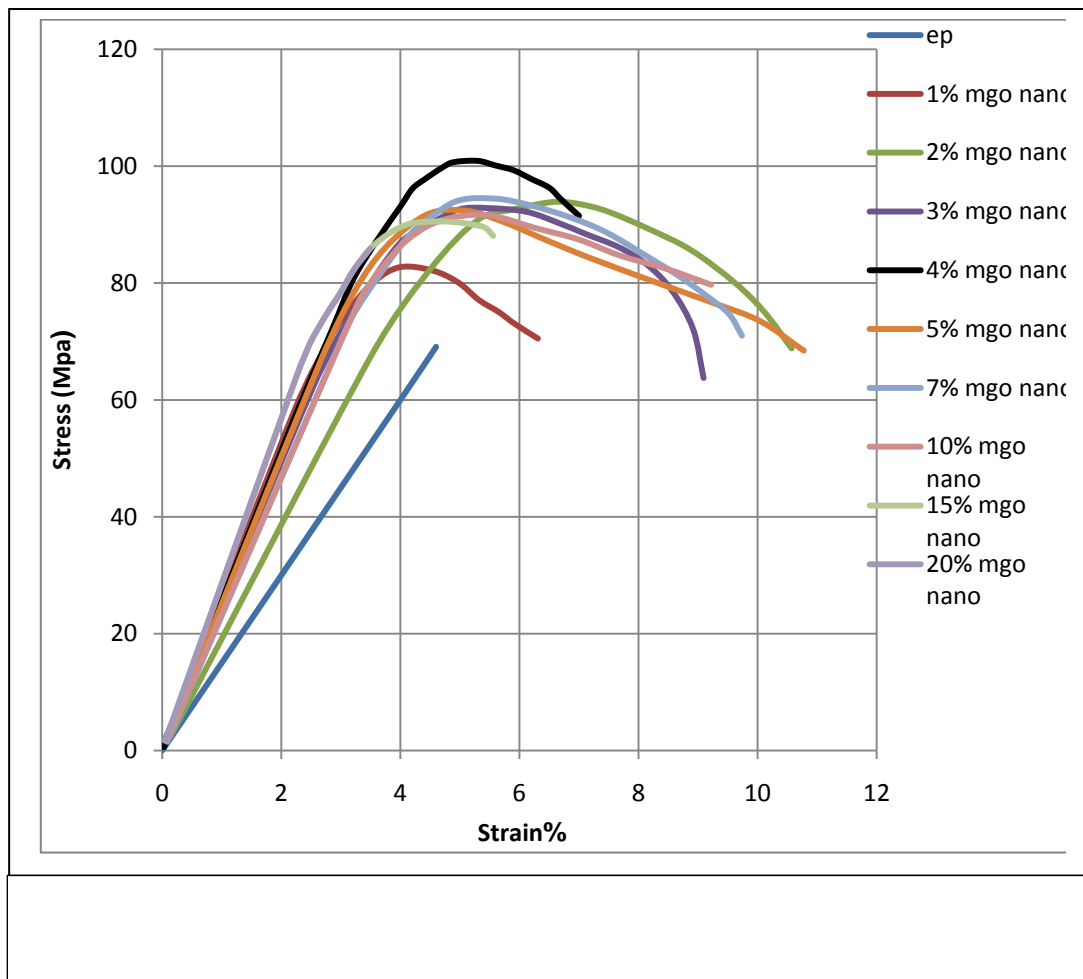


Table (4-3) illustrated; maximum stress (MPa), maximum strain (%), flexural strength, flexural modulus and fracture toughness for EP/MgO nanocomposites with illustrates 1, 2, 3, 4, 5, 7, 10, 15 and 20% vol. fraction. The maximum strain illustrated random difference as the volume fraction of MgO nanoparticles rise, maximum strain happens at 10% vol., fraction of MgO nanoparticles. ductility performance of EP/MgO nanocomposites was very clear from Stress-Strain curves at concentration of MgO nanoparticles (\leq 15% vol. fraction),

Table (4-3) Maximum stress (MPa), maximum strain (%), flexural strength, flexural modulus and fracture toughness of epoxy and EP/MgO nanocomposites.

sample	Maximum stress (MPa)	Maximum strain (%)	Flexural strength (MPa)	flexural modulus (GPa)	Fracture Toughness (J/m ²)
EP	69.1	4.6	69.1	1.5	158.9
EP/ 1% nano MgO	82.71	6.3	82.8	2.01	375.3
EP/ 2% nano MgO	92.7	8.8	92.8	2.10	580.2
EP/ 3% nano MgO	92.8	8	94.4	2.50	635.5
EP/4% nano MgO	101.2	9.5	101.2	2.61	720.3
EP/5% nano MgO	92.3	10.7	95.3	2.51	757.4
EP/7% nano MgO	94.4	9.7	93.4	2.531	686.6
EP10% nano MgO	91.5	13.6	91.7	3.1	589.4
EP/15% nano MgO	90.5	5.5	91.3	3.21	351.2
EP/20% nano MgO	85.4	3.4	80.2	3.01	340.7

Ductility behaviour of EP/MgO nanocomposites, could be explain using multipolar model of MgO structure, the nature of epoxy chains in presence of network of MgO nanoparticles that is creating at the mixing period perform to variation the epoxy chains distribution in a very dramatically manner by a complicated epoxy chains (without increasing crosslink density) , lead to transfer some of imposed stresses on nanocomposites from matrix to nanoparticles which makes EP/ MgO nanocomposites to bear extra forces compared with epoxy and EP/ZrO₂ nanocomposites. Also the nature of metallic core of MgO nanoparticles lead to transfer some of metallic properties (ductile) from nanoparticles (MgO) to the epoxy matrix (brittle) which decrease brittle behaviour of epoxy matrix of nanocomposites as illustrated in figure (4-21).

From Table (4-3) we can see the flexural strength values rise with increasing the filler content of MgO nanoparticles at low concentration (5% vol. fraction), maximum increase occur at 4% vol. fraction of MgO nanoparticles, this performance is in a good agreement with Rosso et al [101]. Rise of MgO nanoparticles into epoxy matrix (5% vol. fraction) lead to reduce of flexural strength of EP/MgO nanocomposites and then vanishing improvement in flexural strength, figure (4-22) show the difference of flexural strength with increasing of filler content of MgO nanoparticles. EP/MgO nanocomposites illustrated that the flexural strength difference due to reduce in space distance between chains caused by addition MgO nanoparticles which are multipolar particles, forming attractive polar forces, and Van der-Waals between chains and nanoparticles this perform to increase restraint between (i) particles/epoxy chains and (ii) epoxy chains itself, complex epoxy chains which contact one another, will decrease free volume space. This influence of MgO nanoparticles perform epoxy chains to stand extra loading. Beyond 4% vol. fraction of MgO nanoparticles flexural strength start to reduce from maximum improvement. Raising the filler content of MgO nanoparticles perform to increment the restraint between epoxy chains, which reduce the length of epoxy chains perform to reduce flexural strength. The flexural strength relied highly on free volume space and chains length (decreasing free volume space refer to the rise in immobility of epoxy chains for matrix system). Flexural strength beyond the 4% vol. fraction of MgO nanoparticles still higher than that of epoxy resin due to Van der-Waals bonds which is weak bond but with huge numbers.

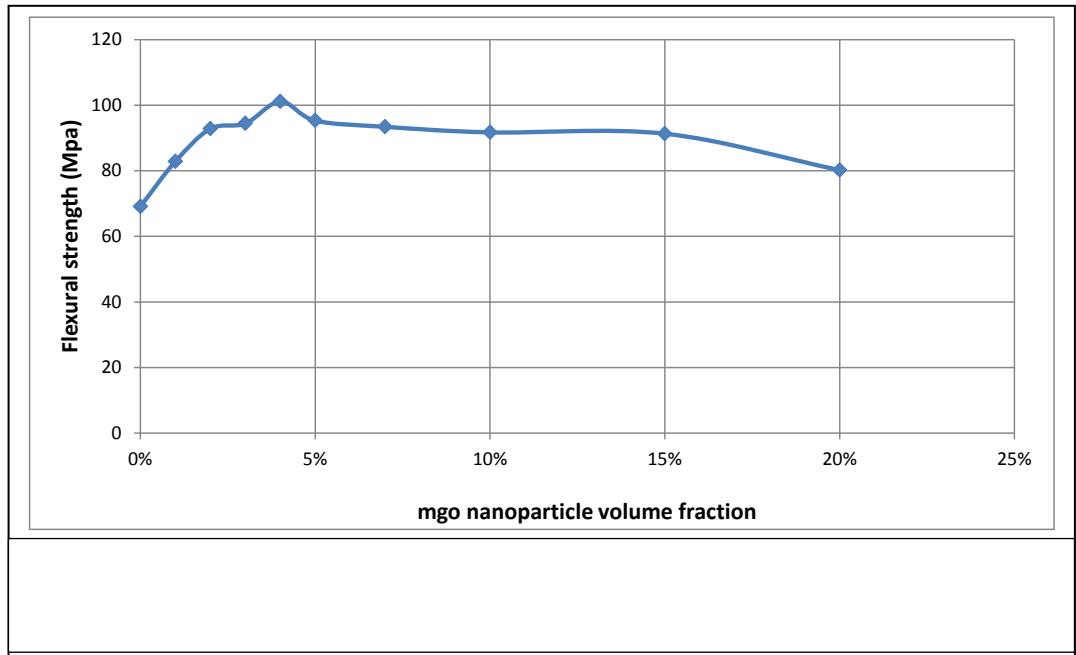


figure (4-23) shows EP/MgO nanocomposites which have a higher value of flexural modulus than that of neat epoxy , which, rise with raising the filler content of MgO nanoparticles in small fraction of addition($< 5\%$) and higher values of addition ($>10\%$), this performance in a good accord with L.S. Schadler [38]. Raising flexural modulus because of rise filler content of MgO nanoparticles which perform to raise the restriction between epoxy chains decreasing the mobility of epoxy chains.

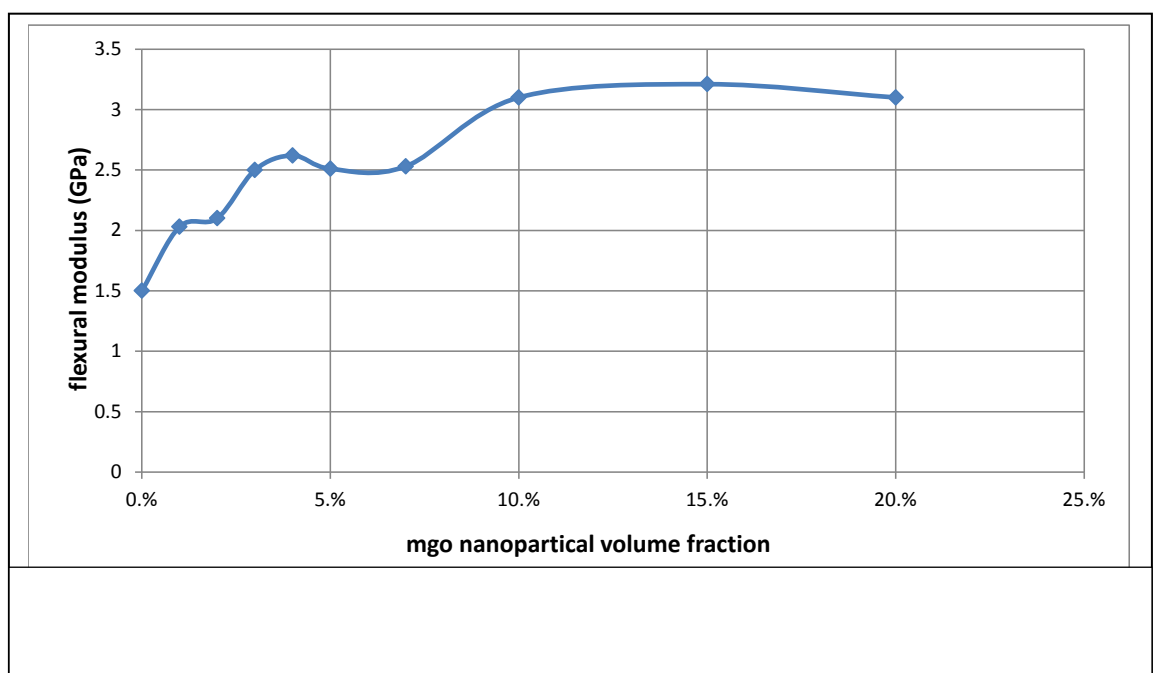
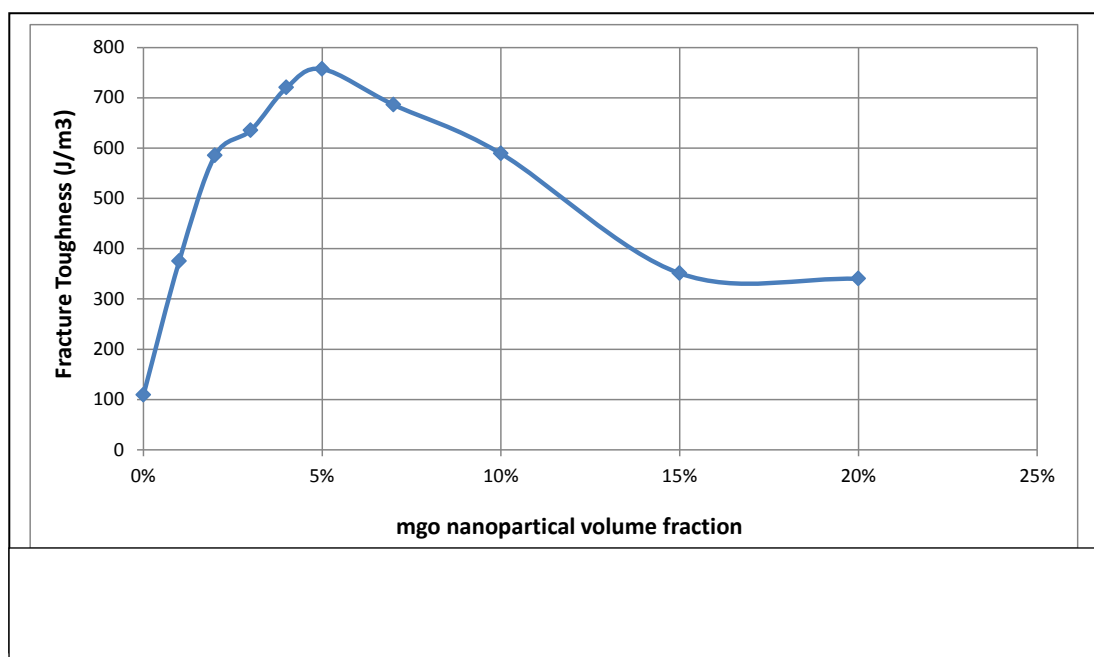


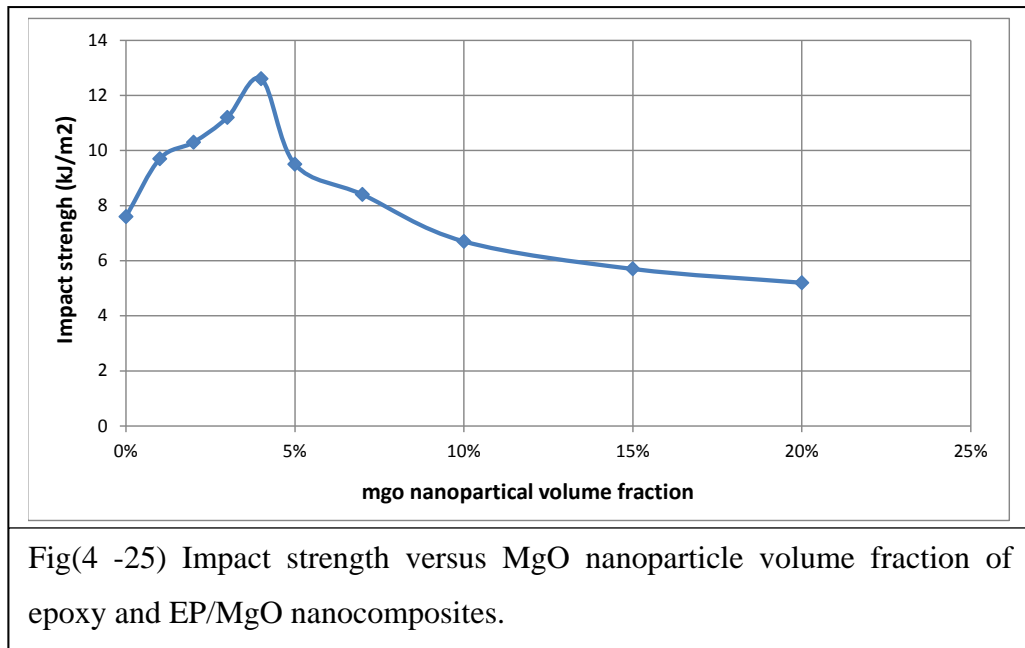
Table (4-3) shows that the fracture toughness rise with increment filler content of MgO nanoparticles, until 5% vol. fraction of MgO nanoparticles, then fracture toughness starts to reduce after this percentage. Figures (4-24) show the performance of difference of fracture toughness with the change of the filler content of MgO nanoparticles, this performance is in a good agreement with L.S. Schadler [38] . Some mechanisms explain the enhancement of fracture toughness e.g. crack deflection, ;when more than one crack propagation direction refer to crack deflection, also crack pinning mechanism where structure uniform matrix with minimum defect of nanocomposites rise crack pinning and plastic deformation lead to rise fracture toughness;

Fracture toughness start to reduce beyond the 5% volume fraction, this performance is in good agreement with Justice et. al., [102]. this performance may be because of particles agglomerations which lead to rise the space distance (free volume space) between epoxy chains, therefore, growing free volume space perform to epoxy chains that will not stand extra-forces.

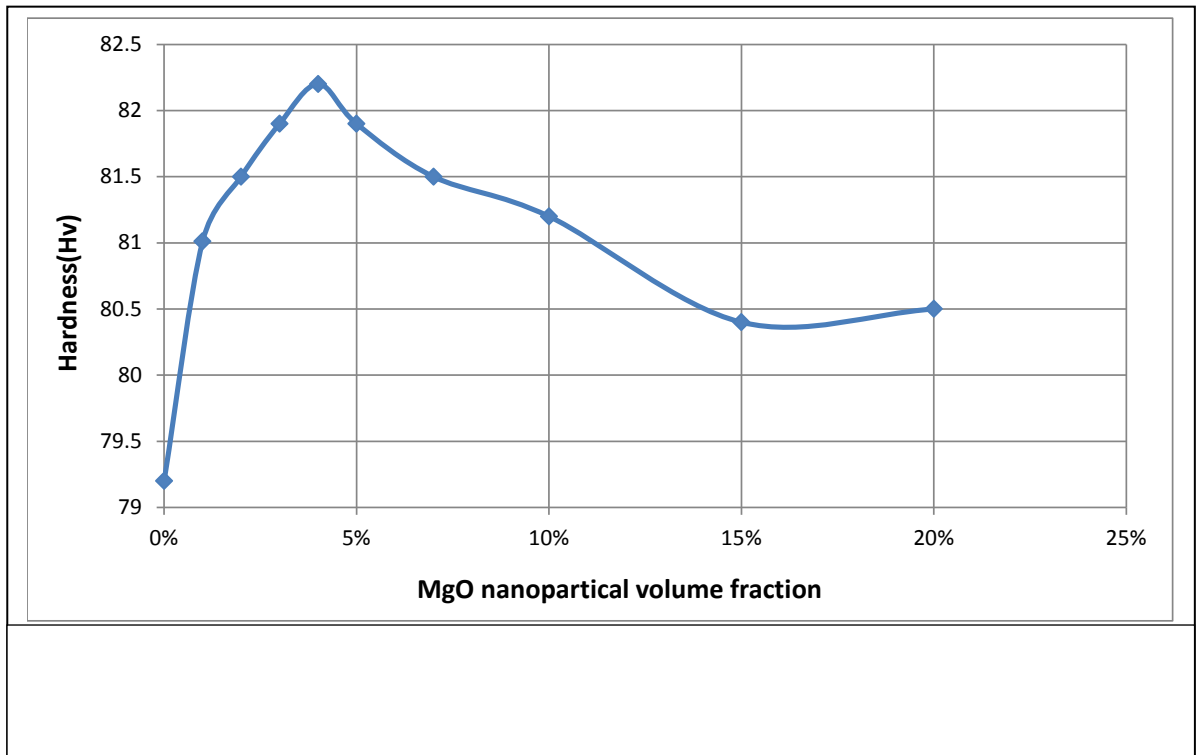


figure(4-25) show; the behaviour of variation of impact strength with the change of the volume fraction of MgO nanoparticles, this behaviour is in a good agreement with Wazzan et al [41].

The impact strength have a higher value volume fraction of MgO nanoparticles, until 4% vol. fraction of MgO nanoparticles, then impact strength begin to decrease after this vol. fraction due to The aggregation of modified nano- MgO that lead to the decrease in impact strength because of higher surface area of the fillers, which may reached to μm in size, so stress concentration about this aggregation which lead to crack proportion.



figure(4-26) show the hardness which is increasing with increasing of concentration of MgO nanoparticles until 4% vol., fraction of MgO nanoparticles . It seems reasonable to suppose that a better impregnation of the 4% vol., fraction of MgO nano-filler will amplify the effect of stress transfer under loaded condition due to increased filler-matrix bonding and degree of crosslinking action ,then hardness begin to decrease after this vol., fraction.



4-2.5 Mechanical Properties of EP/MgO Microcomposites

The stress-strain curves for epoxy and EP/MgO microcomposites with 0,1, 2, 3, 4, 5, 7, 10, 15 and 20% vol., fraction of MgO microparticles, that are shown in figure (4-27).

From the stress - strain curves it was determined the maximum stress, maximum strain, flexural strength, flexural modulus and fracture toughness for epoxy and EP/MgO microcomposites with 0,1, 2, 3, 4, 5, 7, 10, 15, and 20% vol., fraction which shown in Table (4-4).

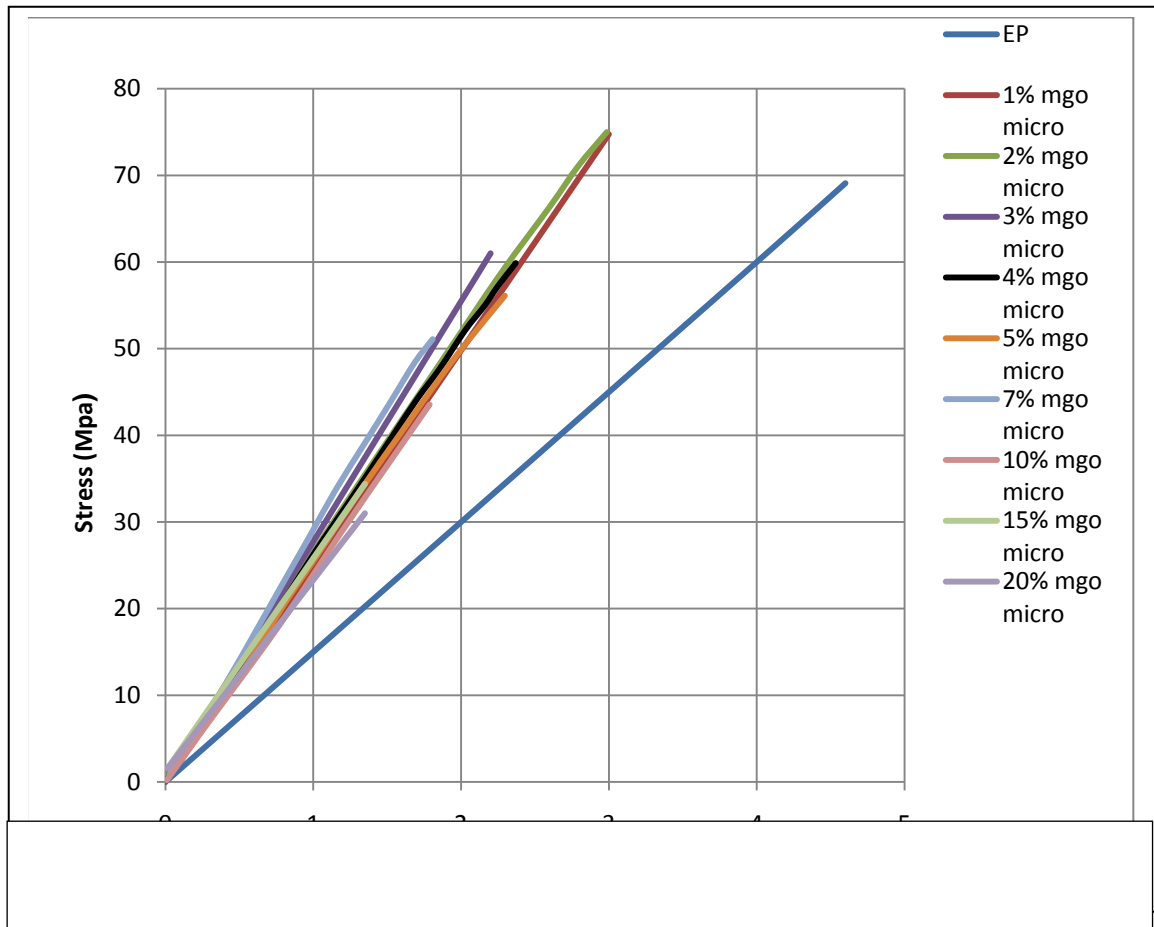
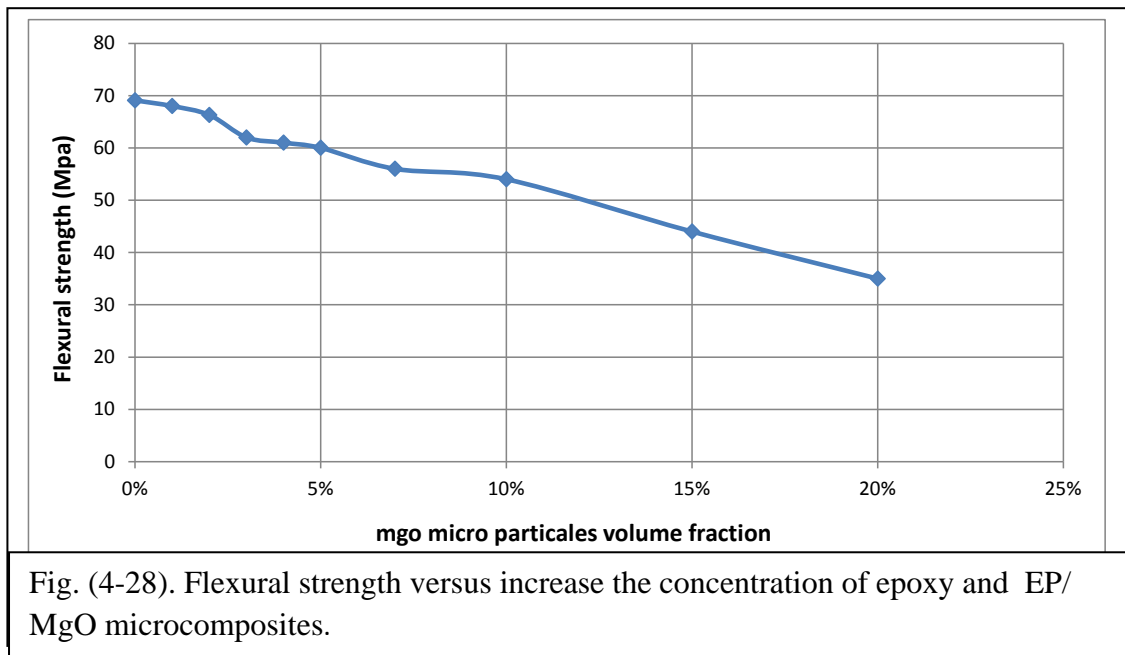


Table (4-4): Maximum stress (MPa), maximum strain (%), flexural strength, flexural modulus and fracture toughness of epoxy and EP/MgO microcomposites.

sample	Maximum stress (MPa)	Maximum strain (%)	Flexural strength (MPa)	Flexural modulus (GPa)	Fracture Toughness (J/m ²)
EP	69.1	4.6	69.1	1.5	158.9
EP/1% micro MgO	74.71	2.9	68.0	2.72	115.3
EP/2% micro MgO	74.9	2.9	66.3	2.8	108.5
EP/3% micro MgO	61.0	2.3	62.0	2.91	71.4
EP/4% micro MgO	59.0	2.3	61.1	2.94	70.2
EP/5% micro MgO	56.1	2.2	60.2	2.5	64.1
EP/7% micro MgO	51.1	1.8	56.0	2.62	47.3
EP/10 %micro MgO	43.5	1.7	54.1	2.64	39.2
EP/15% micro MgO	34.4	1.3	44.2	2.69	36.1
EP/20% micro MgO	31.4	1.28	35.1	2.3	23.3

Maximum strain (%) follows the same performance of maximum strain (%) of EP/ZrO₂ microcomposites. This kind of performance indicates increasing brittle properties of the microcomposites. Flexural strength of EP/MgO microcomposites, Table (4-4) reduce with increasing the concentration of MgO microparticles. Figure (4-28), shows the difference of flexural strength with concentration of MgO microparticles. This performance in microcomposites is because of low or lost interfacial strength (adhesion), de-bonding and cavitation seems due to particles shape, particles size and concentration of MgO microparticles.



Maximum value of flexural modulus of EP/ MgO microcomposites in Table (4-4), was with 4% vol., fraction of MgO microparticles. In general flexural modulus was increased with increasing the concentration of MgO microparticles up to 4% volume fraction of addition as shown in figure (4-29), this is because of particles size, where it leads to growing the restriction between epoxy chains (chains immobility rise).

While, fracture toughness reduce with increasing the concentration of MgO microparticles, minimum value was (23.3 J/m²) at 20% vol. fraction of

MgO microparticles, some mechanisms were responsible of reducing fracture toughness; such as; microparticles size that increment space distance among epoxy chains, reducing epoxy chains length over certain critical chains length because of distribution microparticles into epoxy matrix, low porosity of microparticles surface preform to de bonding and cavitation seems. Figure (4-30) shows the behaviour of difference; fracture toughness with changing the concentration of MgO microparticles.

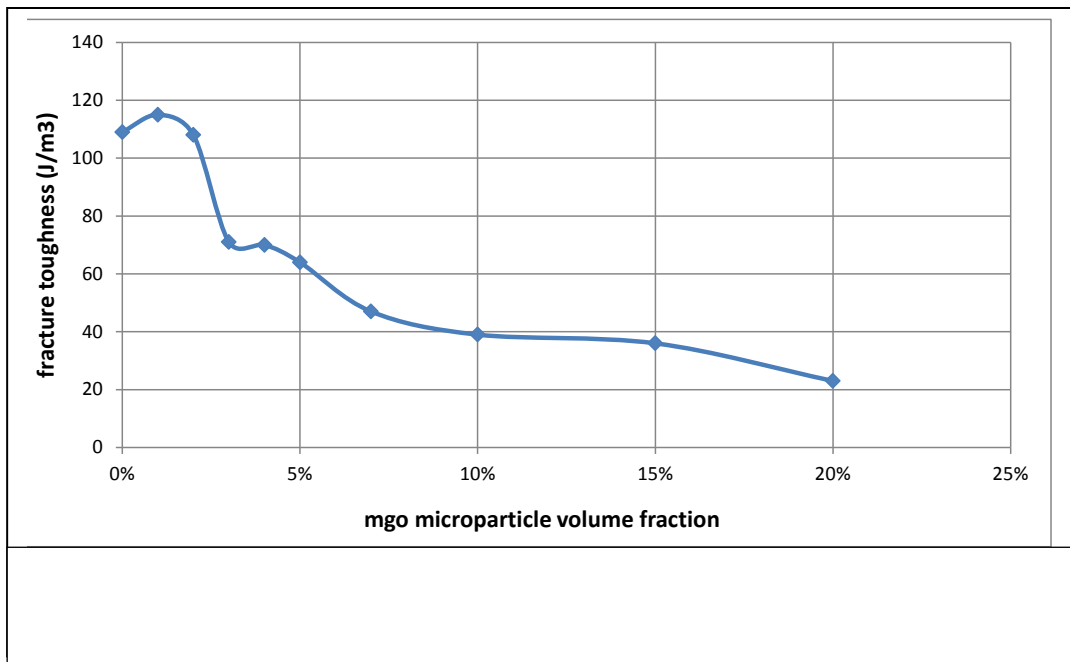
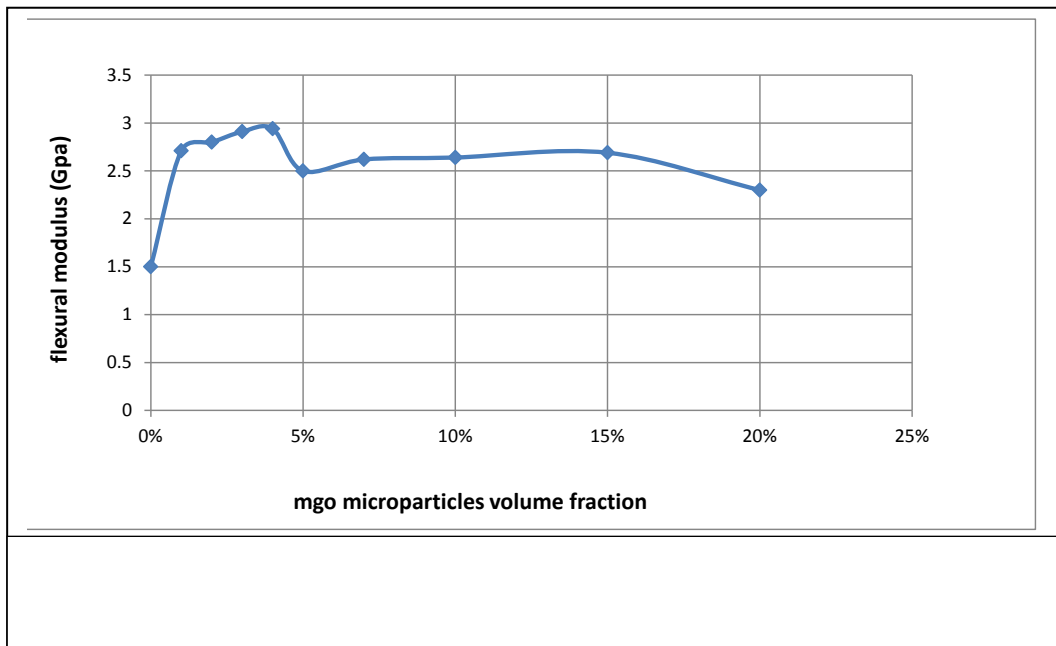


Figure (4-31) illustrate the behaviour of variation impact strength of EP/MgO microcomposites vs., MgO microparticles volume fraction. The Impact strength of EP/MgO microcomposites reduce with increasing the concentration of MgO microparticle

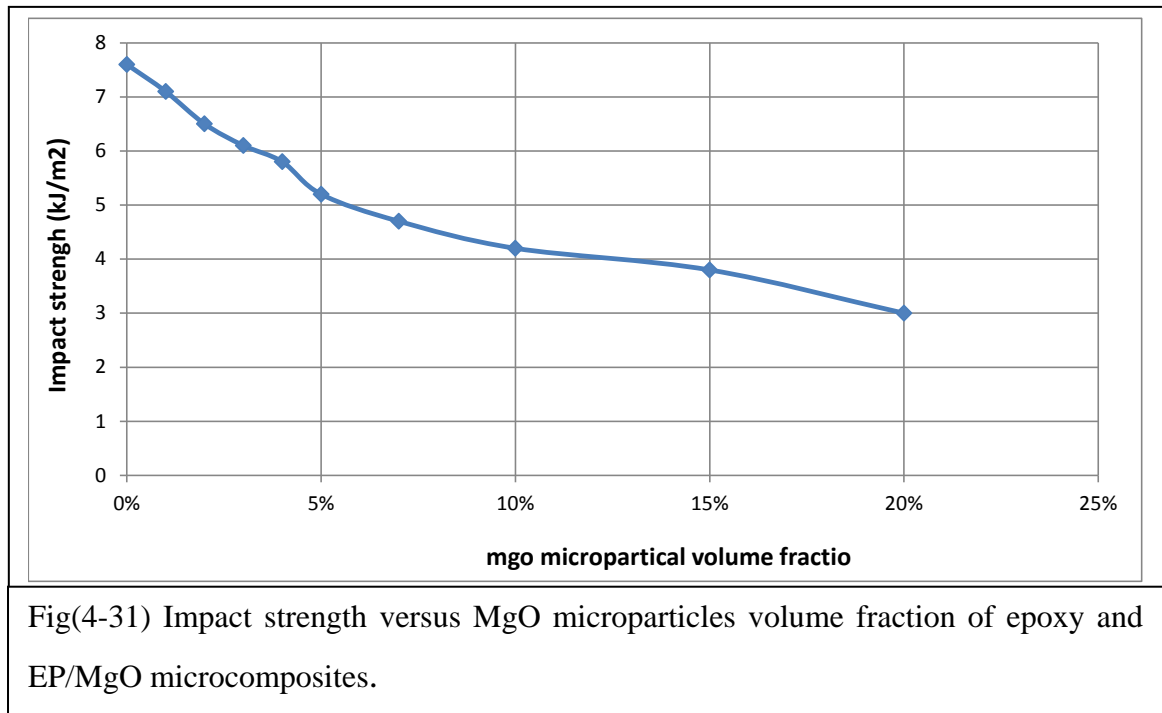
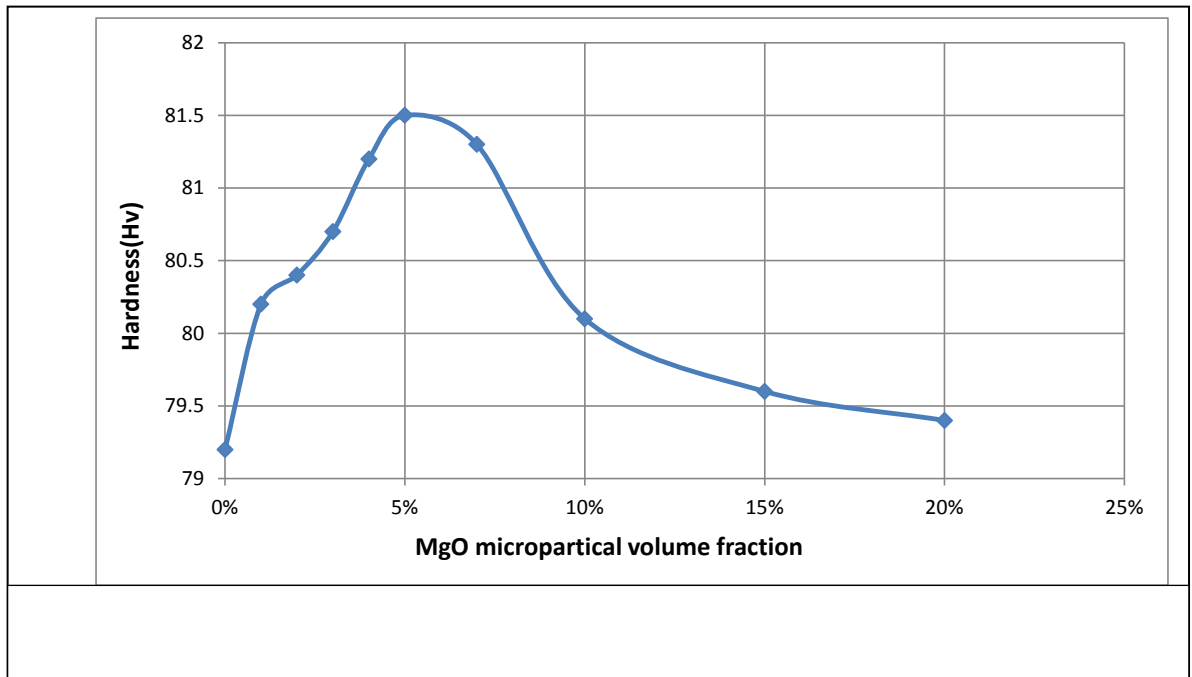


Figure (4-32) show the behaviour of variation hardness of EP/MgO microcomposites vs., MgO microparticles volume fraction. It can be observed that the addition of nano fillers into epoxy showed increases in the hardness of composites up to (< 5%) of addition. Then hardness begin to reduce



4-2.6 Scanning Electron Microscope (SEM) image of EP/MgO Nanocomposite topography of Fractured Structure

Figures ((4-33) – (4-40)) illustrate SEM image of the fractured structure topography of epoxy and EP/ MgO nanocomposites magnified to 30,000X its original scale.

Figure (4-33) shows; SEM image of the topography of fractured structure of epoxy while Figures (4-34, 4-35 and 4-36) illustrate; SEM images of the topography of fractured structure of EP/MgO nanocomposites with 1 ,2 and 3% vol. fraction of MgO nanoparticles have nanocracks of good agreement mode with figure (4-33) but less length ,width and distribution. Some of big agglomerations seemed signed by square, particles

de bonding also seemed signed by circle. New performance of fractured structure begin to appeared due to addition MgO nanoparticles.

Figure (4-37), illustrates SEM image of the of fractured structure of EP/MgO nanocomposites with 4% vol. fraction of MgO nanoparticles have different mode of nanocracks comparing with figures (4-34, 4-35 and 4-36). The nanocraks almost vanish from the structure due to MgO nanoparticles at 4% volum fraction of addition, MgO nanoparticles have good cohesion force between nanoparticles/epoxy chains arising from the polar of MgO nanoparticles and good surface porosity increasing resin viscosity, filling space distance between epoxy chains, all these reasons lead to chains contact one another and overcome issues of polymerisation begin at numerous regions and speeds, so, decreasing nanocracks structure (width and length) increasing crack resistance and crack pinning initiation. Agglomerations and particles de-bonding almost vanish from the structure because the balancing between MgO nanoparticles and epoxy matrix volume fraction ratio. Figures (4-38,4-39 and 4-40) illustrate SEM image of the of fractured structure of nanocomposites with 5,7and 10 % vol., fraction of

MgO nanoparticles, have a good agreement mode of nanocracks with figures (4-34, 4-35 and 4-36). In addition, figures (4-38, 4-39 and 4-40)illustrate nanoparticles agglomerations due to high volume fraction of MgO nanoparticles

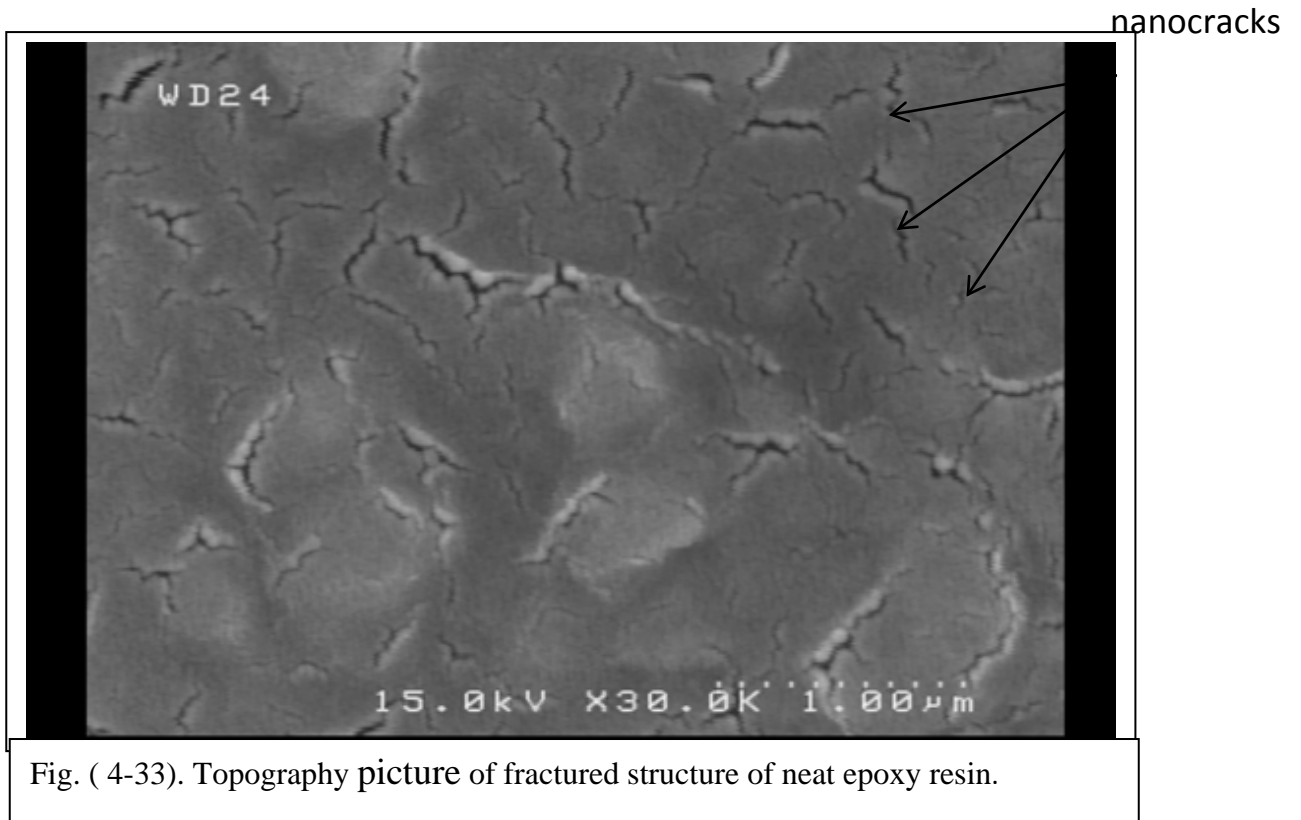
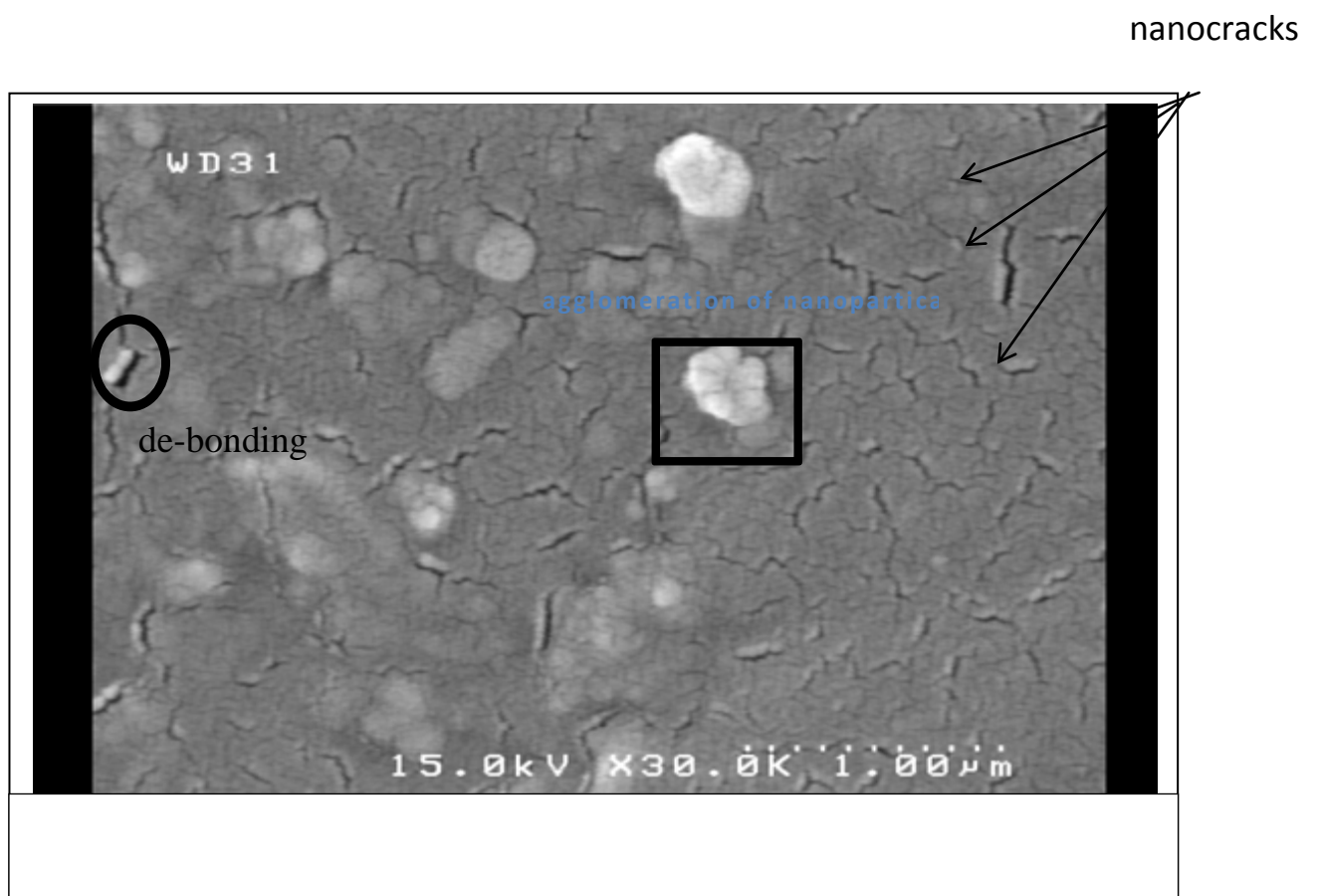


Fig. (4-33). Topography picture of fractured structure of neat epoxy resin.



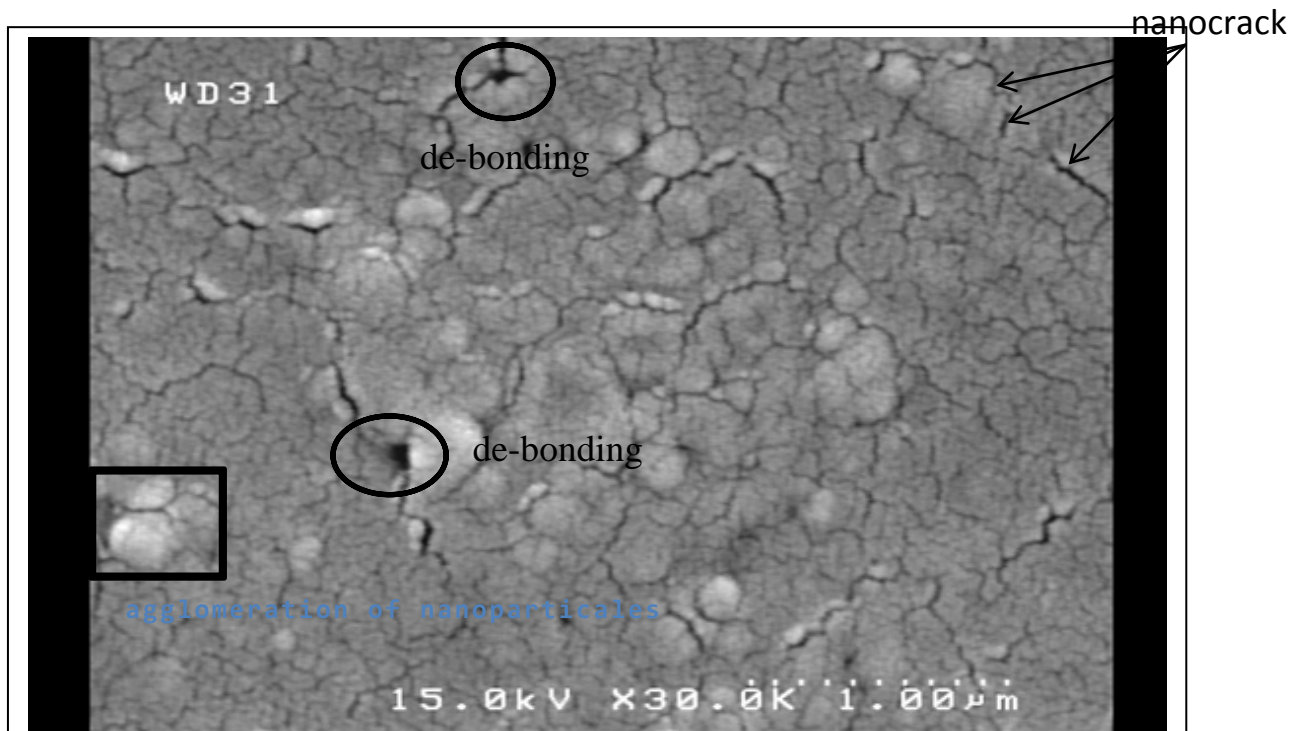
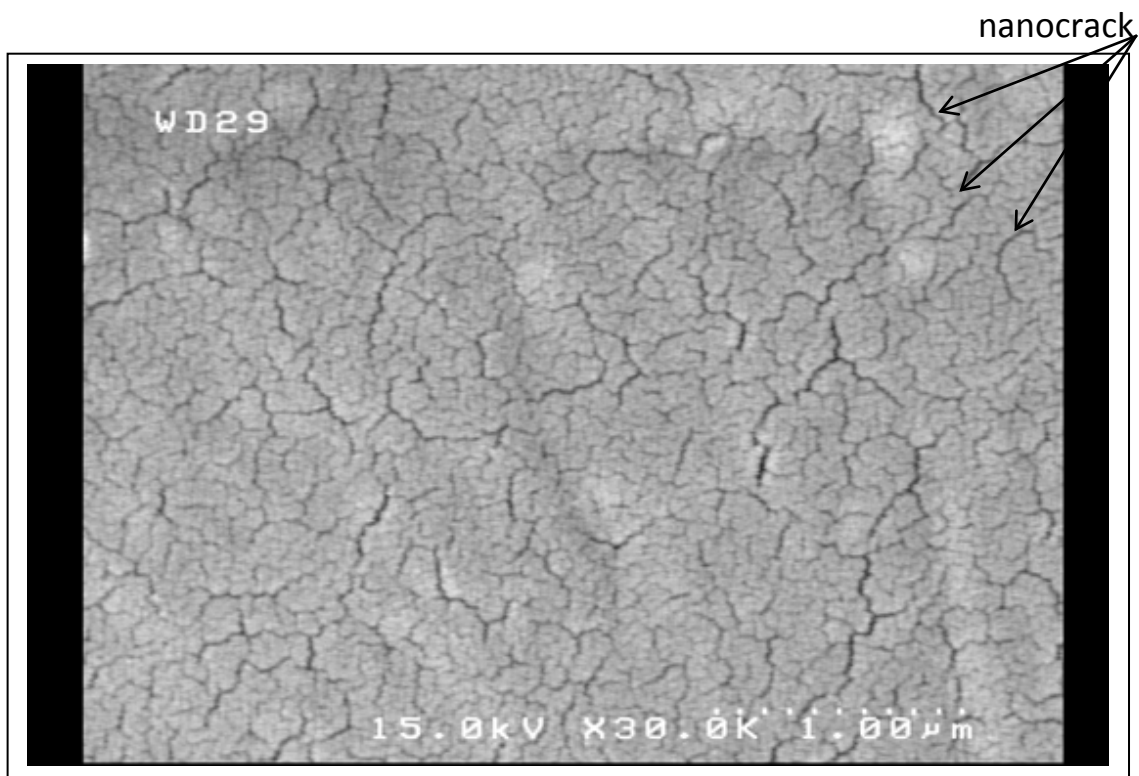
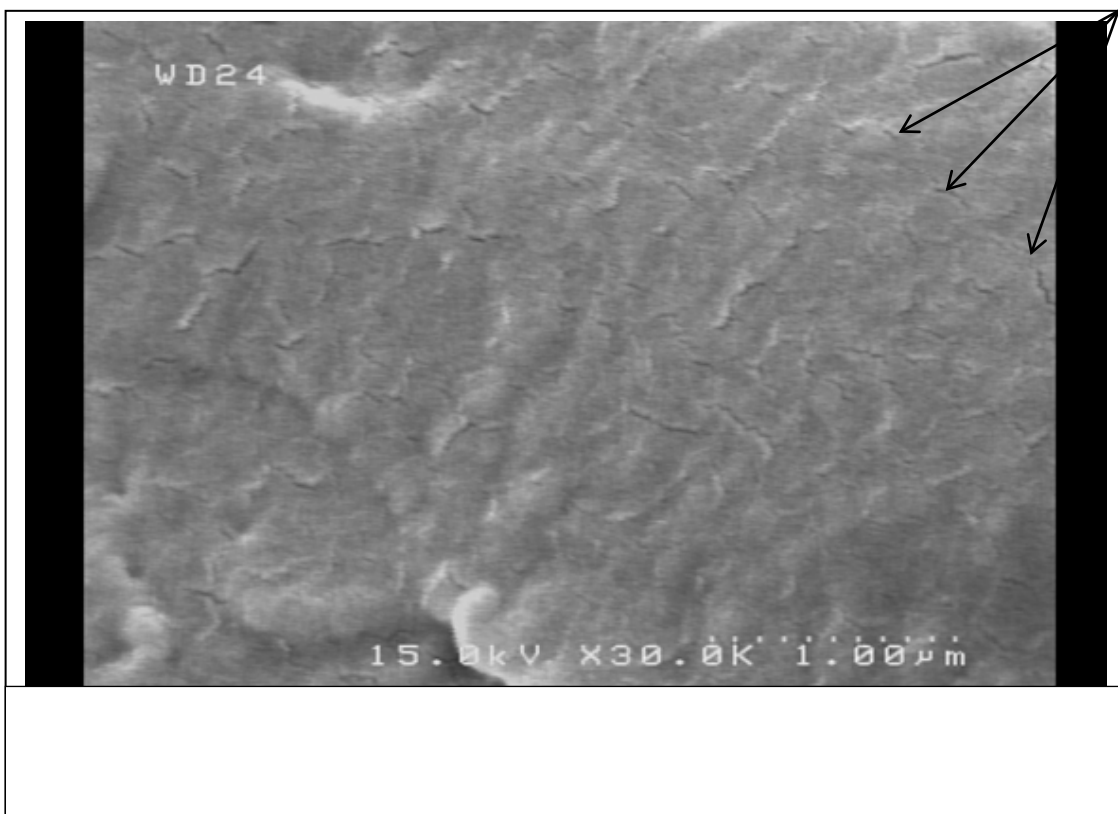


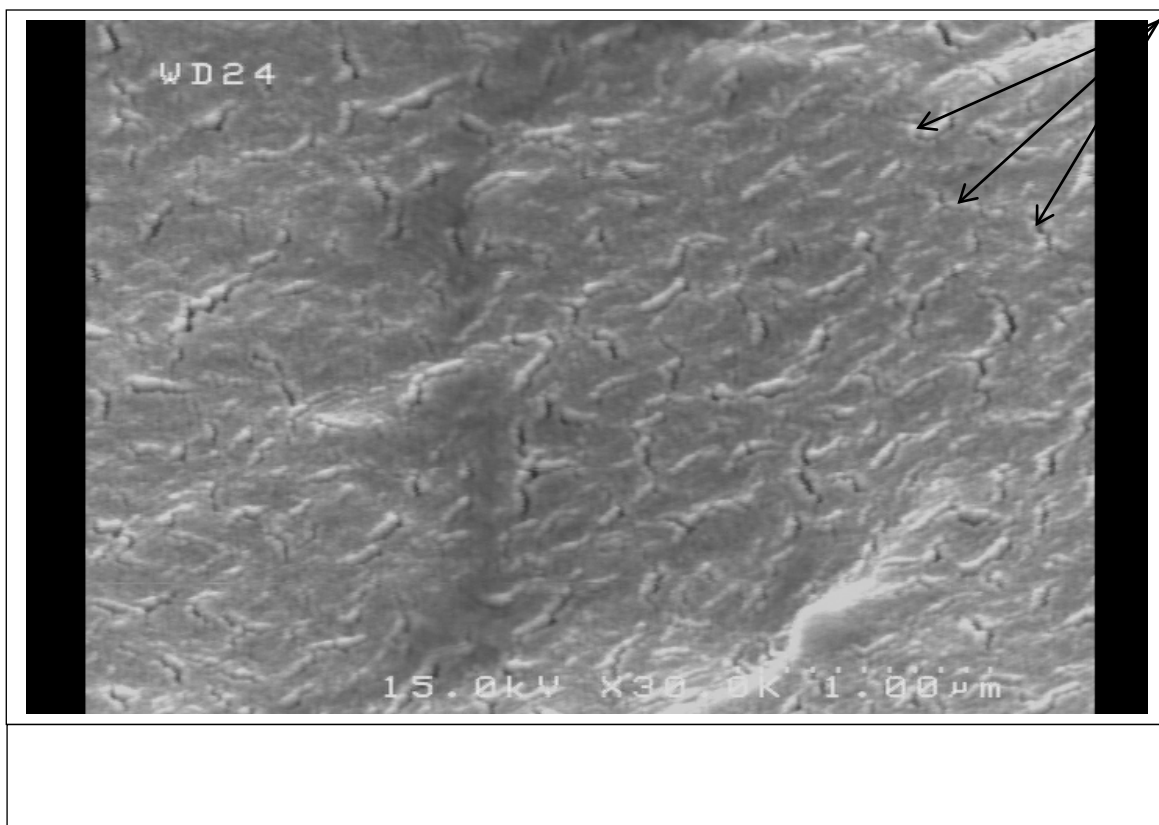
Fig. (4-35). Topography of fractured structure of EP/MgO nanocomposites (2% vol. fraction of / MgO).

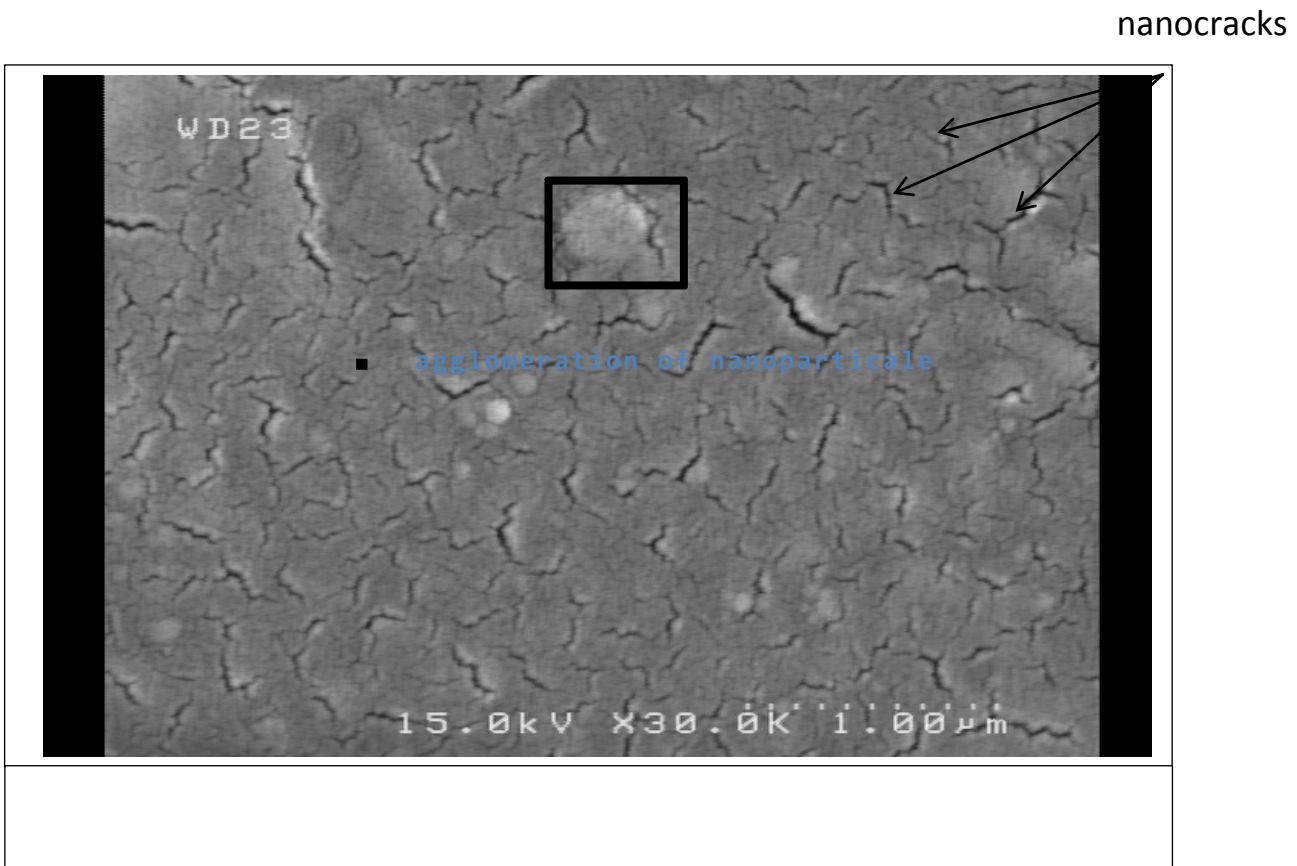
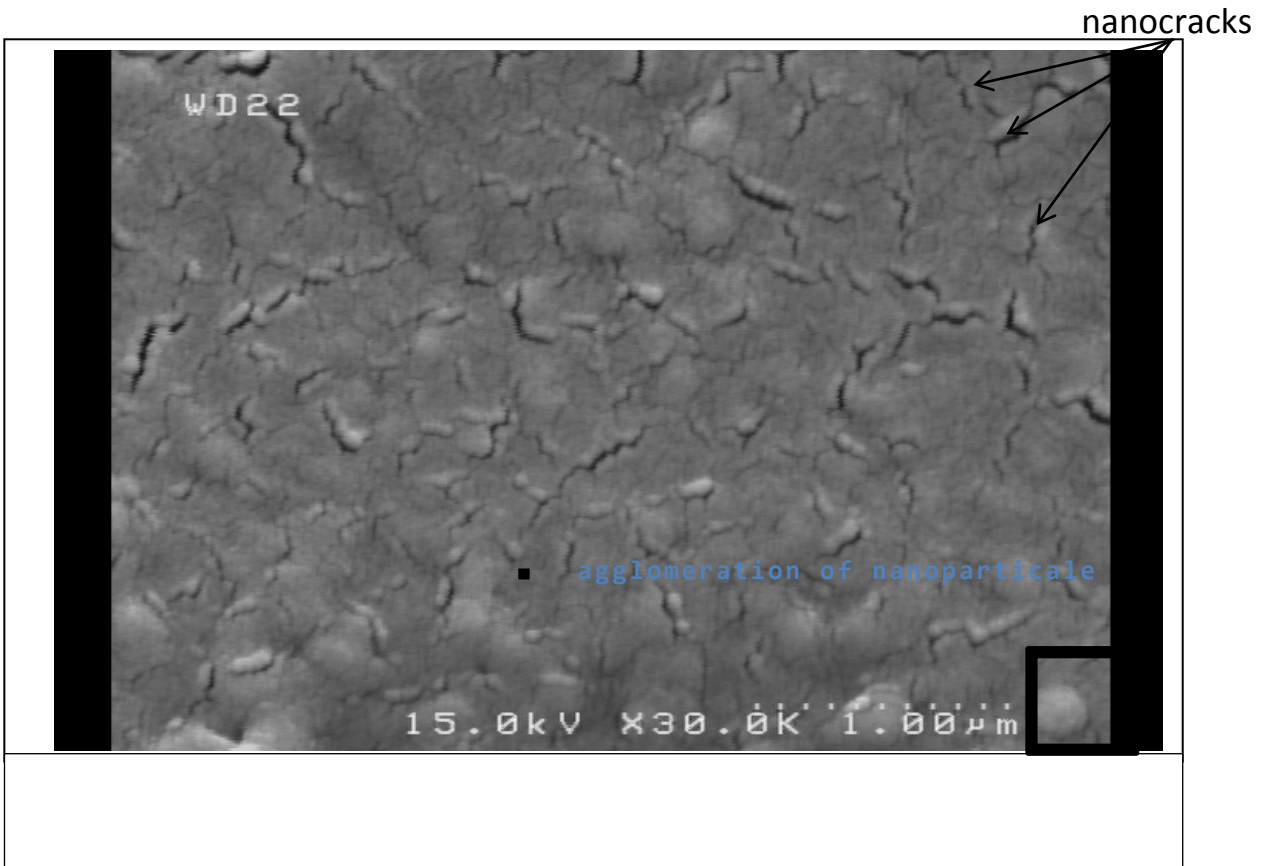


nanocrack



nanocracks

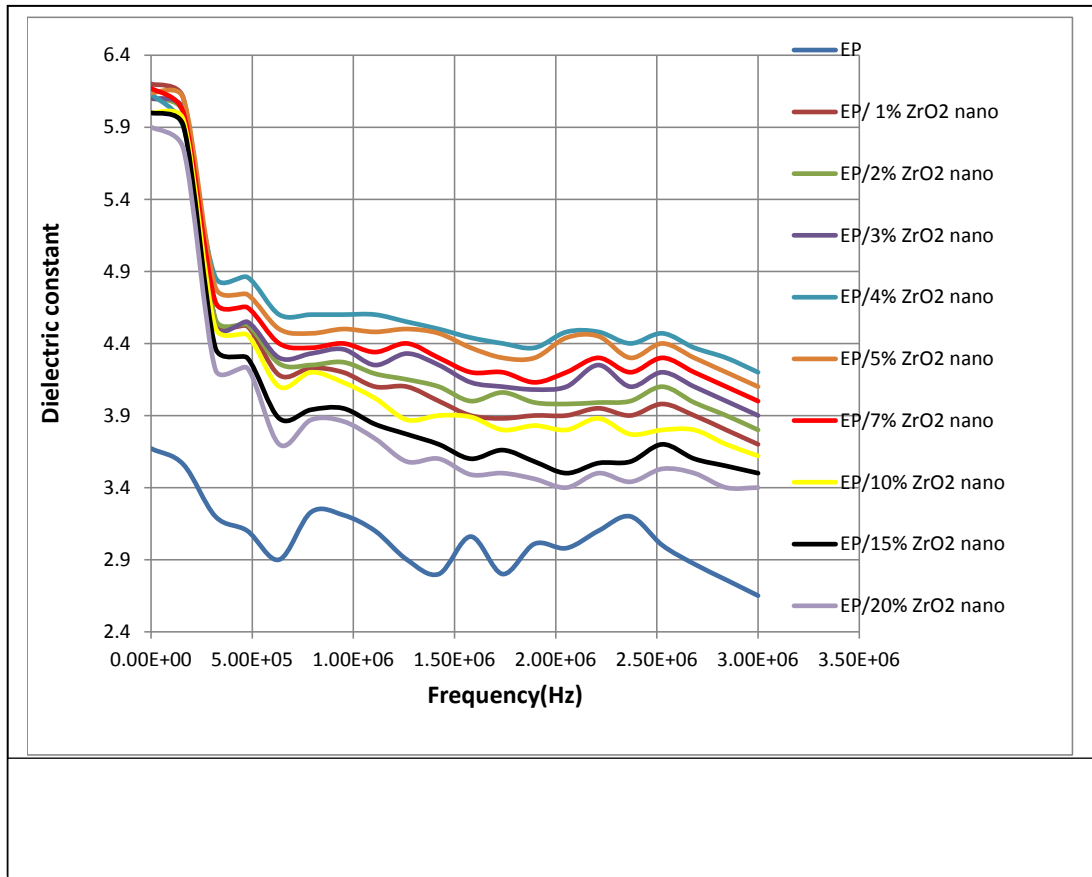




4-3 Electrical Properties

4-3.1 Dielectric constant of EP/ ZrO₂ Nanocomposites:

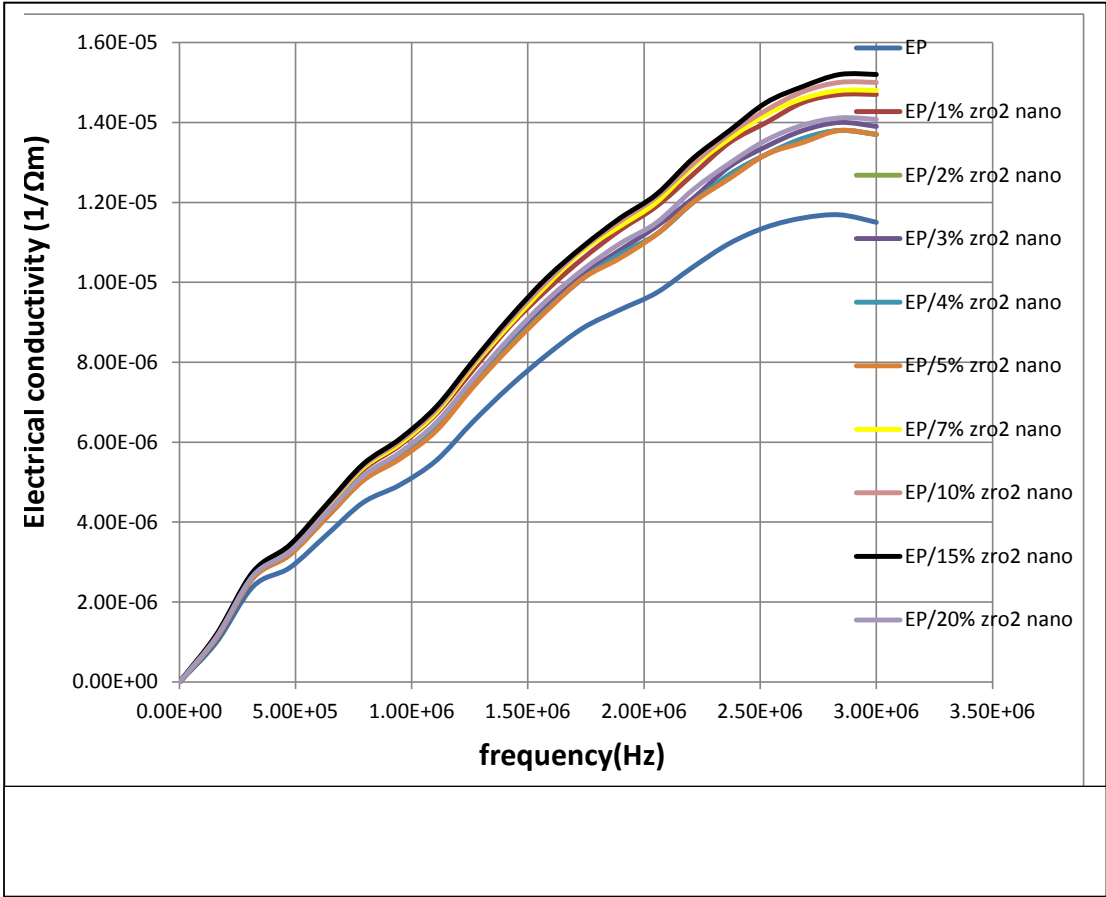
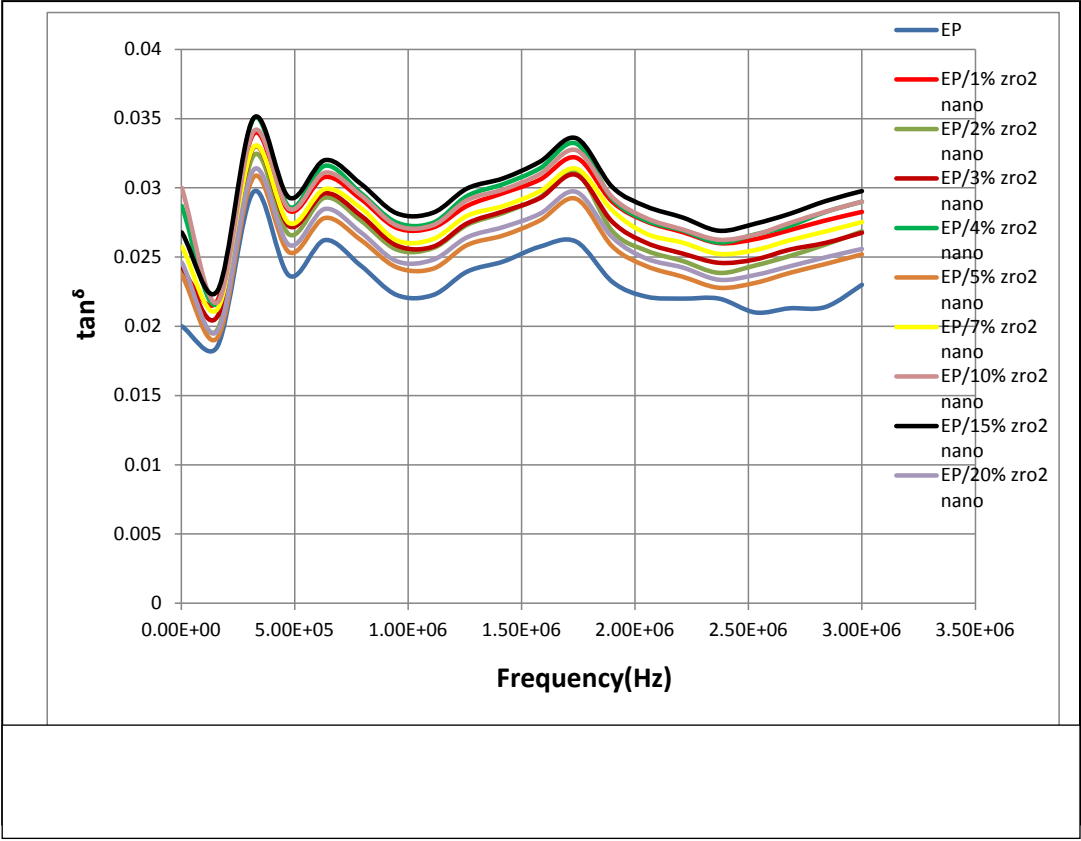
The variations of dielectric constant at frequency range 2×10^3 up to 3×10^6 for the epoxy and EP/ ZrO₂ nanocomposites with 1, 2, 3, 4, 5, 7, 10, 15 and 20% vol. fraction of ZrO₂ nanoparticles are shown in illustration (4-41) at room temperature. Nanocomposites have a large concentration of epoxy-nanoparticles interfaces because of large surface zone of nanoparticles, therefore the most dominated polarizations kind are interfacial polarizations [42]. The high dielectric constant value of the epoxy and EP/ ZrO₂ nanocomposites at low frequencies of imposed voltage is due to free dipolar functional sets of epoxy chains which orientate themselves with the imposed voltage, this preform to high dielectric constant, while at intermediate and higher frequencies of imposed voltage (duration of imposed voltage is very short) several of non-free dipolar functional sets will not respond to the imposed voltage which lead to decrease dielectric constant [103], as shown in illustration (4-41). The dielectric constant of EP/ZrO₂ nanocomposites illustrated almost flat region till to 3×10^6 Hz . The dielectric constant of EP/ ZrO₂ nanocomposites with 1, 2, 3, 4, 5 and 7% vol. fraction of ZrO₂ nanoparticles increase in clear manor comparing with the dielectric constant of the epoxy, this behavior of the dielectric constant of EP/ ZrO₂ nanocomposites could be due to the influence of the dielectric constant of ZrO₂ nanoparticles which have higher dielectric constant [54] than that of epoxy.



The dielectric constant of EP/ ZrO₂ nanocomposites with 10, 15 and 20% vol. fraction of ZrO₂ nanoparticles begin to reduce from maximum improvement with increasing concentration of ZrO₂ nanoparticles, but still higher than that of epoxy. The rise of high immobile epoxy nano-layer formed around ZrO₂ nanoparticles is due to the rise of the concentration of nanoparticles, and hence epoxy chains about and close to the nanoparticles surface, decrease the dielectric constant of EP/ ZrO₂ nanocomposites in addition to the overlapping of interaction region of nanoparticles with percolation during the interaction region, working together in reverse way of the effect of the dielectric constant of ZrO₂ nanoparticles to decrease the dielectric constant of EP/ ZrO₂ nanocomposites, this behavior is in a good agreement with Najiba [54] and Singha [42].

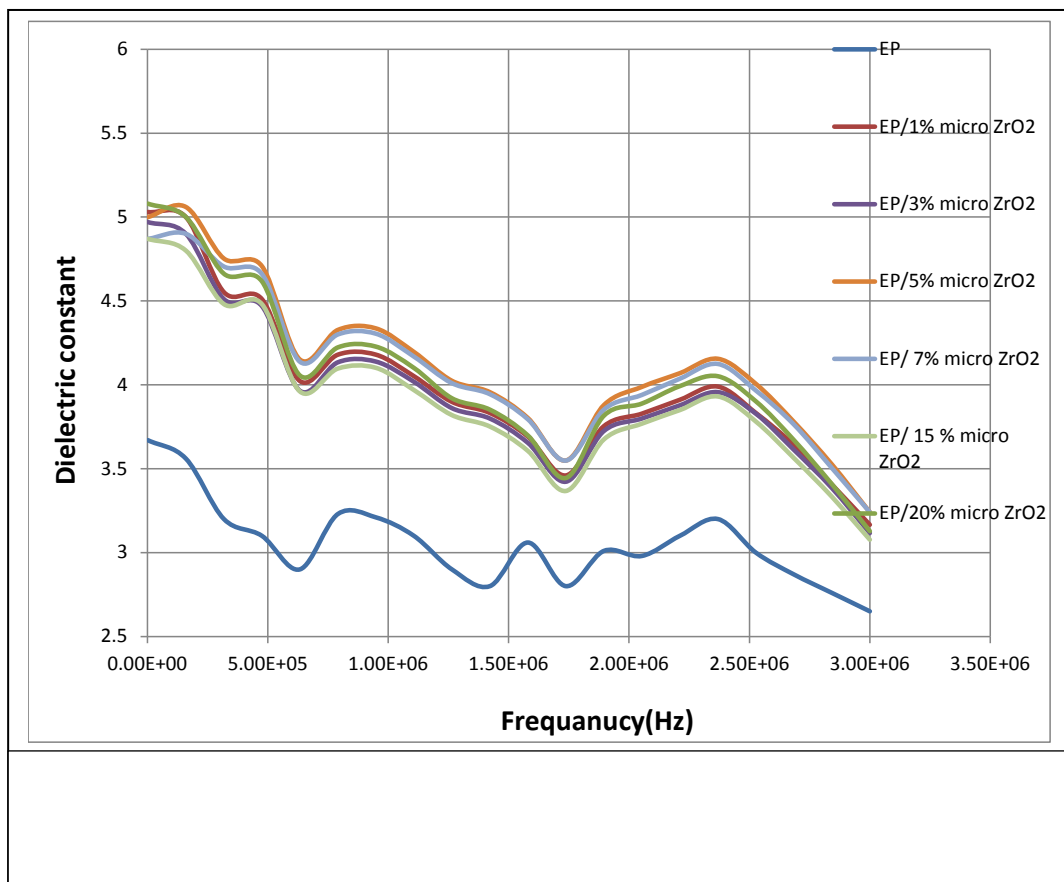
4-3.2 Tan Delta of EP/ ZrO₂ Nanocomposites

The differences of tan delta at the frequency for epoxy and EP/ ZrO₂ nanocomposites with 1, 2, 3, 4, 5, 7, 10, 15, 20% vol. fraction of ZrO₂ nanoparticles at room temperature are shown in illustration (4-42). Some mechanisms dominate the value of tan delta. First, tan delta adopted on the electrical conductivity into composites material and the electrical conductivity adopted on the number of charge carriers and frequency of the imposed electric field on the composites. The rises of volume fraction of ZrO₂ nanoparticles in epoxy/ZrO₂ nanocomposites improved the sources of charge carriers. The charge carriers can passage though the overlapping interaction regions of (ZrO₂,) nanoparticles into the epoxy matrix of EP/ (ZrO₂,) nanocomposites. The overlapping of interaction region (percolation influence) depends on; filler content of (ZrO₂) nanoparticles, dispersion of (ZrO₂) nanoparticles and the size of (ZrO₂) nanoparticles. The differences of tan delta at frequency for the epoxy and both epoxy- ZrO₂ nanocomposites with 1, 2,3, 4, 5, 7, 10,15 and 20 % vol. fraction of epoxy-ZrO₂ nanoparticles at room temperature are shown in figure (4-42). Tan delta of EP/ ZrO₂ nanocomposites have the same behavior with deferent frequency . This behaviour refer to balancing in the mechanisms that effect on the electrical conductivity as shown in figure (4-43)



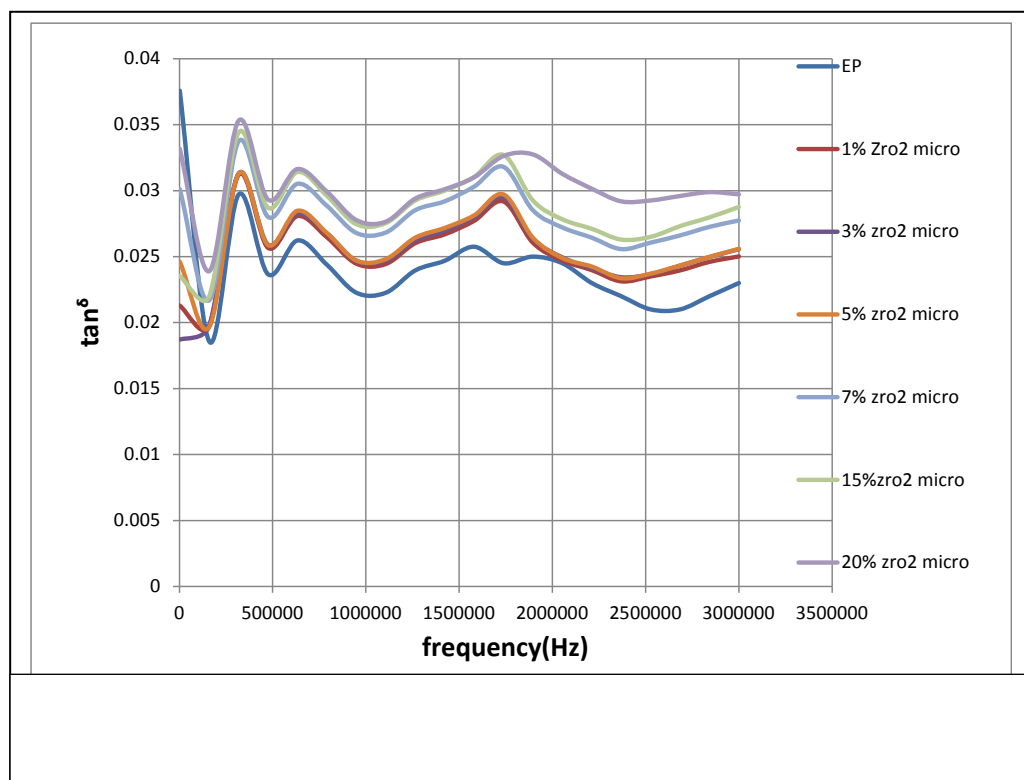
4-3.3 Dielectric constant of EP/ ZrO₂ Microcomposites

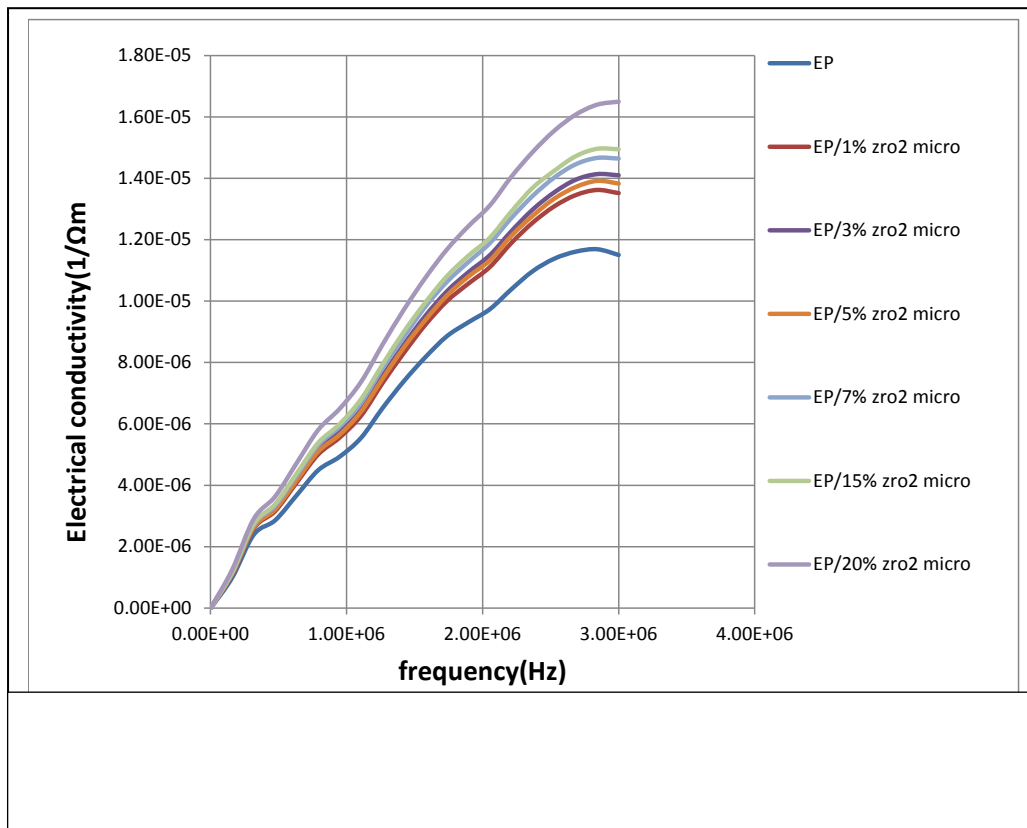
The variations of dielectric constant at frequency for epoxy and EP/ ZrO₂ microcomposites with 1, 3, 5, 7, 15, 20% vol. fraction of ZrO₂ microparticles at room temperature are shown in illustration (4-44). The dielectric constant of the epoxy and EP/ ZrO₂ microcomposites reduce with increasing frequency of the imposed electric field. The dielectric constant of ZrO₂ microcomposites have almost the same performance for all volume fraction of ZrO₂ microparticles, where the influence of the dielectric constant of ZrO₂ microparticles which is higher than that of epoxy increasing the dielectric constant of EP/ ZrO₂ microcomposites. The dielectric constant of EP/ ZrO₂ microcomposites are slightly lower than that of EP/ ZrO₂ nanocomposites, that probably because of the fact that there are large number of charge carriers in ZrO₂ nanoparticles then that for ZrO₂ microparticles .



4-3.4 Tan Delta of EP/ ZrO₂ Microcomposites

The differences of tan delta at frequency for epoxy and EP/ZrO₂ microcomposites with 1, 3, 5, 7, 15 and 20% vol. fraction of ZrO₂ microparticles at room temperature are shown in illustration (4-45). At low concentrations (1, 3, and 5% vol. fraction of ZrO₂ microparticles) tan delta show the same performance of tan delta of epoxy where no increase in charge carriers at low vol. fraction of ZrO₂ microparticles. The rise in volume fractions of ZrO₂ microparticles (7, 15 and 20% vol. fraction of ZrO₂ microparticles) show slightly rise in tan delta at intermediate frequency when increasing charge carriers. The electrical conductivity as shown in figure (4-46) could be happen from water molecules present in the surface of ZrO₂ microparticles, this performance in a good agreement with Nelson [104].

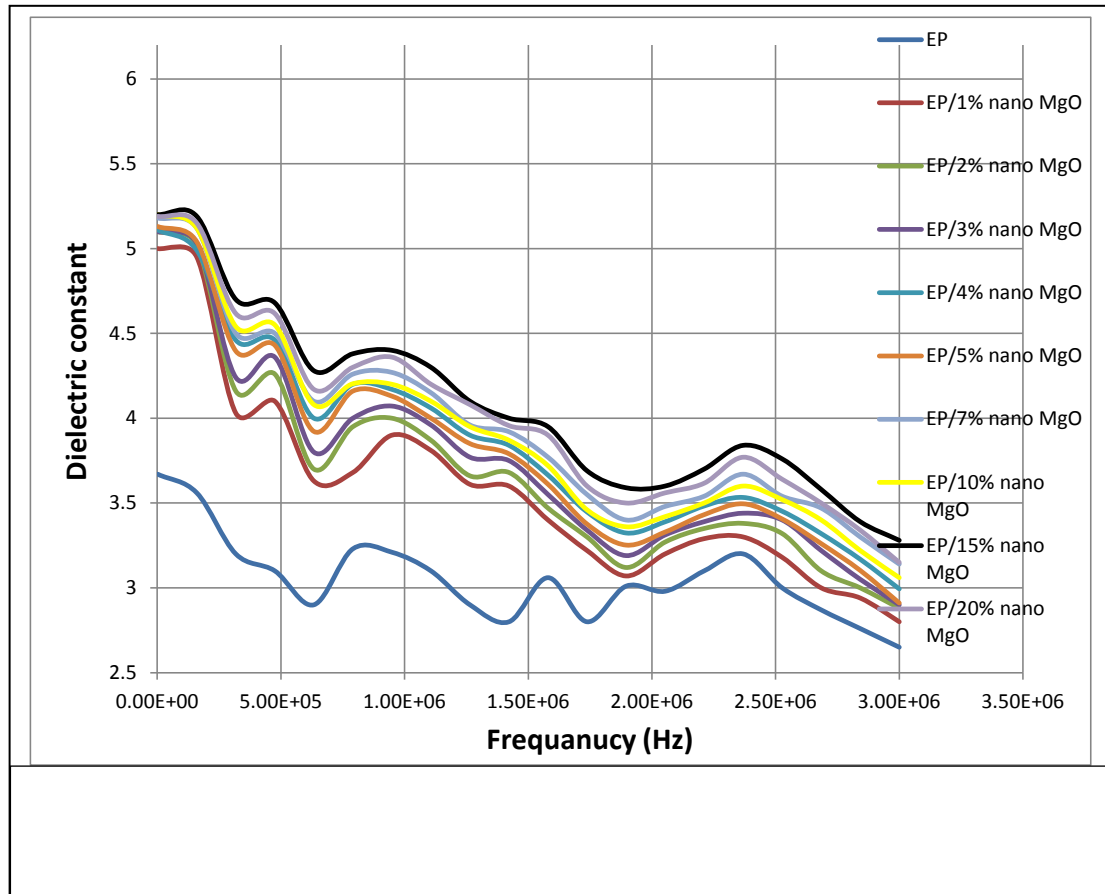




4-3.5 Dielectric constant of EP/ MgO Nanocomposites:

The variations of dielectric constant at frequency for epoxy resin and EP/MgO nanocomposites with 1, 2, 3, 4, 5, 7, 10, 15, 20% vol. fraction of MgO nanoparticles at room temperature are shown in illustration (4-47). The general performance of dielectric constant of the epoxy and EP/ MgO nanocomposites is reduce with increasing of the frequency of the imposed voltage. There are some theories to explain and discuss the performance of the dielectrical properties of epoxy nanocomposites in many investigates, on other hand, there are some parameters could be affect the dielectrical properties of epoxy nanocomposites such as the concentration of nanoparticles, imposed field frequency, distribution and dispersion of nanoparticles and size and kind of nanoparticles. The dielectric constant is ruled by the number of orient able

dipoles existing in the epoxy matrix (also in epoxy nanocomposites) and their ability to orient under an imposed electric field [73].



The dielectric constant of EP/ MgO nanocomposites at low volume fraction (1,2,3,4,5 and 7% vol. fraction of MgO nanoparticles) was higher increased comparing to the dielectric constant of epoxy, this behavior of the dielectric constant of EP/ MgO nanocomposites because the effect of the dielectric constant of MgO nanoparticles in the dielectric constant of EP/ MgO

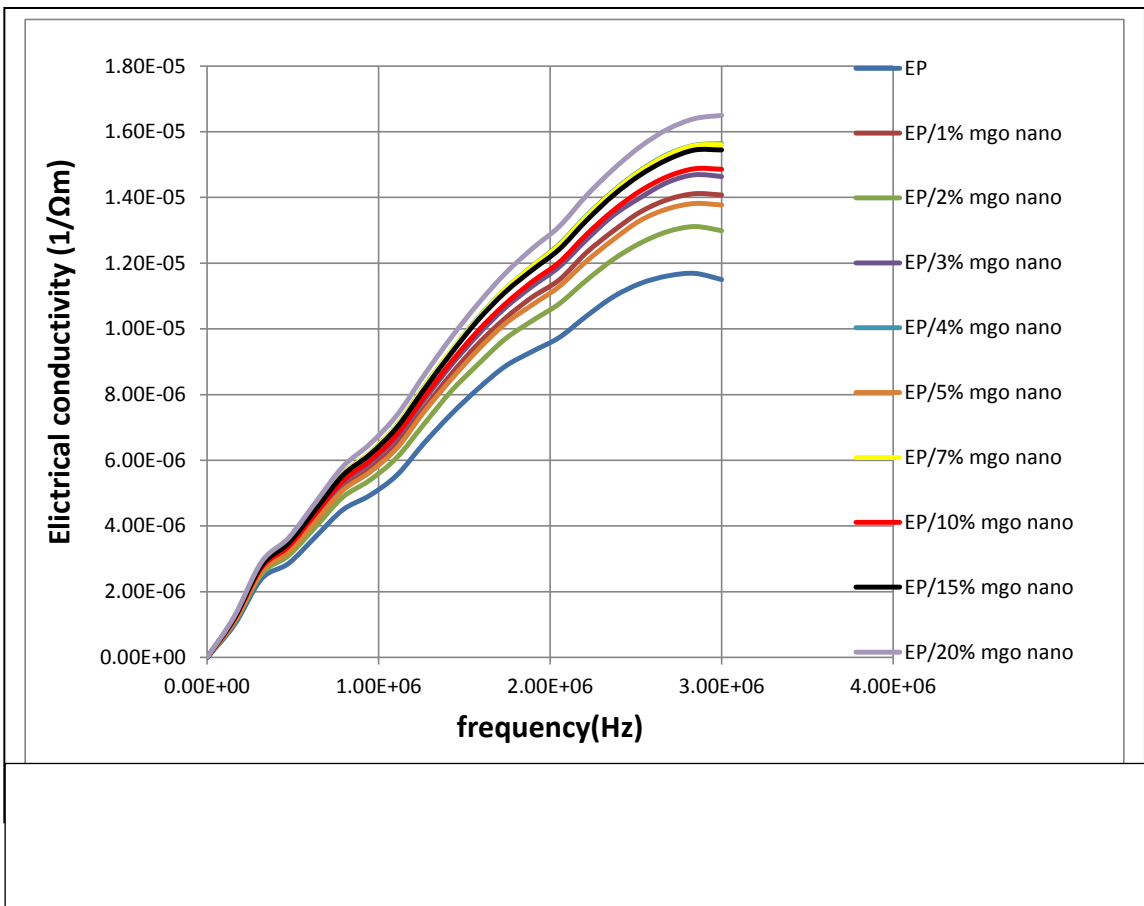
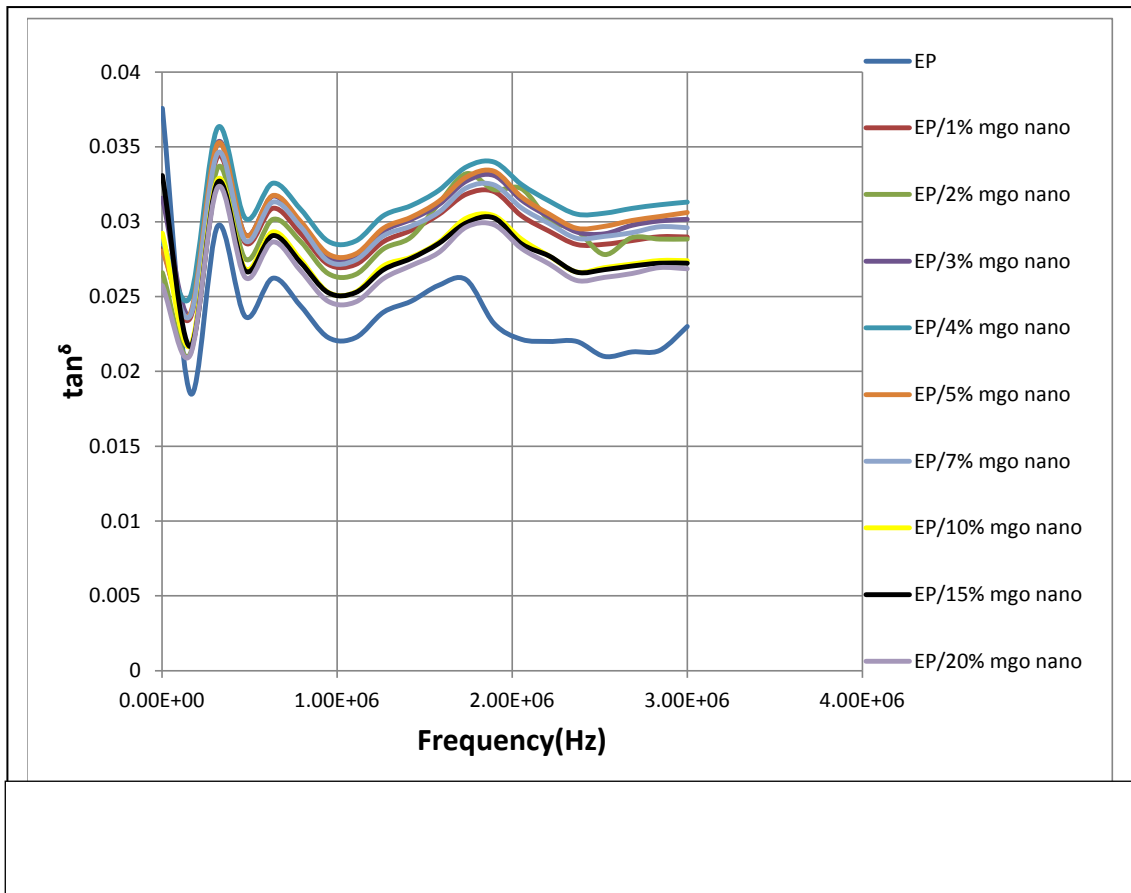
. The corporation of the dielectric constant of MgO nanoparticles was the controlled mechanism in increasing the dielectric constant of EP/ MgO nanocomposites, this performance is in a good agreement with Singha [42]. The dielectric constant of EP/ MgO nanocomposites reduce again at 10 and 20% vol. fraction of MgO nanoparticles. The effect of the overlapping of the

interaction region of nanoparticles and the percolation influence through the interaction region decrease the dielectric constant of EP/ MgO nanocomposites.

4-3.6 Tan Delta of EP/ MgO Nanocomposites

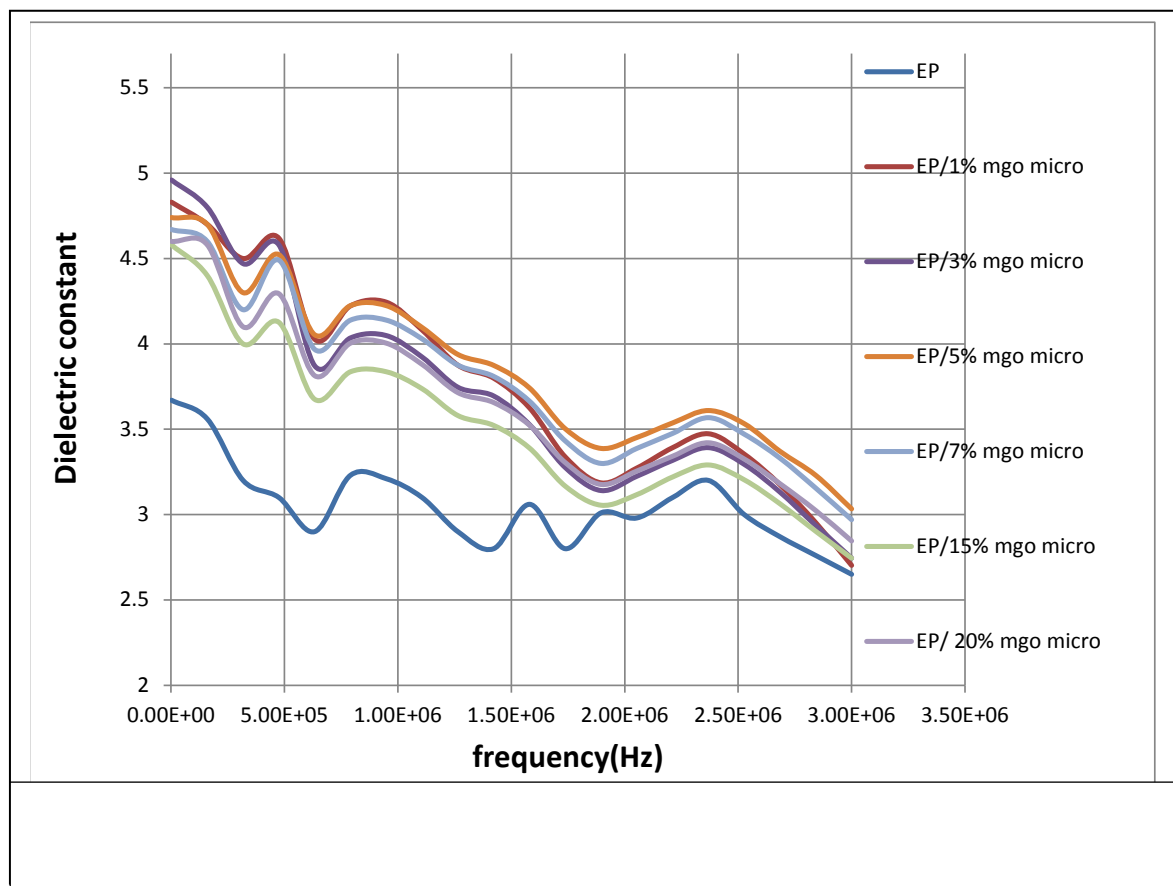
The differences of tan delta at the frequency for epoxy and EP/ MgO nanocomposites with 1, 2, 3, 4, 5, 7, 10, 15, 20% vol. fraction of MgO nanoparticles at room temperature are shown in illustration (4-48). Tan delta rises with increasing the concentration of MgO nanoparticles in EP/ MgO nanocomposites specially at low concentration with 1,2,3,4,5 and 7% vol. fraction of MgO nanoparticles comparing with tan delta of epoxy. MgO nanoparticles rise the charges carrier in the nanocomposites through; the nature of MgO nanoparticles (metal structure) and the interaction region. The overlapping of interaction region depends on the volume fraction of MgO nanoparticles, dispersion of MgO nanoparticles and the size of MgO nanoparticles, when, as small as nanoparticles size the overlapping of interaction regions and percolation effect increased. The tan delta of EP/ MgO nanocomposites with changed volume fractions show almost the same performance, this performance of unchanged tan delta denote to balancing in the mechanisms that affect tan delta. The low concentration lead to low percolation effect with low immobile epoxy nano-layer formed about nanoparticles, at high volume fraction high percolation effect with high immobile epoxy resin nano-layer formed about nanoparticles .

Increasing the concentration of MgO nanoparticles and small nanoparticles size improve electrical conductivity as shown in illustration. (4-49). , and hence, tan delta. This performance is in a good agreement with Singha [42].



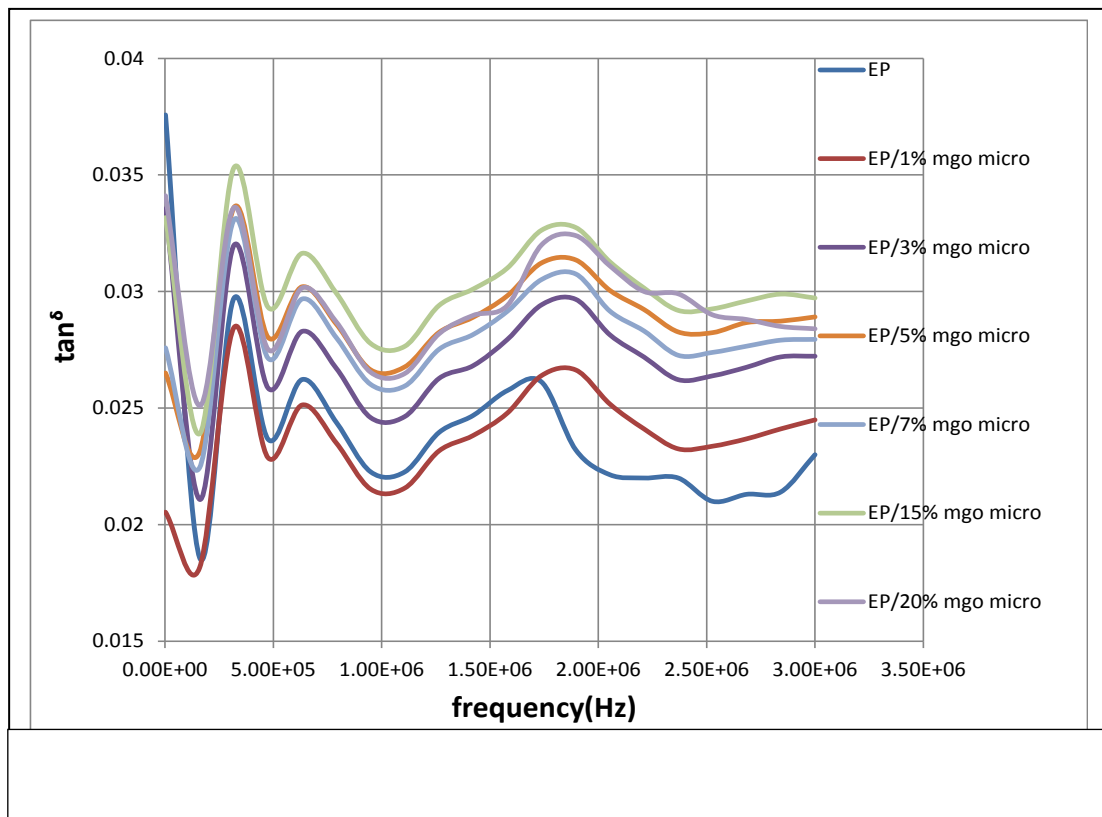
4-3.7 Dielectric constant of EP/ MgO Microcomposites

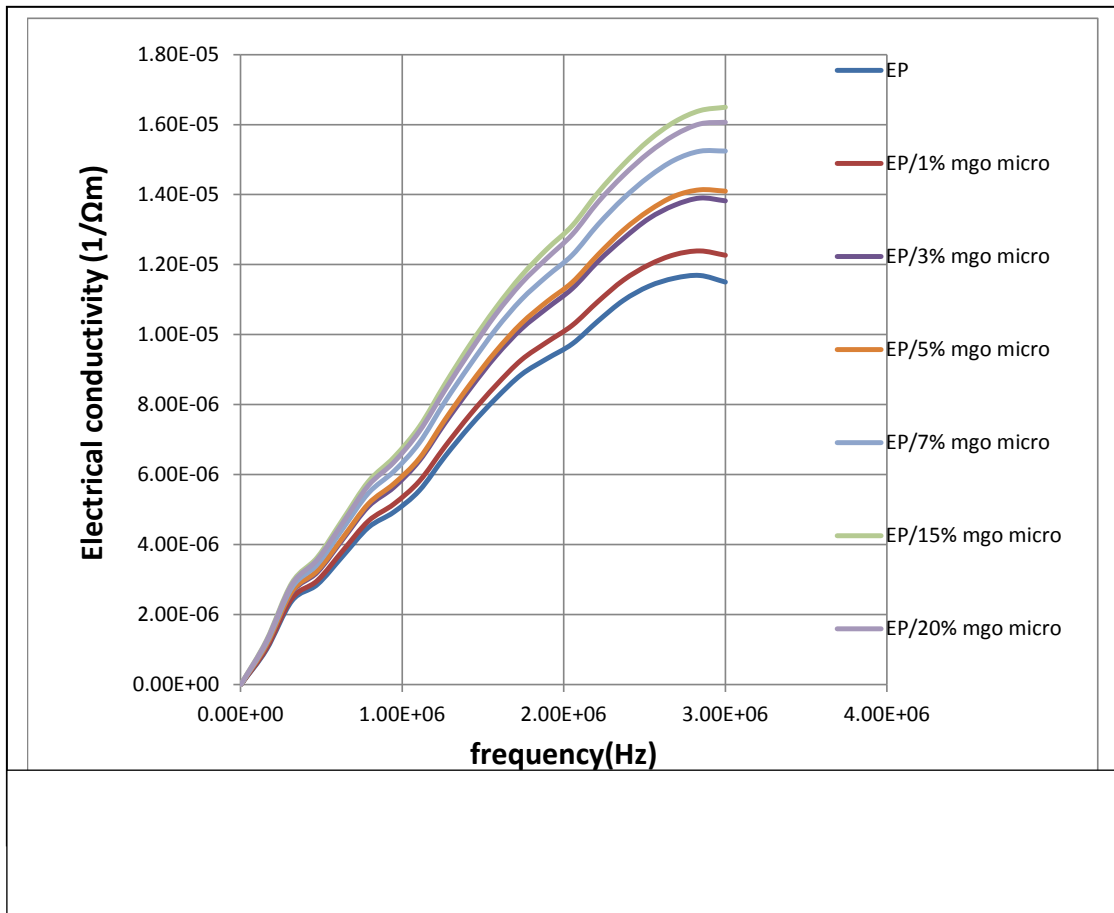
The variations of dielectric constant with frequency for epoxy and EP/ MgO microcomposites with 1, 3, 5, 7, 15, 20% vol. fraction of MgO microparticles at room temperature are shown in illustration (4-50). The dielectric constant of epoxy and EP/ MgO microcomposites reduce with increasing frequency of imposed electric field. The dielectric constant of MgO microcomposites have almost the same performance for all concentration of MgO microparticles, where the effect of the dielectric constant of MgO microparticles which is higher than that of epoxy increasing the dielectric constant of EP/ MgO microcomposites. The dielectric constant of EP/ MgO microcomposites are slightly lower than that of EP/ MgO nanocomposites, that probably because of the fact that there are large number of charge carriers in MgO nanoparticles then that MgO microparticles.



4-3.8 Tan Delta of EP/ MgO Microcomposites:

The differences of tan delta with frequency for the epoxy and EP/ MgO microcomposites with 1, 3, 5, 7, 15 and 20% vol., fraction of MgO microparticles at room temperature are shown in illustration (4-51). Tan delta in composites material adopted on the number of charge carriers and the frequency of the imposed electric field in the composites. The tan delta of EP/ MgO microcomposites have similar performance tan delta of EP/ MgO nanocomposites ,where growing charge carriers in microcomposites arise from; defects, poor particles-epoxy bonding, the nature of MgO microparticles which have tendency to absorb water at the surface lead to tan delta increments. illustration (4-52), shows that the electrical conductivity are increasing with increasing the vol., fraction of addition of MgO microparticles.





4-4. Thermal properties

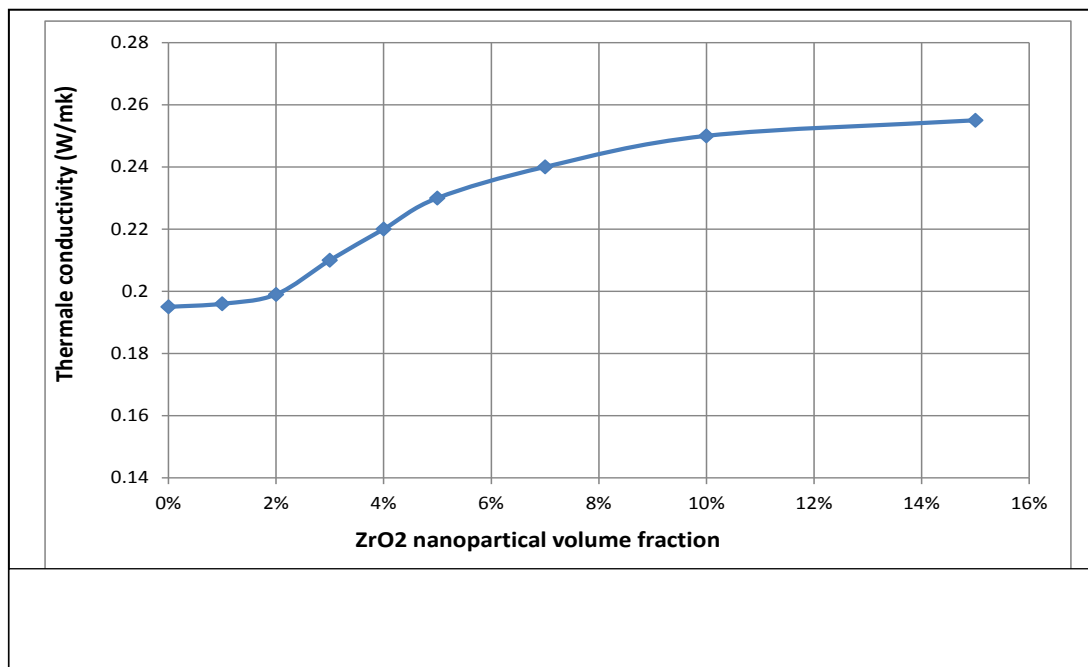
4-4.1. Thermal conductivity

4-4.1.1 Thermal conductivity of EP/ ZrO₂ nanocomposites

Thermal conductivity behaviour for epoxy and EP/ZrO₂ nanocomposites filled with 0,1, 2, 3, 4, 5, 7, 10, 15 and 20% vol. fraction are shown in figure (4-53). The general performance of thermal conductivity of EP/ ZrO₂ nanocomposites is increase with increasing of the volume fraction ZrO₂ nanoparticle. there are some parameters could be affect the thermal conductivity of epoxy nanocomposites such as It has been found that filler size, , concentration ,geometry, dispersion, crystal structure, orientation, and

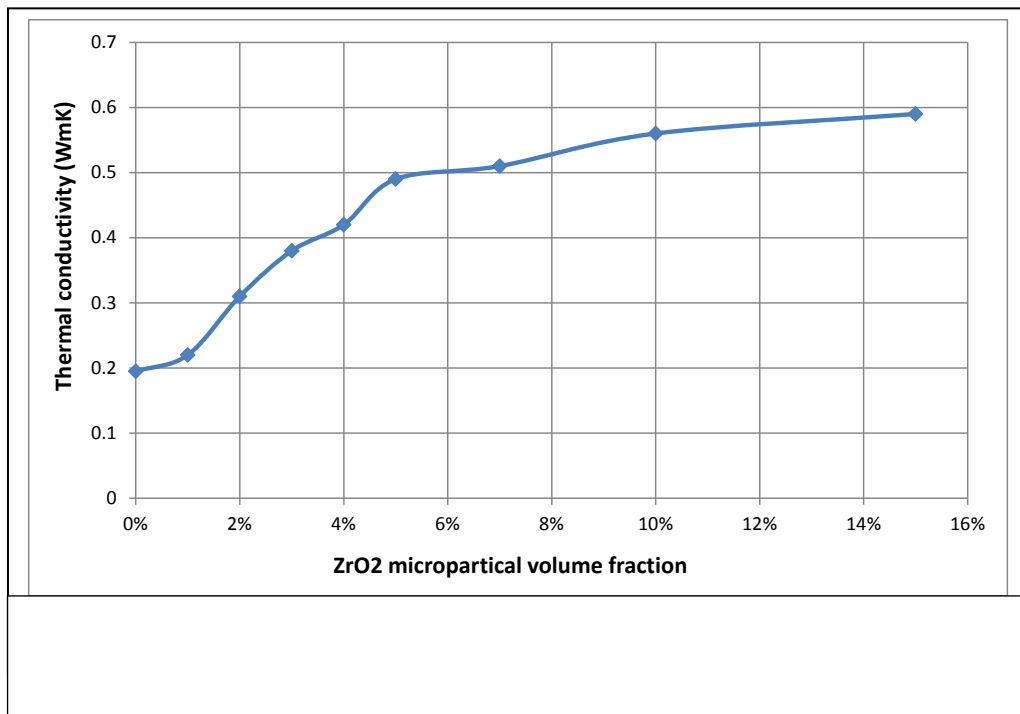
interface between the polymer matrix and filler affect the thermal conductivity of the host polymer [13].

The thermal conductivity of EP/ ZrO₂ nanocomposites at low volume fraction (1 and 2% vol. fraction of ZrO₂ nanoparticles) was slightly increased comparing to the thermal conductivity of epoxy because of ZrO₂ nanoparticles have the large interfacial areas and interfacial thermal resistance, which cause higher levels of phonon scattering. The thermal conductivity of EP/ ZrO₂ nanocomposites at higher volume fraction (3, 4, 5,7,10 and 15% vol. fraction of ZrO₂ nanoparticles) increases because the effect of the thermal conductivity of ZrO₂ nanoparticles in the thermal conductivity of EP/ ZrO₂ nanocomposites begin to appear in obvious manner , That is because the porosity of the pure sample is greater than the other samples which are doped with ZrO₂, and also because the thermal conductivity of ZrO₂ is larger than epoxy resin.



4-4.1.2 Thermal conductivity of EP/ ZrO₂ microcomposites

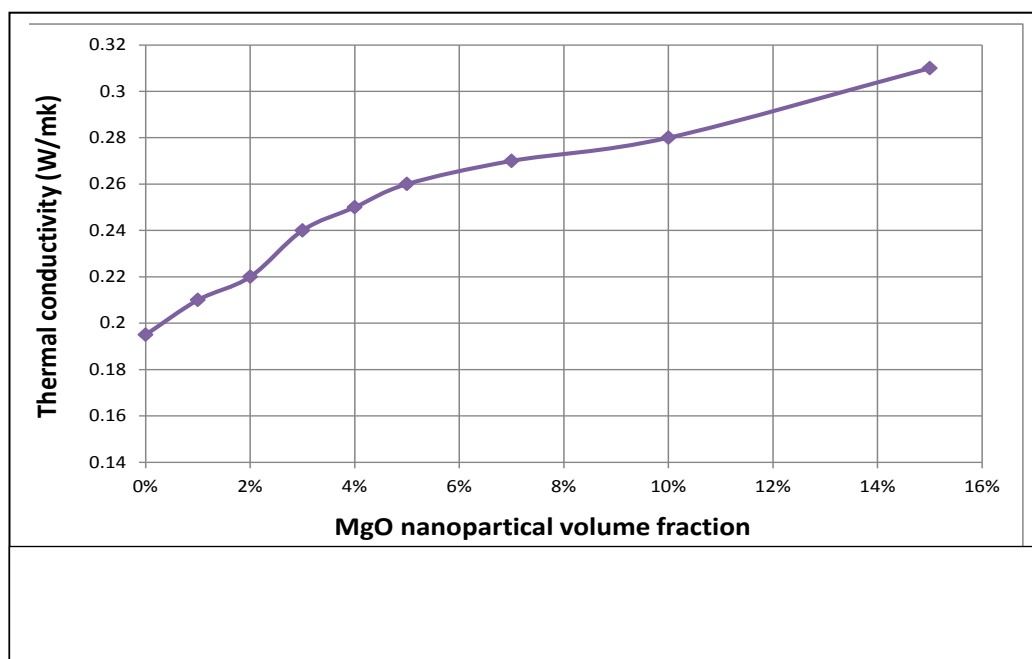
Fig(4-54).shows the Thermal conductivity of EP/ ZrO₂ microcomposites , where the Thermal conductivity values increase with increasing the volume fraction of ZrO₂ microparticles. This behavior in microcomposites is due to low or lost interfacial thermal resistance. The epoxy-based composites filled with ZrO₂ microparticles have much higher thermal conductivity values



4-4.1.3 Thermal conductivity of EP/ MgO nanocomposites

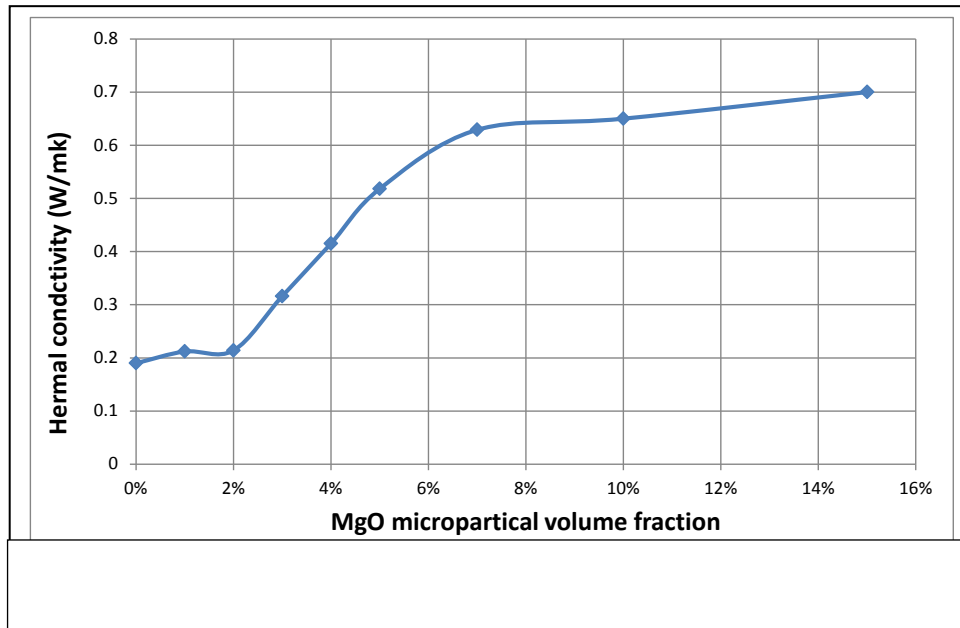
The results of thermal conductivity of EP/MgO nanocomposites in figure(4-55) show an increase thermal conductivity with increasing the MgO nanoparticles volume fraction, this performance is due to incorporating MgO nanoparticles in epoxy matrix producing an increase scattered at the interface between unlike materials. the heat passage is controlled by the interface provided by a

combination agent that connects inorganic particles on one side and the polymer host on the other side. It was found that the thermal conductivity improvement of the composites is dependent on the filler loading. this performance of EP/ MgO nanocomposites agree with the behavior obtained by Wereszczak et al. [52].



4-4.1.4 Thermal conductivity of EP/ MgO microcomposites

From figure (4-56) thermal conductivity increased with increasing volume fraction of MgO microparticles of EP/ MgO microcomposites. At 15 % vol. fraction of MgO nanoparticles thermal conductivity reach maximum increment. The increasing in volume fraction of MgO microparticles lead to increase of constraint of epoxy chains, since heat conduction mainly occurs through the fillers. The epoxy is a thermal barrier for heat propagation, while the filler material transmits the heat much faster therefore the thermal conductivity increased with increasing volume fraction of MgO microparticles. In general all the results obtained after the addition of MgO microparticles to epoxy were higher than that of epoxy and MgO nanocomposites.



4-4.2 Differential Scanning Calorimeter (DSC) Spectra of EP/ ZrO₂Nano/Microcomposites

The measurements value of DSC test were done to epoxy, EP/ ZrO₂ microcomposites at 2% vol. fraction of ZrO₂ microparticles, and EP/ ZrO₂ nanocomposites at 2% and 10% vol. fraction of ZrO₂ nanoparticles with heating rate (5 °C/min), the results are shown in illustration (4-57). Glass transition temperature (T_g) of the specimen were delineates from the tangents of (DSC) spectra as a function of temperature.

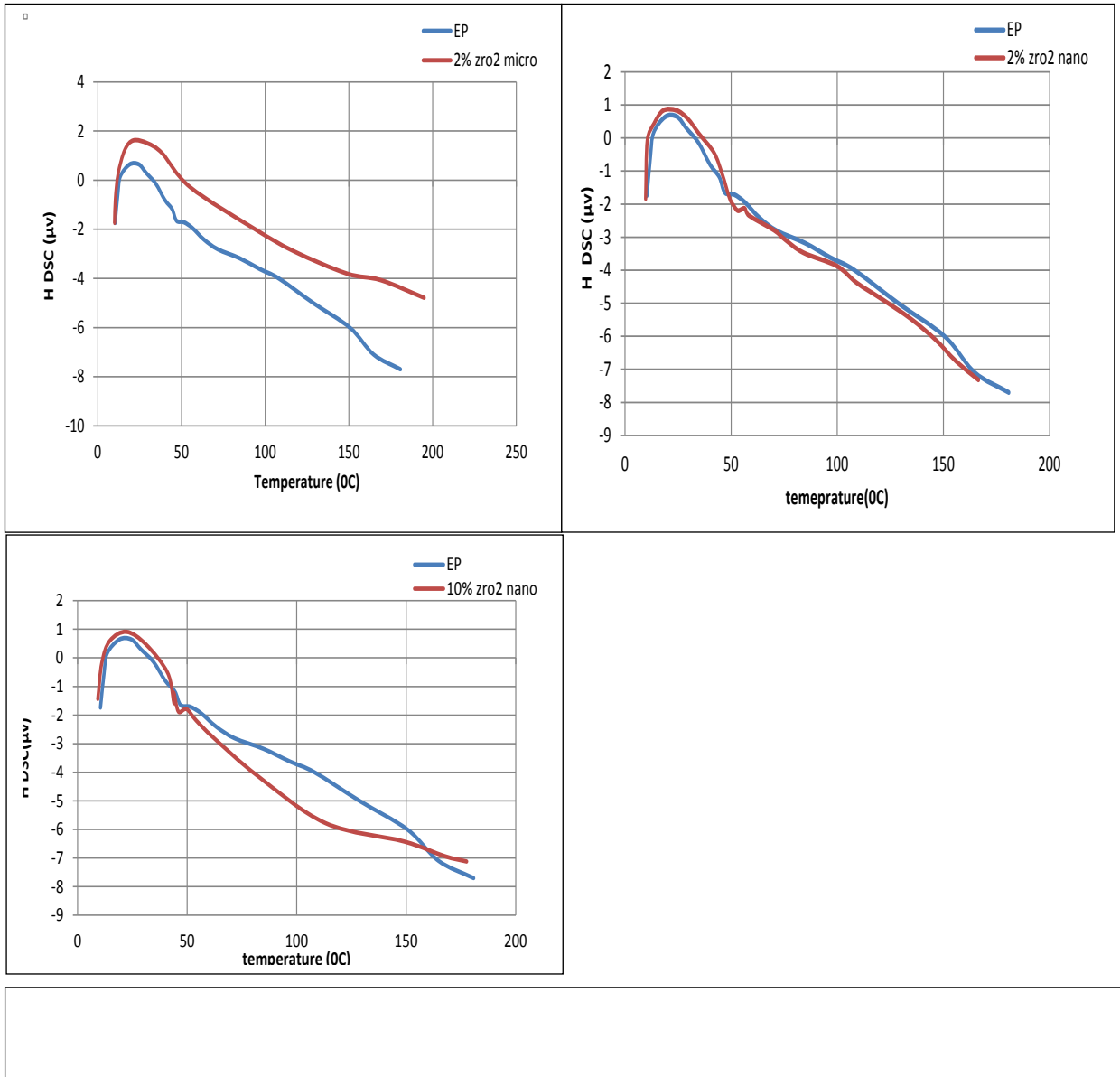


Table (4-5) offers information linked to Glass transition temperature (T_g) for epoxy, EP/ ZrO₂ microcomposites with (2% vol. fraction of ZrO₂ microparticles) and EP/ ZrO₂ nanocomposites with (2, 10% vol. fraction of ZrO₂ nanoparticles).

Table (4-5). Glass transition temperature (T_g) for epoxy, EP/ ZrO₂ microcomposites, and EP/ ZrO₂ nanocomposites at (5 °C/min heating rat

Samples	EP	EP/2% micro ZrO ₂	EP/2% nano ZrO ₂	EP/10% nano ZrO ₂
T _g (oC)	47	45	53	44

The glass transition temperature (T_g) of Epoxy sample illustrated higher value than that of the EP/ ZrO₂ microcomposites with (2% vol. fraction) and EP/ ZrO₂ nanocomposites with (10% vol. fraction). While (T_g) value of EP/ ZrO₂ nanocomposites at (2% vol. fraction) was higher than that of epoxy, EP/ ZrO₂ microcomposites at (2% vol. fraction) and EP/ ZrO₂ nanocomposites at (10% vol. fraction), this performance of EP/ ZrO₂ nanocomposites are in a good agreement with the performance obtain by Dorigato et al. [45].

The increasing of glass transition temperature (T_g) for EP/ ZrO₂ nanocomposites with (2% vol. fraction) could be increase by the attractive of nanoparticles with matrix when good space distribution of nanoparticles, Van der-Waals bonding and adhesion of polar force of nanoparticles in nanocomposites compared to epoxy and EP/ ZrO₂ microcomposites, preform to increase the value of (T_g) glass transition temperature.

Glass transition temperature (T_g) of EP/ ZrO₂ nanocomposites at 10% vol. fraction of ZrO₂ nanoparticles was lower than that of epoxy and EP/ ZrO₂ nanocomposites with 2%vol. fraction of ZrO₂ nanoparticles, this performance could be explanation by an rise in the concentration of nanoparticles up to a critical value leads to reducing in glass transition temperature because of reducing the amount of epoxy in the specific volume and lesser crosslink density, therefore less energy requiring for molecular and hence epoxy chains

motion this performance of EP/ ZrO₂ nanocomposites in a good agreement with the performance obtain by Kotesilkova et al. [105].

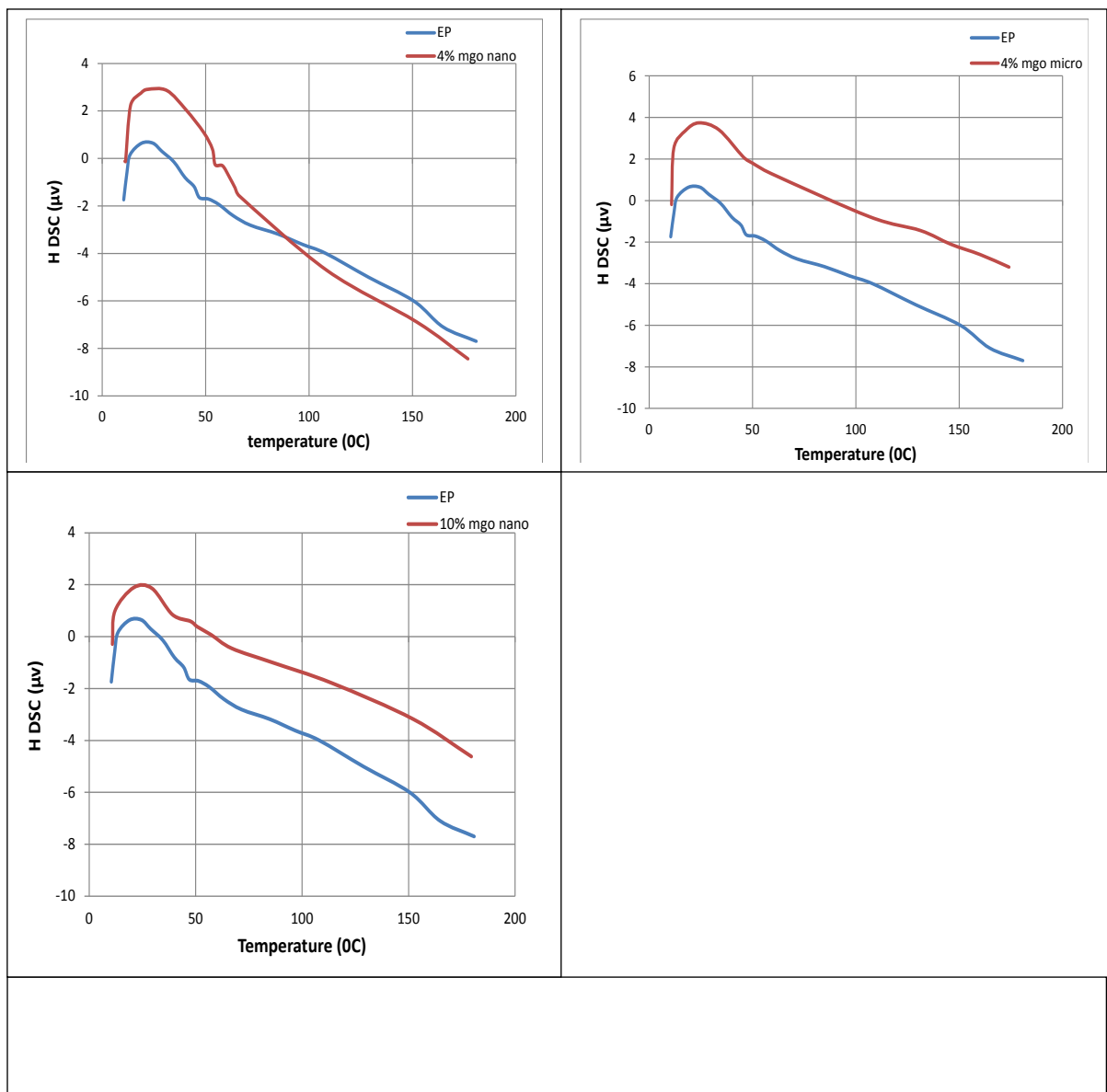
4-4.3 Differential Scanning Calorimeter (DSC) Spectra of EP/ MgO Nano/Microcomposites

The measurements value of (DSC) tested to epoxy, EP/ MgO microcomposite at 4% vol. fraction of MgO microparticles, and EP/ MgO nanocomposites at 4% and 10% vol. fraction of MgO nanoparticles with heating rate (5 °C/min), the results are illustrated in illustration (4-58). Glass transition temperature (T_g) of the specimen were delineates from the tangents of (DSC) spectra as a function of temperature Table (4-18) offers information linked to Glass transition temperature (T_g) for epoxy, EP/ MgO microcomposites with (4% vol. fraction of MgO microparticles) and EP/ MgO nanocomposites with (4, 10 % vol. fraction of MgO nanoparticles).

Table (4-6). Glass transition temperature (T_g) for epoxy, EP/ MgO microcomposites, and EP/ MgO nanocomposites at (5 0C/min heating rate).

Samples	EP	EP/2% micro MgO	EP/2% nano MgO	EP/10% nano MgO
T _g (oC)	47	44	55	46

The result glass transition temperature (T_g) value of epoxy illustrated higher value than that of EP/ MgO nanocomposites with 10% vol. fraction of MgO nanoparticles and EP/ MgO microcomposites with 4% vol. fraction of MgO microparticles While, glass transition temperature (T_g) value of EP/ MgO nanocomposites with 4% vol. fraction of MgO nanoparticles was higher than that of epoxy, this performance of EP/ MgO nanocomposites in a good agreement with Chatterjee et al. [43]



The increasing in the value of glass transition temperature (T_g) value of EP/ MgO nanocomposites 4% vol. fraction of MgO nanoparticles was probably due to the attractive of nanoparticles with matrix when good space distribution of nanoparticles, Van der-waals bonding and adhesion of polar force of nanoparticles into nanocomposites compared to epoxy and EP/ MgO microcomposites

4-5 Conclusions

- 1- ZrO₂ nanoparticles enhance all mechanical properties of epoxy matrix with most vol. fraction of addition , The best value of addition of ZrO₂ nanoparticles which is used to improvement of mechanical properties like (flexural strength, fracture toughness and impact strength) at 2% and (flexural modulus ,hardness) at 3% vol. fraction.
- 2- SEM images show that ZrO₂ and MgO nanoparticles enhance epoxy chains structure by decreasing structure defects appearance like; nanocrack created by numerous polymerization zone. the nanocracks almost vanish from the structure because of adding ZrO₂ nanoparticles was at minimum value at 2% vol. fraction of ZrO₂ nanoparticles and adding MgO nanoparticles is 4% vol. fraction of MgO nanoparticles.
- 3- Incorporation of ZrO₂ results in improvement of thermal conductivity of epoxy resin. The thermal conductivity was found to increase with increased in volume fraction of filler content.
- 4- MgO nanoparticles enhance all mechanical properties of epoxy matrix with most vol. fraction of addition. The best value of addition of MgO nanoparticles is 4% which is used to improvement of mechanical properties like (flexural strength, flexural modulus, fracture toughness impact strength and hardness)
- 5- Ductile behavior almost appears in stress-strain curves of EP/ MgO nanocomposites.
- 6- Dielectric constant of EP/ ZrO₂ nanocomposites at higher concentration (> 10% vol. fraction) dielectric constant of EP/ ZrO₂ nanocomposites decrease increasing volume fraction of ZrO₂ nanoparticles,

while Tan delta of EP/ ZrO₂ nanocomposites little increase with increasing volume fraction ZrO₂ nanoparticles.

7- Dielectric constant EP/ MgO nanocomposites increase with increasing volume fraction of MgO nanoparticles ,.while tan δ of EP/MgO nanocomposites rise with increasing concentration of MgO nanoparticles in the epoxy matrix of EP/ MgO nanocomposites.

4-6 Future work

1-Estimation the lifetime of using TGA temperature EP/ZrO₂ nanoparticles and EP/MgO nanoparticles .

2- Study the outdoor weathering of EP/ZrO₂ nanoparticles and EP/MgO nanoparticles.

3- Study the tear test on some epoxy composites and some epoxy blends.

4-Study the influence of metal nanoparticles multi-sizes on mechanical, thermal and dielectrical properties of epoxy nanocomposites.

5-Study the influence of nano/micro-hybrids metal oxides nanoparticles on mechanical, thermal and dielectrical properties of epoxy composites.

References

1. J. H. Koo, (**Polymer Nanocomposite, Processing, Characterization and Application**) Mc. GrawHill companies, USA (2006)
2. F. Hussain, M. Hojjati, M. Okamoto, and R. E. Gorga. (**Review article: Polymer-matrix Nanocomposites, Processing, manufacturing and Application: An overview**) Journal of Composite Materials. 40 (2006) 17, 1511-1574.
3. R. K. Gupta, E. Kennel and K. J. Kim (**Polymer Nanocomposites Handbook**) 2010 by Taylor and Francis Group, LLC
4. R. Sarathi, R.K. Sahu and P. Rajeshkumar (**Understanding the thermal, mechanical and electrical properties of epoxy nanocomposites**) Materials Science and Engineering A 445–446 (2007) 567–578.
5. L. L. Zhai, L. GP, W. YW.. (**Effect of nano-Al₂O₃ on adhesion strength of epoxy adhesive and steel**) International Journal of Adhesion & Adhesives 2007;28:23
6. P. Singh ·M ·Zhang ·D ·Chan (**Toughening of a brittle thermosetting polymer: Effects of reinforcement particle size and volume fraction**) J. Mater. Sci. 37 (2002) 371
7. George Odain, (**Principle of Polymerization,**) John Wiley and Sons Inc., Fourth edition, USA (2004).
8. J. P. Pascault and R. J. Williams (**Epoxy Polymers**) 2010 WILEY-VCH Verlag GmbH & Co. KGaA, Weinheim
9. W. D. Callister, Jr., and D. G. Rethwisch. (**Fundamentals of Materials Science and Engineering An Integrated Approach**) Third edition 2008 John Wiley and sons Inc.
10. J. P. Pascault and R. J. J. Williams, (**Epoxy Polymers**) WILEY-VCH Verlag GmbH & Co. KGaA, Weinheim, Germany (2010).
11. D. Chondhury and A. Thompson, (**Introduction to Materials Science**) University Tennessee, USA (2006).
12. M. Ruben and R. H. Colby, (**Polymer Physics**) Oxford University Press, USA (2003).
13. R. Kochetov, (**Thermal and Electrical Properties of Nanocomposites**) *Including Material Processing*. 2012, p. 197.
14. X. Chen, and S. S. Mao (**Titanium Dioxide Nanomaterials: Synthesis, Properties, Modifications, and Applications**) Chem. Rev. 107 (2007), 2891- 2959.
15. W. R. Fahrner (**Nanotechnology and Nanoelectronics Materials, Devices, Measurement Techniques**) (2005) Springer-Verlag Berlin Heidelberg.

- 16.R. N. Rothon (**Particulate-Filled Polymer Composites**) 2003, Rapra Technology Limited.
- 17.K. J. Klabunde, (**Nanoscale Materials in chemistry**) 2001 John G.
- 18.G.Zhang (**Dispersion structure and properties of Nanocomposites**) M.Sc. thesis, Department of Chemical and Materials Engineering of the College of Engineering, University of Cincinnati.
- 19.Wang .J, Hu .X.G, Tian .M and Stengler .R, (Study on mechanical and tribological property of nanometer ZrO₂ filled polyoxymethylene composites) Polymer-Plastics Technology and Engineering, 46, 2007, 469–473 -
- 20.BAE D S, KIM E J, PARK S W, HAN K S.(Synthesis and characterization of nanosized Zn_xMn_{1-x}Fe₂O₄ powders by glycothermal process) [J]. Mater Sci Foru, 2005, 486: 436–439
- 21 J. S. Kim, D. H. Lee, S. Kang, D. S. Bae, H. Y. Park, and M. K. Na, (Synthesis and microstructure of zirconia nanopowders by glycothermal processing) Trans. Nonferrous Met. Soc. China (English Ed., vol. 19, p.p. 16–19, 2009.
- 22 D. Mehta and R. Shetty, (Bonding to Zirconia : elucidating the confusion) Int. Dent. SA, vol. 12, no. 2, p.p. 7–46, 2010.
- 23 S. W. Baker, (Chapter 2 Literature Survey) p.p. 7–37, 1996.
- 24 A. Note, (Temperature-Dependent Phase Transitions of ZrO₂) Design, p.p. 1–4.
- 25 A. Mahshad; J. Mona; R. Alimorad (Simple and Economical Method for the Preparation of MgO Nanostructures with Suitable Surface Area) vol. 33, no. 1, p.p. 21–28, 2014.
- 26 H. Zulkefle, L. N. Ismail, R. A. Bakar, M. H. Mamat, M. Rusop, and A. S. Preparation, (Enhancement in Dielectric Constant and Structural Properties of Sol-Gel Derived MgO Thin Film using ZnO / MgO Multilayered Structure) vol. 2, no. 1, 2012.
- 27 E. Grades, (Functionalization and Immobilization of MgO Nanocubes Funktionalisierung und Immobilisierung von MgO Nanowürfeln,) 2012.
28. S. Advani (**Processing and Properties of Nanocomposites**) 2007 by World Scientific Publishing Co. Pte. Ltd.
- 29.D. Devaprakasam, P.V. Hatton, G. Mobus and B.J. Inkson (**Effect of microstructure of nano- and micro-particle filled polymer composites on their tribo-mechanical performance**) Journal of Physics: Conference Series 126 (2008) 012057.

30. J. Yuan, S. Zhou, G. Gu and L. Wu (Effect of Particles Size of Nanosilica on Performance of Epoxy/silica Composites Coatings) *Journal of Materials Science* 40 (2005) 3927-3932
31. M. Cakir, I. Kartal, H. Demirer and R. Samur (Effect of water absorption on the wear behavior of sol-gel processed epoxy/silica hybrids) *Scientific Research and Essays* Vol. 7(7) (2012) p.p. 805-812, .
32. L. F. Nielsen (Composite Materials: Properties as Influenced by Phase Geometry) 2008 Springer
33. V. Mittal (Optimization of Polymer Nanocomposite Properties) 2010 WILEY-VCH Verlag GmbH & Co
34. G. Akovali (Handbook of Composite Fabrication) 2001 Rapra Technology Limited
35. D.R. Pau, L.M. Robeson (Polymer nanotechnology: Nanocomposites) *Polymer* 49 (2008) 3187–3204.
36. R. Kotsilkova (Thermoset Nanocomposites for Engineering Applications) 2007, Smithers Rapra Technology Limited.
37. A. Boudenne, L. Ibos, Y. Candau and S. Thomas (Handbook of Multiphase Polymer Systems) volume 1 2011 John Wiley and Sons Ltd.
38. C.B. Ng, L.S. Schadler and R.W. Siegel (Synthesis and mechanical properties of TiO₂-Epoxy nanocomposites) *Nanostructured materials* Vol. 12 (2001), 507-510.
- 39- Y. Shan and L. Gao, “**CHAPTER 7,**” p.p. 129–157, 2004.
- 40- F. Bondioli, V. Cannillo, E. Fabbri, M. Messori, and R. Emilia, (Preparation and characterization of epoxy resins filled with submicron spherical zirconia particles) no. 11, p.p. 794–798, 2006.
- 41- A. Wazzan and H. A. Al-Turaif (Influence of Submicron TiO₂ Particles on the Mechanical Properties and Fracture Characteristics of Cured Epoxy Resin) *Polymer-Plastics Technology and Engineering*, 45 (2006) 1155–1161.
- 42- S. Singha and M. J. Thomas (Dielectric Properties of Epoxy Nanocomposites) *IEEE Transactions on Dielectrics and Electrical Insulation* Vol. 15 (2008) No.1 p12-
- 43- A. Chatterjee and M. S. Islam (Fabrication and characterization of TiO₂-epoxy nanocomposite) *Materials Science and Engineering A* 487 (2008) 574–585.
- 44- 58. J K Nelson and Y Hu (Nanocomposite dielectrics—properties and implications) *J. Phys. D: Appl. Phys.* 38 (2005) 213–222.
- 45- A. Dorigato, A. Pegoretti, F. Bondioli, and M. Messori, (Improving Epoxy Adhesives with Zirconia Nanoparticles) vol. 17, p.p. 873–892, 2010.

- 46- Jeong, J. Kim, J. Lee, and J. Hong, (Electrical Insulation Properties of Nanocomposites with SiO₂ and MgO Filler) vol. 11, no. 6, p.p. 261–265, 2010.
- 47-. Cho, Y. Kim, J. Kwon, K. Lim, E. Jung, and H. Lee, (**Improvement of Electrical and Thermal Characteristics of Nano-Micro Epoxy Composite**) vol. 12, no. 4, p.p. 160–163, 2011.
- 48- M. A. Sithique (Processing And Characterization Of Zirconium Oxide Nanocomposites From Epoxidized Soy Bean Oi Systems) vol. 6, no. 1, p.p. 1-31,2011.
- 49- S. Halder, P. K. Ghosh, and M. S. Goyat, (High Performance Polymers) 2012.
- 50- Q. Wang and G. Chen (**Effect of nanofillers on the dielectric properties of epoxy nanocomposites**) Advances in Materials Research, Vol. 1, No. 1 (2012) 93-107.
- 51- K. S. Harishanand, H. Nagabhushana, B. M. Nagabhushana, P. Panda, R. Gupta, and M. S. Muruli, (ISSN 2277 – 7164 Original Article Comparitive Study on Mechanical Properties of ZnO , ZrO₂ and CeO₂ Nanometal Oxides Reinforced Epoxy Composites) vol. 3, no. 1, p.p. 7–13, 2013.
- 52- A. a. Wereszczak, T. G. Morrissey, C. N. Volante, P. J. Farris, R. J. Groele, R. H. Wiles, and H. Wang, (**Thermally conductive MgO-filled Epoxy molding compounds**) IEEE Trans. Components, Packag. Manuf. Technol., vol. 3, no. 12, p.p. 1994–2005, 2013.
- 53- M. Edm, (Corrosion Resistance of Modified Nano-ZrO₂/epoxy Coating ZHAO) vol. 26, no. 5, pp. 139–140, 2012.
- 54- N. A. Al-hamadani and N. D. Al-shwak, (Dielectric Properties of ZrO₂ / PMMA Nanocomposites) vol. 7, no. 1, pp. 55–58, 2015.
- 55- Widad Hamdi .J (**Advances in Physics Theories and Application**)vol.44 (2015)
- 56.Z. D. Jastrzebski (**The Nature and Properties of Engineering Materials**) John Wiley and sons, Inc. 1976.
- 57.L. E. Nielsen and R. F. Landel (**Mechanical properties of polymers and composites**) 1994 by Marcel Dekker, Inc.
- 58.W. Soboyejo (**Mechanical Properties of Engineered Materials**) 2002 by Marcel Dekker, Inc.
59. D. Gross and T. Seelig (**Fracture Mechanics With an Inroduction to Micromechanics**) 2006 by Springer-Verlag Berlin Heidelberg.

- 60-A. S. Khleel, (**Study the Effect of Additives on Some Mechanical and Thermal Properties for Epoxy Resin**) Ph. D. Thesis, Department of Physics, University of Baghdad, Iraq (2007).
- 61.N. Perez (**FRACTURE MECHANICS**) 2004 Kluwer Academic Publishers Boston.
- 62.W. F. Hosford (**Mechanical Behavior of Materials**) 2010, William F. Hosford.
- 63.A. F. Liu (**Mechanics and Mechanisms of Fracture: An Introduction**) 2005 by ASM International.
64. S. L. kakapli and A. kakani, (**Material Science and Engineering,**) New Age International (P) Ltd. (2004).
65. J. F. Shackelford, (**Introduction to Material Science and Engineering**) USA (2005).
- 66.Basarkar A.and Singh J., "poly(lactide-co-glycolide)-polymethacrylate nanoparticles for intramuscular delivery plasmid encoding interleukinco to prevent autoimmune diabetes in mice," Journal of Pharmaceutical Research, Vol. 26 No. 1,72-81 (2009).
- 67.D. R. Askeland and P. P. Fulay (**Essentials of Materials Science and Engineering**) 2009 Cengage Learning.
- 68.V. V. Vasiliev and E. V. Morozov (**MECHANICS AND ANALYSIS OF COMPOSITE MATERIALS**) 2001 Elsevier Science Ltd.
- 69.D.R. Moore (**THE APPLICATION OF FRACTURE MECHANICS TO POLYMERS, ADHESIVES AND COMPOSITE**) 2004 Elsevier Ltd and ESIS.
70. M. Ward and J. Sweeney (**An Introduction to the Mechanical Properties of Solid Polymers**) 2004 John Wiley & Sons Ltd.
71. G. H. Michler and F. J. Balta-Calleja (**Mechanical Properties of Polymers Based on Nanostructure and Morphology**) 2005 by Taylor & Francis Group.
- 72.S. Kumar and W. A. Curtin (**Crack interaction with microstructure**)2007 VOLUME 10: NUMBER 9
73. J. K. Nelson (**Dielectric Polymer Nanocomposites**) 2010 Springer Science and Business Media, chapter
74. W. D. Callister, (**Materials Science and Engineering an Introduction**) John Wiley and Sons Inc., USA. (2007).
75. A. Harper, (**Plastics Testing Technology**) John wielly and Sons, London (1984).
76. S.L .kakani and Amit kakani (**Material science**) 2004,new age interntional(p) Ltd,publishers

77. R. L. Ellis, (**ballistic impact resistance of graphite epoxy composites with shape memory alloy and extended chain polyethylene spectraTM**) 1996,p.4
78. M. Technologies, “**Shore (Durometer) hardness test,**” vol. 8890, p. 75070.
79. J. M. Jewell, M. S. Spess, and R. L. Ortlando, (**Effect of Heat- Treatment Temperature on The Properties of Lithium Aluminosilicate Glass**), journal of American Society Vol.74, 92-97(1991).
80. H. Semat and R. Katz, (**Capacitance and Dielectrics**), University of Nebraska-Lincoln, Rober Katz Publication, USA (1958).
- 81.D.B. Sirdeshmukh, L. Sirdeshmukh and K.G. Subhadra (**Micro- and Macro-Properties of Solids: Thermal, Mechanical and Dielectric Properties**) 2006 Springer-Verlag Berlin Heidelberg.
- 82.K. C. Kao (**dielectric phenomena in solide**) 2004, Elsevier, Inc.
- 83.P. J. Harrop (Dielectrics) 1972 Butterworth and Co.
- 84.K. A. Krishnamuthy & M. R. Raghuveer, (**Electrical and Electronics Engineering**) Wiley Eastern, Canada (1993).
- 85.B. S. Mitchell, (**An Introduction to Materials Engineering and Science**) John Wiley and Sons Inc., New Jersey, USA (2004).
- 86.A. Chelkowski (**Dielectric physics**) 1980 PWN-Polish Scientific Publishers (Warszwa).
- 87.C. P. Smyth (**Dielectric Behavior and structure**) 1955 Princeton University.
- 88.S. C. Tjong and Y. W. Mai (**Physical properties and applications of polymer nanocomposites**) 2010 Woodhead Publishing Limited
- 89.R. E. Newnham (**Properties of Materials Anisotropy, Symmetry, Structure**) 2005 Oxford University Press.
- 90.W. Liu, S. Hoa, M. Pugh (**Fracture toughness and water uptake of high-performance epoxy/nanoclay nanocomposites**). Compos Sci Tech 65(2005) 2364–2373
- 91.K. F. Young and H. P. R. Frederikse, (**Compilation of Static Dielectric Constant of Inorganic Solids**) Institute for Materials Research, vol.2, No.2 (1973).
- 92.B. Tareev, (**Physics of Dielectric Materials**) Mir publisher, Moscow(1979)
- 93.P. S. Halasyamani & K.R. Poeppelmeier, (**Noncentrosymmetric Oxides**) Chem. Mater., vol. 10, 2753- 2769(1998).
- 94 D.D.L. Chung, (**Materials for electronic packaging**), Butterworth-Heinemann, 1995.

- 95 Y.K. Godovsky, (**Thermophysical properties of polymers**) Springer-Verlag, 1992
96. H.S. Tekce, D. Kumlutas, I.H. Tavman, (**Effect of particle shape on thermal conductivity of copper**), 2007.
- 97 D. Hansen, G.A. Bernier, (**Thermal conductivity of polyethylene: the effect of crystal size, density and orientation on the thermal conductivity**) *Polymer Engineering and Science, Vol. 12, №3*, 204-208, 1972
- 98 Y. Yang, (**Thermal conductivity**”, *Physical properties of polymers*). *Handbook*, edited by J.E. Mark, Chapter 10, 2nd ed., Springer, 2007
- 99.R. V Kurahatti, a O. Surendranathan, a V. R. Kumar, and C. S. Wadageri, (**Dry Sliding Wear behaviour of Epoxyreinforced with nano ZrO 2 Particles**) *Procedia Mater. Sci.*, vol. 5, p.p. 274–280, 2014.
- 100.H. K. Hameed and H. A. Rahman, (**The effect of addition nano particle ZrO 2 on some properties of autoclave processed heat cure acrylic denture base material**),vol. 27, no. March, p.p. 32–39, 2015.
- 101.B. Wetzel, P. Rosso, F. Hauptert and K. Friedrich (**Epoxy nanocomposites – fracture and toughening mechanisms**) *Engineering Fracture Mechanics* 73 (2006) 2375–2398.
- 102.C. Chen, R. S. Justice, D. W. Schaefer and J. W. Baur (**Highly dispersed nanosilica–epoxy resins with enhanced mechanical properties**) *Polymer* 49 (2008) 3805–3815.
- 103.L. M. Levinson and H. R. Philipp, (**AC Properties of metal oxide varistors**) *J. Appl. Phys.*1976, Vol. 47, No. 3, p.p. 1117-1122.
- 104.J. C. Fothergill, J. K. Nelson and M. Fu, (**Dielectric Properties of Epoxy Nanocomposites containing TiO₂, Al₂O₃ and ZnO fillers**), *IEEE Conf. Electr. Insul. Dielectr. Phenomena (CEIDP)*, p.p. 406-409, 2004
- 105.Kotsilkova R (ed) (**Thermoset nanocomposites for engineering applications**), *Smithers Rapra. Chapter 6: performance of Thermoset Nanocomposites* (2007)

Appendix A1

Certificate of Analysis

Magnesium oxide(MgO)

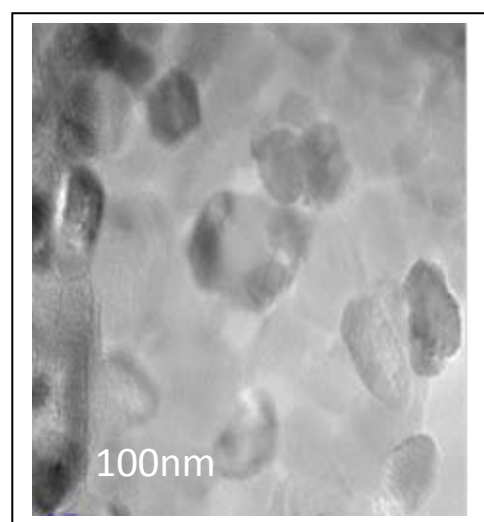
APS 90-100 nm

Stock #: NS613-03-328

Components	Contents (%)
Calcium(Ca)	< 0.05
Potassium(K)	0.05
Sodium(Na)	0.03

Purity: >99%

- Cryst. phases: cubic
- APS: 100nm(90-100) nm
- SSA: > 40 m²/g
- Color: white
- Morphology: polyhedral
- Bulk density: 0.18 g/cm³
- True density: 3.58 g/cm³



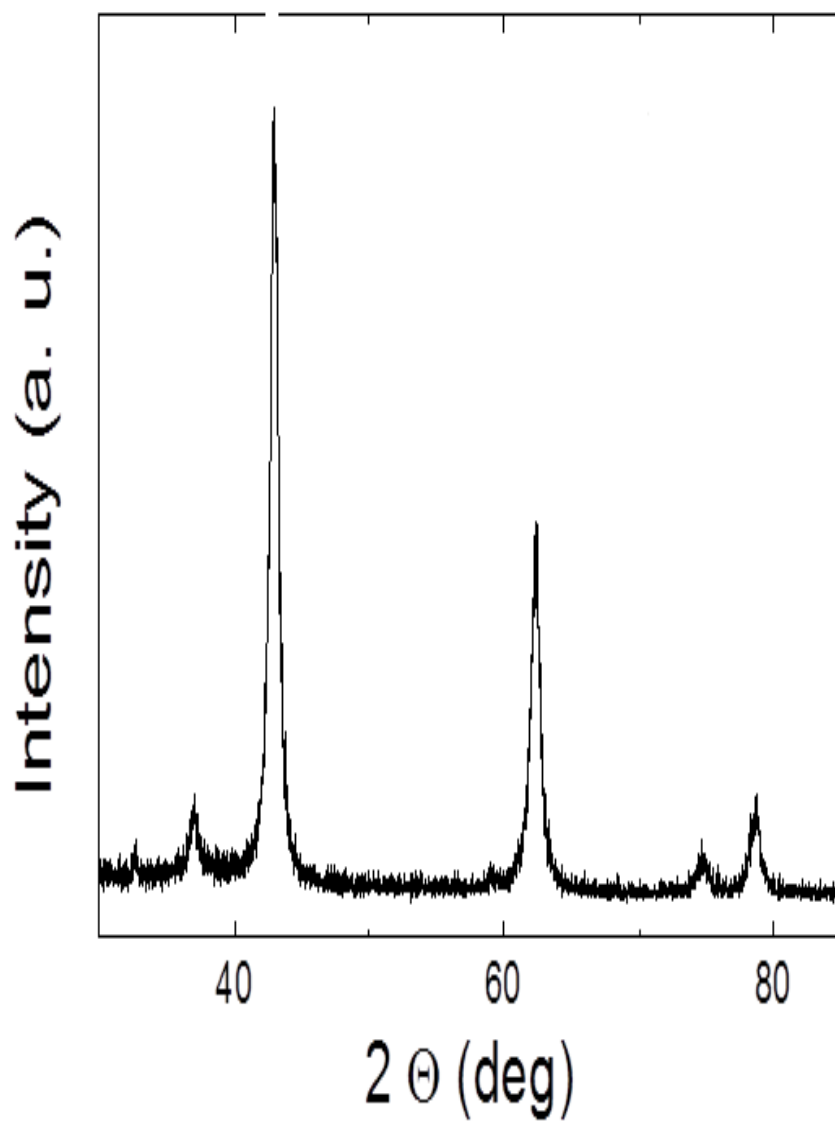


Figure (1): X-Ray diffraction pattern of the nano MgO

Appendix A2

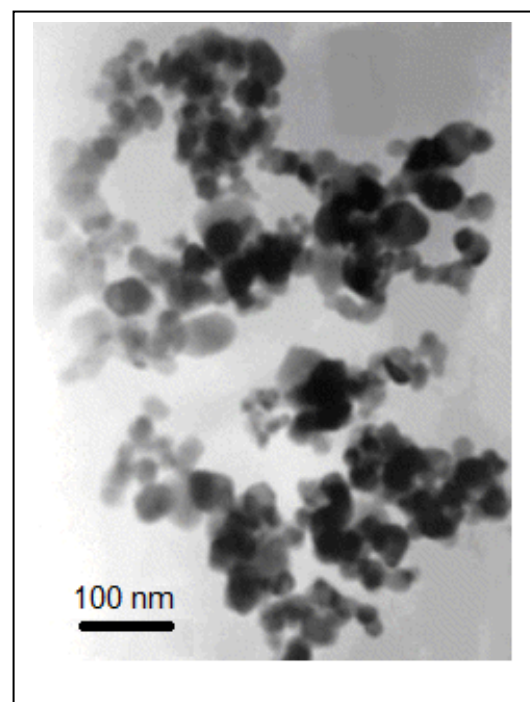
Certificate of Analysis

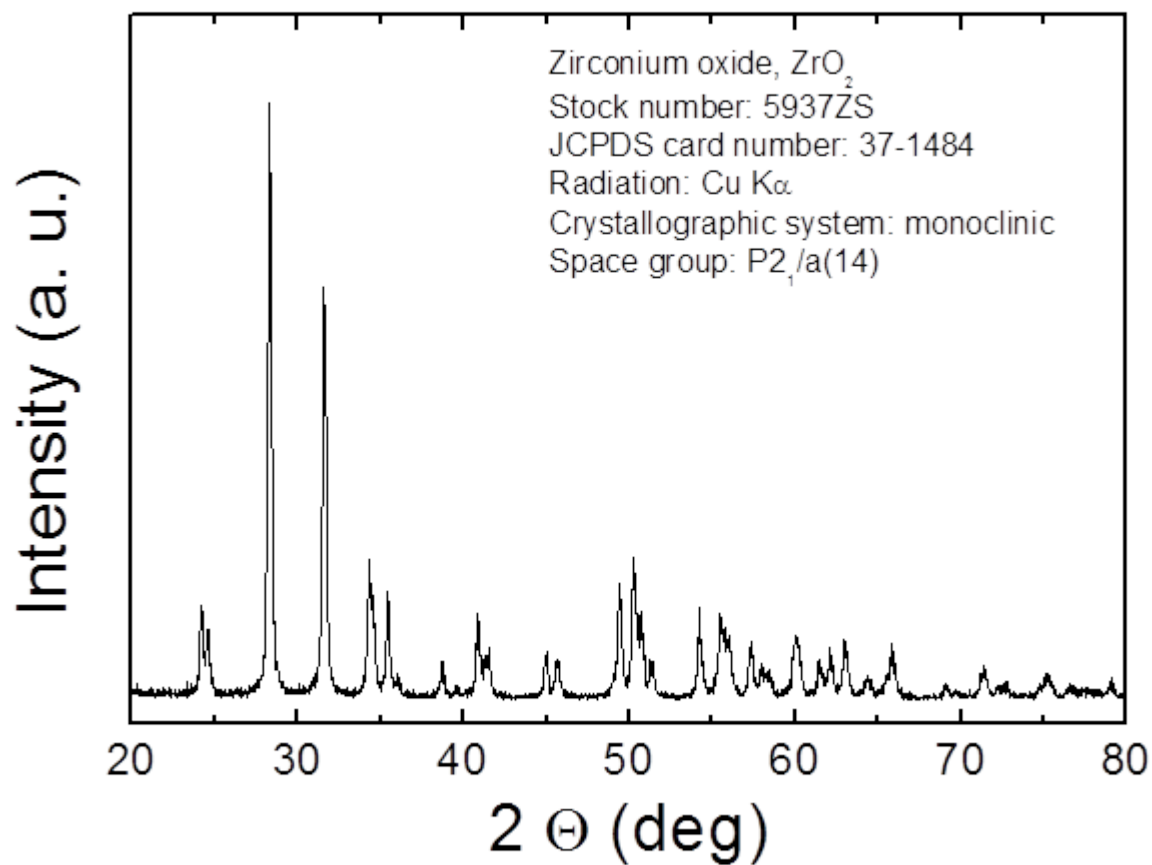
Zirconium oxide
99% (metal basis excluding Hf)
APS 80-100 nm
Stock #: 5937ZS

Components	Contents (%)
HfO ₂	< 3
Fe ₂ O ₃	0.006
Cl ⁻	0.0013
SiO ₂	0.004
TiO ₂	0.005

Analytical Technique: inductively coupled plasma

- Purity: 99%(metal basis excluding Hf, Hf < 3 wt%)
- Cryst. phases: monoclinic
- APS: nm
- SSA: > 100 m²/g
- Color: white
- Morphology: spherical
- Bulk density: 0.4 - 0.5 g/cm³
- True density: 5.89 g/cm³







جمهورية العراق
وزارة التعليم العالي
والبحث العلمي
جامعة بغداد
كلية التربية ابن الهيثم

دراسة بعض الخواص الفيزيائية للايبوكسي المدعم بدقائق نانوية

رسالة مقدمة
الى مجلس كلية التربية-ابن الهيثم - جامعة بغداد
وهي جزء من متطلبات نيل درجة الدكتوراه في علوم الفيزياء

من قبل

صفاء عبد صالح

ماجستير فيزياء – جامعة بغداد

المشرف

أ.م.د. وداد حمدي جاسم

1437 هجري

2016 ميلاد

الخلاصة

تم استخدام مادة الايبوكسي (EP) مع نسب خلط حجمية مختلفة (1، 2، 3، 4، 5، 7، 10، 15 و 20%) من الجسيمات الزركونيا (ZrO_2) والمغنيسا (MgO) النانوية و من الجسيمات ZrO_2 و MgO المايكروية لتحضير متراكبات الايبوكسي النانوية و متراكبات الايبوكسي المايكروية لفحص ودراسة بعض من خصائصها الميكانيكية (متانة الانحناء ومعامل الانحناء و متانة الكسر وقوة الصدمة والصلادة) والخواص الكهربائية العزلية (ثابت العزل الكهربائي و زاوية ظل الفقد والتوصيلية الكهربائية) والخواص الحرارية (التوصيلية الحرارية ودرجة الانتقال الزجاجي)

طريقة تحضير عينات الايبوكسي وعينات متراكبات الايبوكسي النانوية و عينات متراكبات الايبوكسي المايكروية تضمنت مراحل الخلط ال ميكانيكي و مجانس خلط الامواج فوق الصوتية و استخدام منظومة التفريغ . تم استخدام فحص الانحناء ذي النقاط الثلاث و فحص وقوة الصدمة و فحص الصلادة و فحص السعة الكهربائية العزلية و فحص الماسح التفاضلي السعوي الحراري و فحص مجهر المسح الالكتروني و فحص التوصيل الحراري لفحص عينات الايبوكسي و متراكباته النانوية و المايكروية

وقد اظهرت النتائج التي تم الحصول عليها من فحص متانة الانحناء ذي النقاط الثلاث زيادة تدعيم الخصائص الميكانيكية لمتراكبات الايبوكسي الزركونيا النانوية ، ان نسبة 2% من الخلط تؤدي الى اعلى نسبة تدعيم لا متنازع الانحناء بلغت 52% اما معامل الانحناء فتضاعف مرتين عند هذه النسبة وايضا زادة متانة الكسر لتصل الى 86% مقارنة مع نتائج عينة الايبوكسي واما قوة الصدمة فقد بلغت 51% وارتفعت صلادة المادة 5% نسبة التدعيم 2% . وقد ظهر الكسر اللدن بشكل واضح في بعض منحنيات الاجهاد-الانفعال في متراكبات الايبوكسي زركونيا.

كما اظهرت الخصائص الميكانيكية لمتراكبات الايبوكسي مغنيسا النانوية زيادة تدعيمها بزيادة نسب الخلط الحجمية لجسيمات المغنيسا النانوي في التراكيز القليلة (> 5%) حيث اظهرت النسبة 4% من MgO النانوية اعلى قيمة لقوة الانحناء حيث ازداة بنسبة 47% مقارنة (EP) في حين معامل الانحناء ارتفع بنسبة 74% مقارنة (EP) في حين متانة الكسر لمتراكبات الايبوكسي مغنيسا النانوية فتضاعفت بحدود اربع مرات عن الايبوكسي وقد بلغت قوة الصدمة 65% عند نسبة التدعيم وارتفعت صلادة المادة 3% مقارنة (EP) لوحده. وقد ظهر الكسر اللدن بشكل واضح في منحنيات الاجهاد-الانفعال في متراكبات الايبوكسي مغنيسا.

الخصائص الميكانيكية لمتراكبات الايبوكسي زركونيا المايكروية و متراكبات الايبوكسي مغنيسيا المايكروية اظهر انخفاض في خصائصها الميكانيكية بارتفاع نسب الخلط الحجمي للجسيمات المايكروية للزركونيا وللمغنيسيا ما عدا معامل التثني فقد زاد بارتفاع نس ب الخلط الحجمي لجسيمات الزركونيا والمغنيسيا المايكروية .وهذا يظهر تفوق الجسيمات النانوية عن الاخرى المايكروية حيث اضافتها بنسب ضئيلة تؤدي الى تحسين ملحوظ في الصفات الميكانيكية والتي يتم تفسيرها عن طريق الصور المأخوذة عن مجهر الماسح الالكتروني والتي اظهرت البنية التركيبية لسطح الكسر لمتراكبات الايبوكسي زركونيا النانوية و لمتراكبات الايبوكسي مغنيسيا النانوية بوجود شقوق نانوية عند نسب خلط حجمية معينة ،وقد بينت صور الكسر انتهاء اغلب الشقوق من التركيب بسب وجود الاضافات لجسيمات الزركونيا والمغنيسيا النانوية فكانت اقل ما يمكن في نسب 2 % من نسب الخلط الحجمي لجسيمات الزركونيا النانوي وعند 4% من نسب خلط حجمي لجسيمات المغنيسيا النانوي . وهذا معزز من النتائج العملية التي حصلنا عليها عند هذه النسب الضئيلة الاضافة واثرا في تحسين الصفات الميكانيكية للايبوكسي.

ان الخصائص الكهربية العزلية لمتراكبات الايبوكسي زركونيا النانوية و لمتراكبات الايبوكسي مغنيسيا النانوية اظهرت زيادة تدعيم ثابت العزل الكهربائي عند نسب الخلط الحجمية الواطنة لجسيمات الزركونيا والمغنيسيا النانوية في حين في نسب الخلط العالية (< 10%) بدء ثابت العزل الكهربائي لمتراكبات الايبوكسي مغنيسيا النانوي بالارتفاع عن اعلى نسبة تحسن في حين ثابت العزل الكهربائي لمتراكبات الايبوكسي زركونيا بالانخفاض . في حين ان زاوية ظل الفقد لمتراكبات الايبوكسي زركونيا النانوي تزداد زيادة طفيفة بزيادة نسب الخلط الحجمي لجسيمات الزركونيا النانوي في حين زاوية ظل الفقد لمتراكبات الايبوكسي مغنيسيا النانوي تقل بنسب قليلة بزيادة نسب الخلط الحجمي لجسيمات المغنيسيا النانوي.

التوصيل الحراري لمتراكبات الايبوكسي زركونيا النانوية و لمتراكبات الايبوكسي مغنيسيا النانوية لها نفس السلوك نسب خلط حجمية مختلفة (1، 2، 3، 4، 5، 7، 10، 15 و 20%) ان التوصيل الحراري لكلا المتراكبتين (لمتراكبات الايبوكسي زركونيا النانوي و لمتراكبات الايبوكسي مغنيسيا النانوي) يزداد بزيادة نسب الخلط الحجمية لجسيمات زركونيا و مغنيسيا النانوية. تمتلك المتراكبات النانوية توصيل حراري اقل من المتراكبات المايكروية. اما المتراكبات النانوية فقد امتلكت مركبت زركونيا قيما اعلى للتوصيل الحراري مقارنة بمتراكبة المغنيسيا